AD-A088 164 NAVAL AIR DEVELOPMENT CENTER WARMINSTER PA AIRCRAFT --ETC F/G 1/2
INVESTIGATION OF TRANSIENT INDUCED AERODYNAMICS IN A MOVING DEC--ETC(U)
FEB 80 R E PALMER

UNCLASSIFIED NADC-79260-60 NL

1 OF 1
AD
A088 164

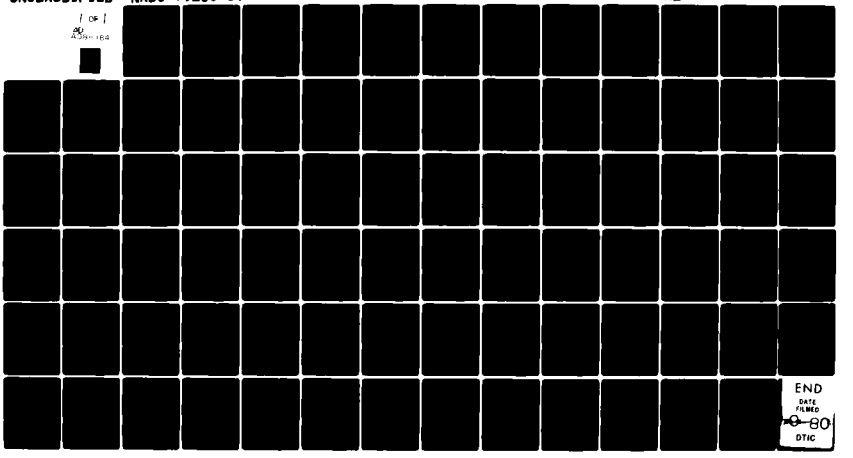

END
DATE FILMED
-80
DTIC

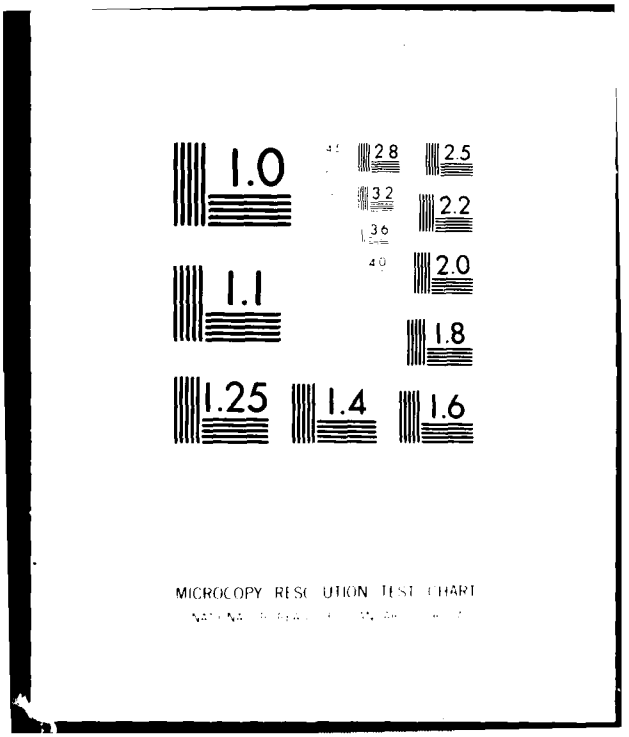
1.0
2.8
2.5
3.2
2.2
3.6
4.0
2.0
1.1
1.8
1.25
1.4
1.6
MICROCOPY RESOLUTION TEST CHART

REPORT NO. NADC-79260-60

AD A088164

INVESTIGATION OF TRANSIENT INDUCED AERODYNAMICS IN A MOVING DECK ENVIRONMENT

R. E. Palmer
NAVAL AIR DEVELOPMENT CENTER
Aircraft and Crew Systems Technology Directorate
WARMINSTER, PENNSYLVANIA 18974

7 FEBRUARY 1980

FINAL REPORT
AIRTASK No. A03V/0000/001B/9F41-400-000
Work Unit No. ZA602

Approved for Public Release; Distribution Unlimited

Prepared for
NAVAL AIR SYSTEMS COMMAND
Department of the Navy
Washington, DC 20361

80 8 21 058

NOTICES

REPORT NUMBERING SYSTEM - The numbering of technical project reports issued by the Naval Air Development Center is arranged for specific identification purposes. Each number consists of the Center acronym, the calendar year in which the number was assigned, the sequence number of the report within the specific calendar year, and the official 2-digit correspondence code of the Command Office or the Functional Directorate responsible for the report. For example: Report No. NADC-78015-20 indicates the fifteenth Center report for the year 1978, and prepared by the Systems Directorate. The numerical codes are as follows:

CODE	OFFICE OR DIRECTORATE
00	Commander, Naval Air Development Center
01	Technical Director, Naval Air Development Center
02	Comptroller
10	Directorate Command Projects
20	Systems Directorate
30	Sensors & Avionics Technology Directorate
40	Communication & Navigation Technology Directorate
50	Software Computer Directorate
60	Aircraft & Crew Systems Technology Directorate
70	Planning Assessment Resources
80	Engineering Support Group

PRODUCT ENDORSEMENT - The discussion or instructions concerning commercial products herein do not constitute an endorsement by the Government nor do they convey or imply the license or right to use such products.

APPROVED BY: _____ DATE: 6/16/80

E. J. STURM
CDR USN

UNCLASSIFIED

SECURITY CLASSIFICATION OF THIS PAGE (When Data Entered)

REPORT DOCUMENTATION PAGE

READ INSTRUCTIONS BEFORE COMPLETING FORM

1. REPORT NUMBER: NADC-79260-60	2. GOVT ACCESSION NO.: AD-A088164
3. RECIPIENT'S CATALOG NUMBER:	
4. TITLE (and Subtitle): Investigation of Transient Induced Aerodynamics in a Moving Deck Environment	5. TYPE OF REPORT & PERIOD COVERED: Final rept. Oct 78-Sep 79
	6. PERFORMING ORG. REPORT NUMBER:
7. AUTHOR(s): Robert E. Palmer	8. CONTRACT OR GRANT NUMBER(s): F41400
9. PERFORMING ORGANIZATION NAME AND ADDRESS: Naval Air Development Center, Aircraft and Crew Systems Technology Directorate, Warminster, PA 18974	10. PROGRAM ELEMENT, PROJECT, TASK AREA & WORK UNIT NUMBERS: P.E. 62241N W.U. No. ZA602 Proj. F41400 AT WF41400000
11. CONTROLLING OFFICE NAME AND ADDRESS: Naval Air Systems Command, Jefferson Plaza, Washington, DC 20361 (AIR-320D)	12. REPORT DATE: 7 February 1980
	13. NUMBER OF PAGES: 86
14. MONITORING AGENCY NAME & ADDRESS (if different from Controlling Office)	15. SECURITY CLASS. (of this report): Unclassified
	15a. DECLASSIFICATION/DOWNGRADING SCHEDULE

16. DISTRIBUTION STATEMENT (of this Report)

Approved for public release, distribution unlimited.

17. DISTRIBUTION STATEMENT (of the abstract entered in Block 20, if different from Report)

18. SUPPLEMENTARY NOTES

19. KEY WORDS (Continue on reverse side if necessary and identify by block number)

VSTOL
VSTOL Aerodynamics
Moving Deck

20. ABSTRACT (Continue on reverse side if necessary and identify by block number)

Transient induced aerodynamic data for a subsonic VSTOL aircraft model operating in a moving deck environment havebeen analyzed. Only single axis deck motions of heave, pitch, and roll were considered. Dynamic effects are discussed with respect to static data and comparisons shown using a developed prediction method.

DD FORM 1 JAN 73 1473 EDITION OF 1 NOV 65 IS OBSOLETE
S/N 0102-LF-014-6601

UNCLASSIFIED
SECURITY CLASSIFICATION OF THIS PAGE (When Data Entered)

393532

SUMMARY

Transient induced aerodynamic data has been analyzed for a subsonic VSTOL aircraft model operating in a moving deck environment. Only the single axis deck motions of heave, pitch, and roll have been considered. The equations governing this analysis are presented along with the methods used to reduce and analyze the data. Dynamic effects are discussed for each deck motion and time history comparisons shown using developed prediction methodology. Conclusions are presented for this analysis along with recommendations for further investigations into this area.

Appendix A presents a detailed discussion of the governing equations along with a description of the computer programs utilized. The transient induced aerodynamic data which were analyzed for heave, pitch, and roll motions are presented in Appendices B, C, and D respectively.

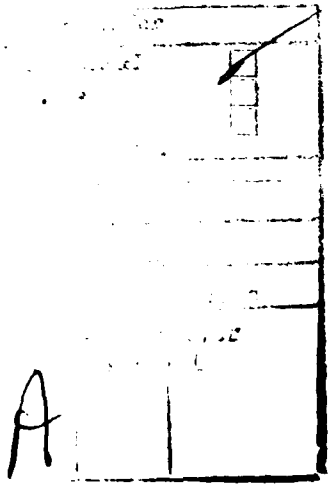

TABLE OF CONTENTS

LIST OF FIGURES

L I S T O F F I G U R E S (C O N T ' D)

I N T R O D U C T I O N

Operating a V/STOL aircraft in ground effect can greatly alter the aerodynamic forces and moments acting on the aircraft. By introducing a moving ground plane, such as the deck of a DD963 class destroyer, the complexity of the resulting flow field is significantly increased. This added complexity makes it even more difficult to perform successful shipboard takeoff and recovery operations. In order to fully utilize the potential shipboard operational capabilities of V/STOL aircraft a better understanding of these phenomena is required.

To accomplish this, the effects of basic single axis deck motions must be examined. Analysis of these independent deck motions (heave, pitch, roll) enable the development of prediction technqiues applicable to a preliminary design environment. These methods provide the designer a tool for estimating the transient induced aerodynamics acting on a V/STOL aircraft in a moving deck environment.

Data for the three-fan subsonic V/STOL configuration of reference (a) was selected for study. A three view drawing of the full scale configuration is shown in Figure 1. As evident in this figure, the aircraft has a low wing and high tail with two lift/cruise fans mounted above the wings and one lift fan in the forward fuselage. The method of analyzing this data in terms of single axis deck motions will be discussed in detail in the following sections.

A P P R O A C H

This analysis was limited to sinusoidal deck motions of heave, pitch, and roll only. Combined motions such as heave and roll were not considered due to the complexity that they introduce. These combined motions, however, should be considered in future analyses of transient induced aerodynamics acting on a VSTOL aircraft.

The dynamic effects caused by a moving deck were investigated through examination of the induced forces or moments in terms of frequency, amplitude, and height-above-deck. For each deck motion the induced force or moment was assumed to be a function of deck position and rate. In the cases of pitch and roll the effect of height-above-deck was also included as shown below:

$$\frac{\Delta L}{T} = f(h,\dot{h}) \qquad (1)$$

$$\frac{\Delta M}{Tc} = g(\theta, \dot{\theta}, h) \qquad (2)$$

$$\frac{\Delta \mathcal{L}}{Tb} = k(\phi, \dot{\phi}, h) \qquad (3)$$

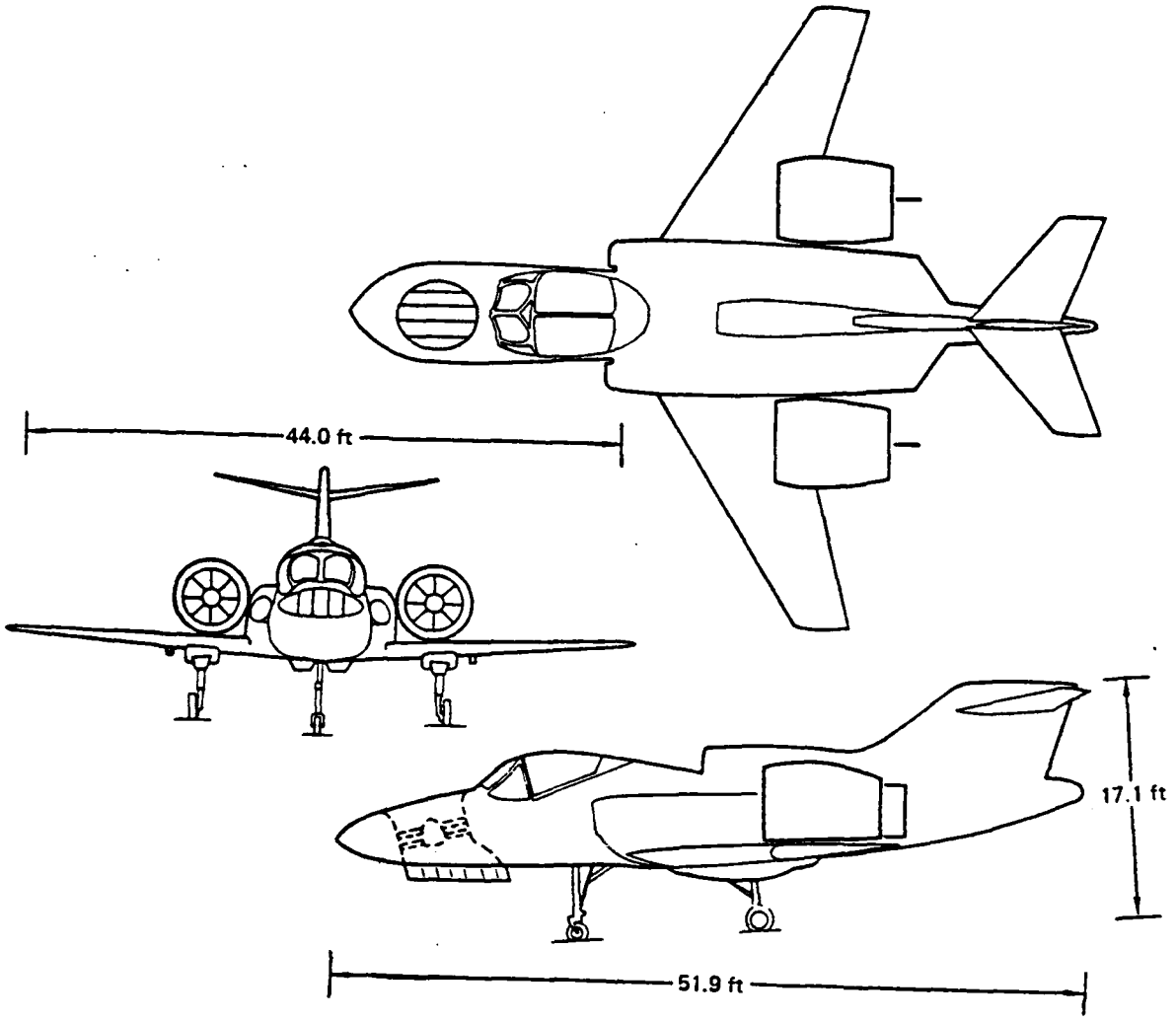

Figure 1. Three View of Subsonic VSTOL Configuration.

The equations defining the deck positions and attitudes at any time, which were differentiated to obtain the desired rates, are presented below:

$$h = h_o + \frac{\Delta h}{2} \sin(\omega t) \quad (4)$$

$$\Theta = \Theta_o + \frac{\Delta \Theta}{2} \sin(\omega t) \quad (5)$$

$$\phi = \phi_o + \frac{\Delta \phi}{2} \sin(\omega t) \quad (6)$$

Figure 2 defines the various parameters of these equations. The deck position and rate are used in a correlative analysis technique to determine the transient induced effects as illustrated in Figure 3 ((a) through (e)). This example is limited to the transient induced lift resulting from variations in deck heave only; this being typical of the method applied to the cases for pitch and roll.

Through selection of a deck rate ($\dot{h}/de$) the corresponding position (h/de) and time (t_1, t_2, ...) were obtained, Figure 3(a). Knowing the measured induced lift as a function of time, Figure 3(b), and the corresponding deck position, the induced lift was cross-plotted with position. Since the deck motion was sinusoidal these data occurred in pairs about the neutral point (ho/de) for the specified deck rate, Figure 3(c). By varying deck rate, an envelope of induced lift versus position was developed corresponding to a given set of test parameters, i.e., deck neutral point, h_o/d_e, frequency, ω, and amplitude, $\Delta h/de$. From this map a quasi-static ($\dot{h}/de = 0$) induced lift was obtained in order to predict the actual transient induced effects, Figure 3(d). Comparisons of these predicted transient effects with the actual test data, Figure 3(e), are presented in subsequent figures for selected test conditions.

R E S U L T S

Each of the three deck motions will be discussed in terms of the accompanying static and dynamic aerodynamic characteristics. Comparisons of actual time histories of dynamic data with predicted time histories will also be presented.

HEAVE

For the heaving deck motion, induced lift is the parameter which is examined. Figures 4, 5, and 6 show induced lift plotted versus height above-deck for frequencies of 1, 2, and 3 Hz. As noted on these figures, the open symbols correspond to positive rates (model heaving away from deck) while the closed symbols represent negative rates (model heaving toward the deck). For clarity, only the data run at the largest amplitude is plotted for each frequency although all amplitudes tested were considered in the analysis. Also, the neutral points for these figures correspond to the data run presented and not necessarily to the other amplitudes.

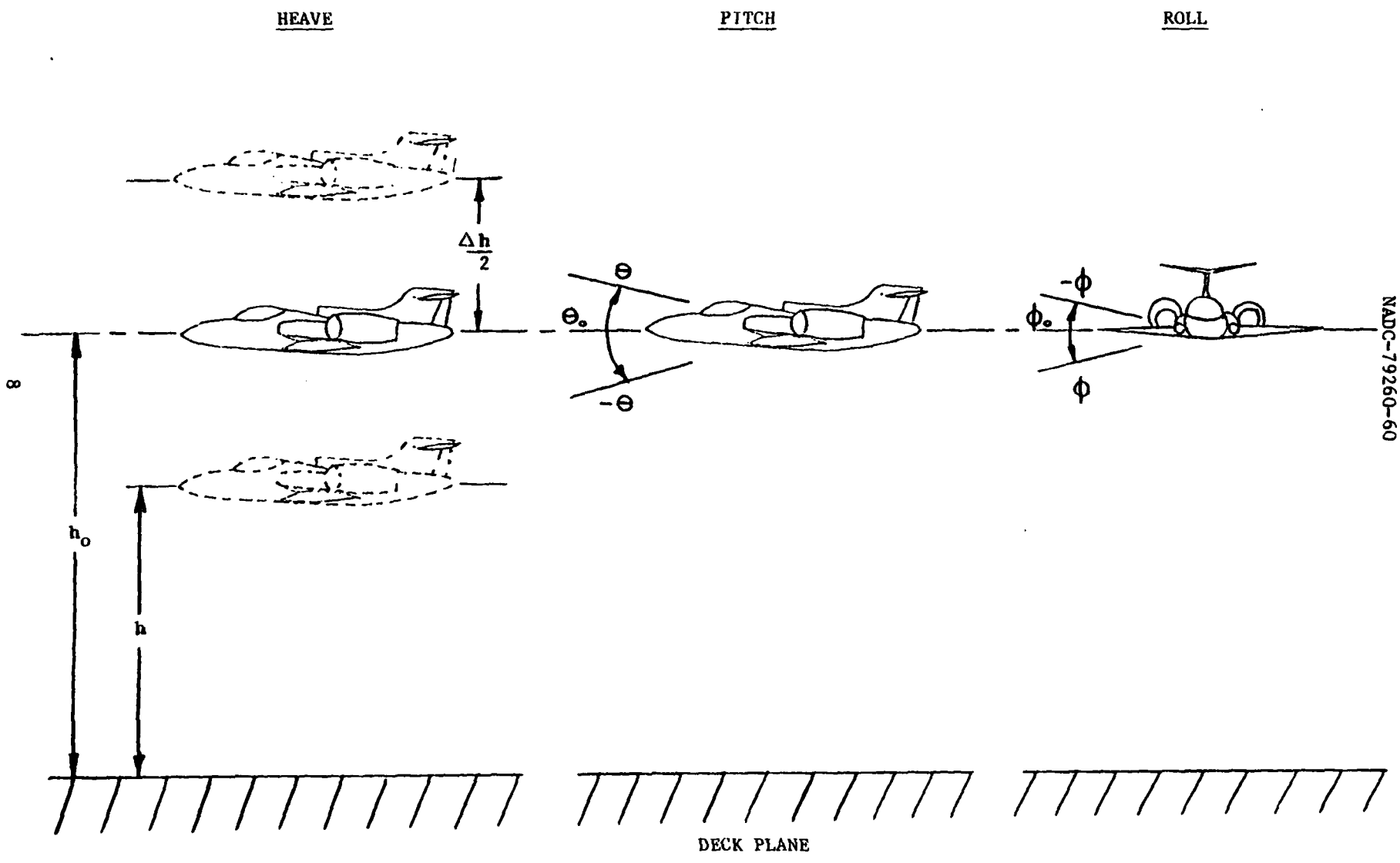

Figure 2. Heave, Pitch, and Roll Coordinate Systems

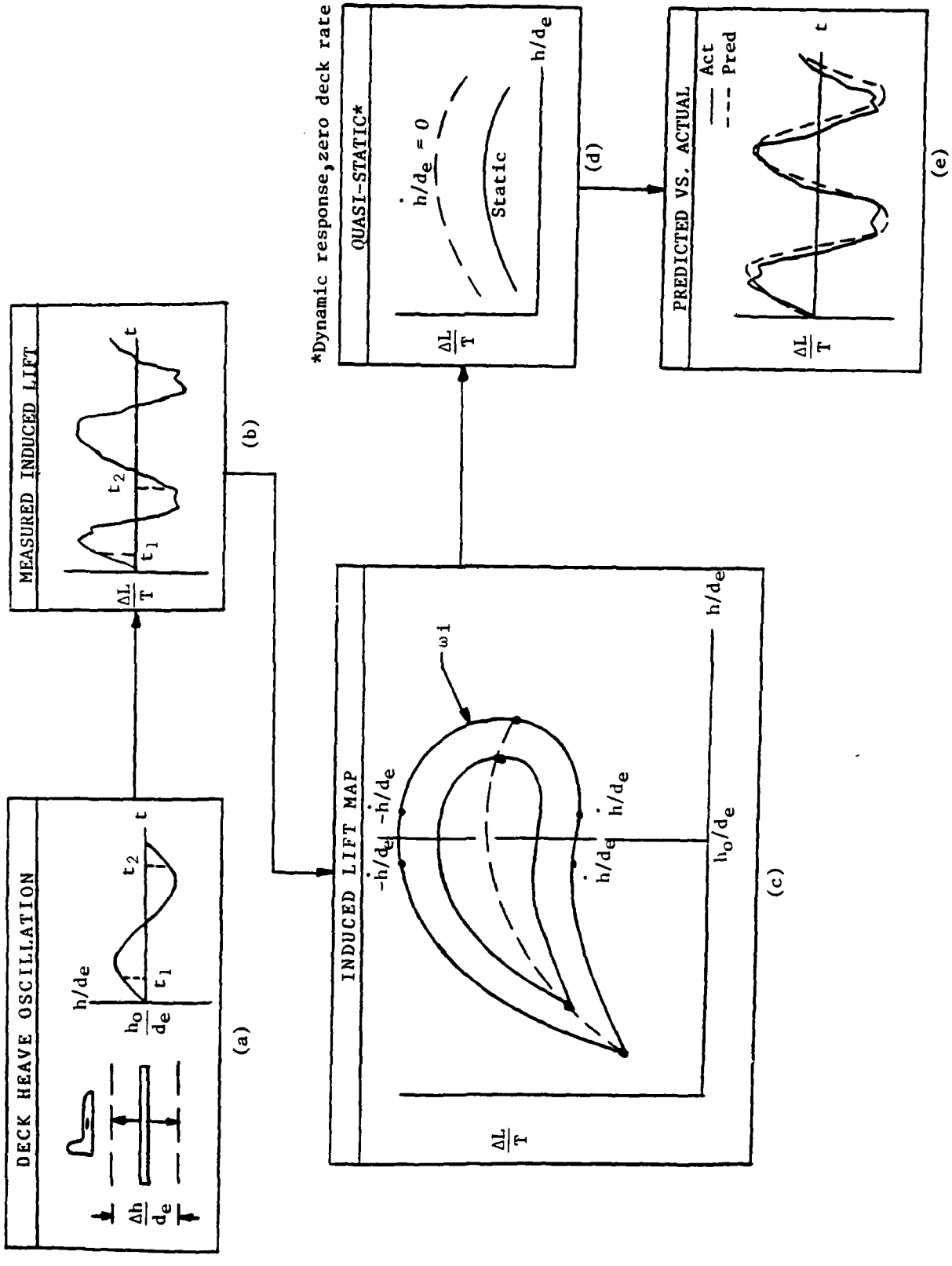

Figure 3. Typical Correlative Analysis Procedure

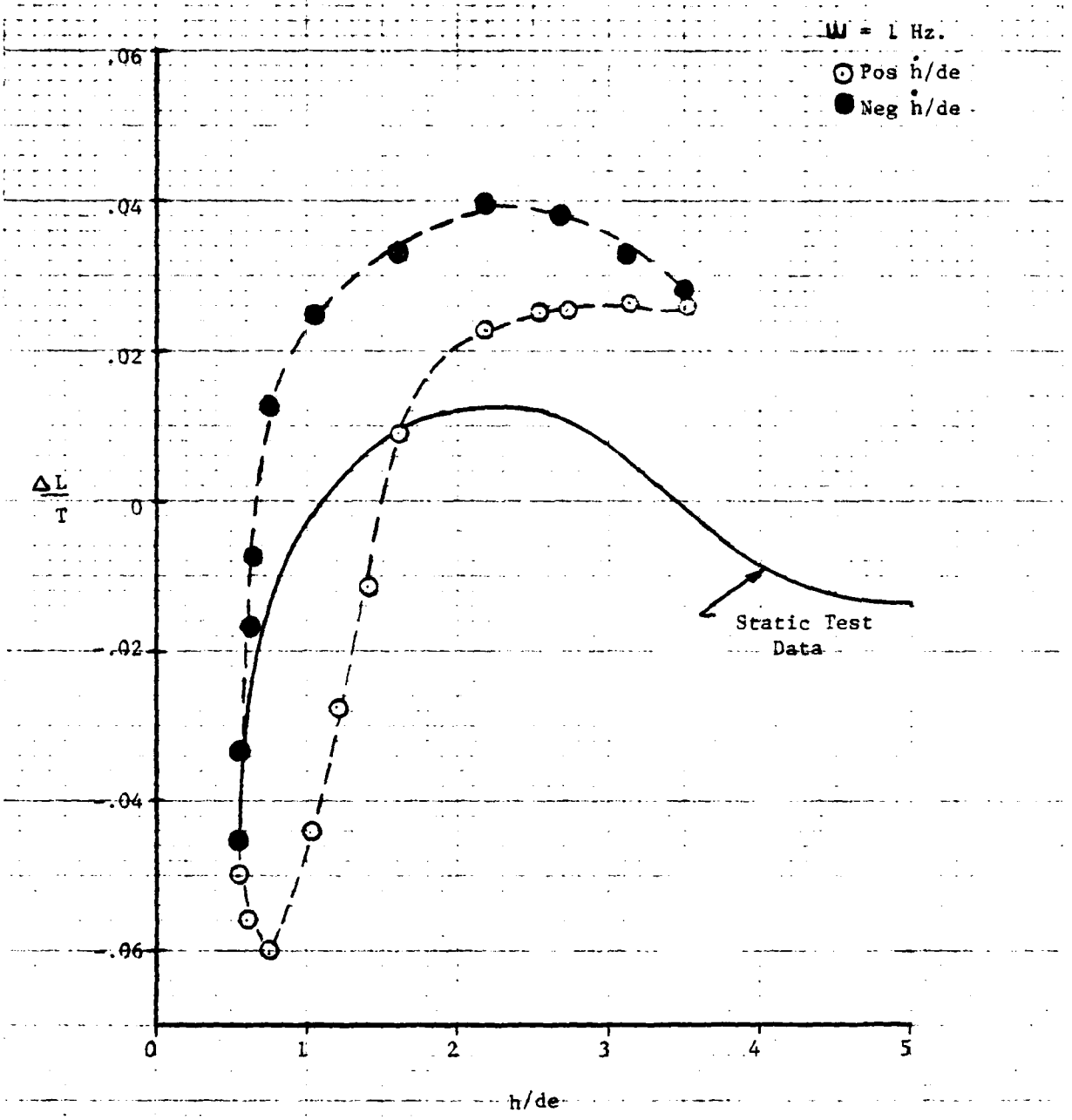

Figure 4. Static and Dynamic Induced Lift in Heave, ω = 1 Hz

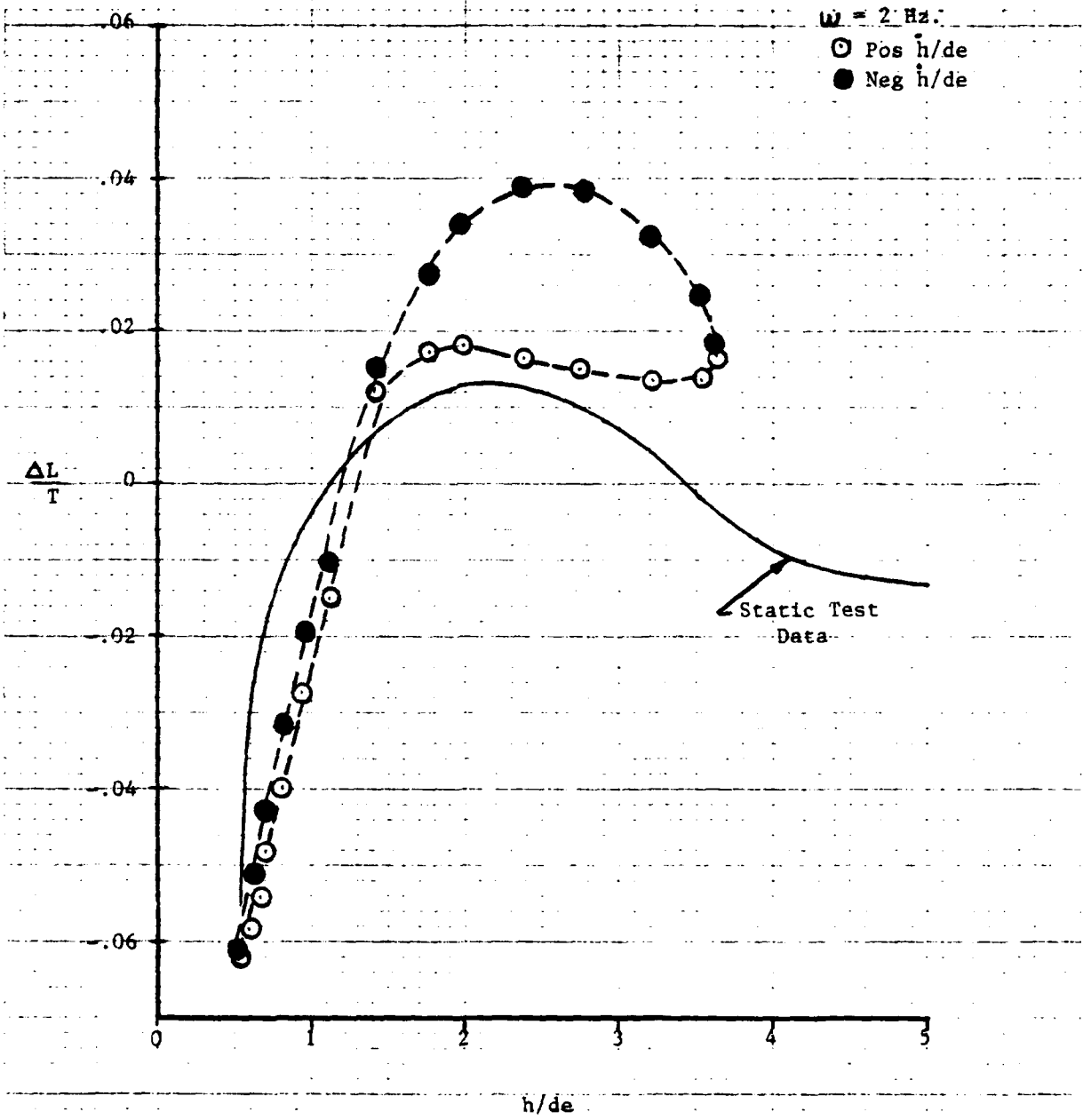

Figure 5. Static and Dynamic Induced Lift in Heave. ω = 2 Hz

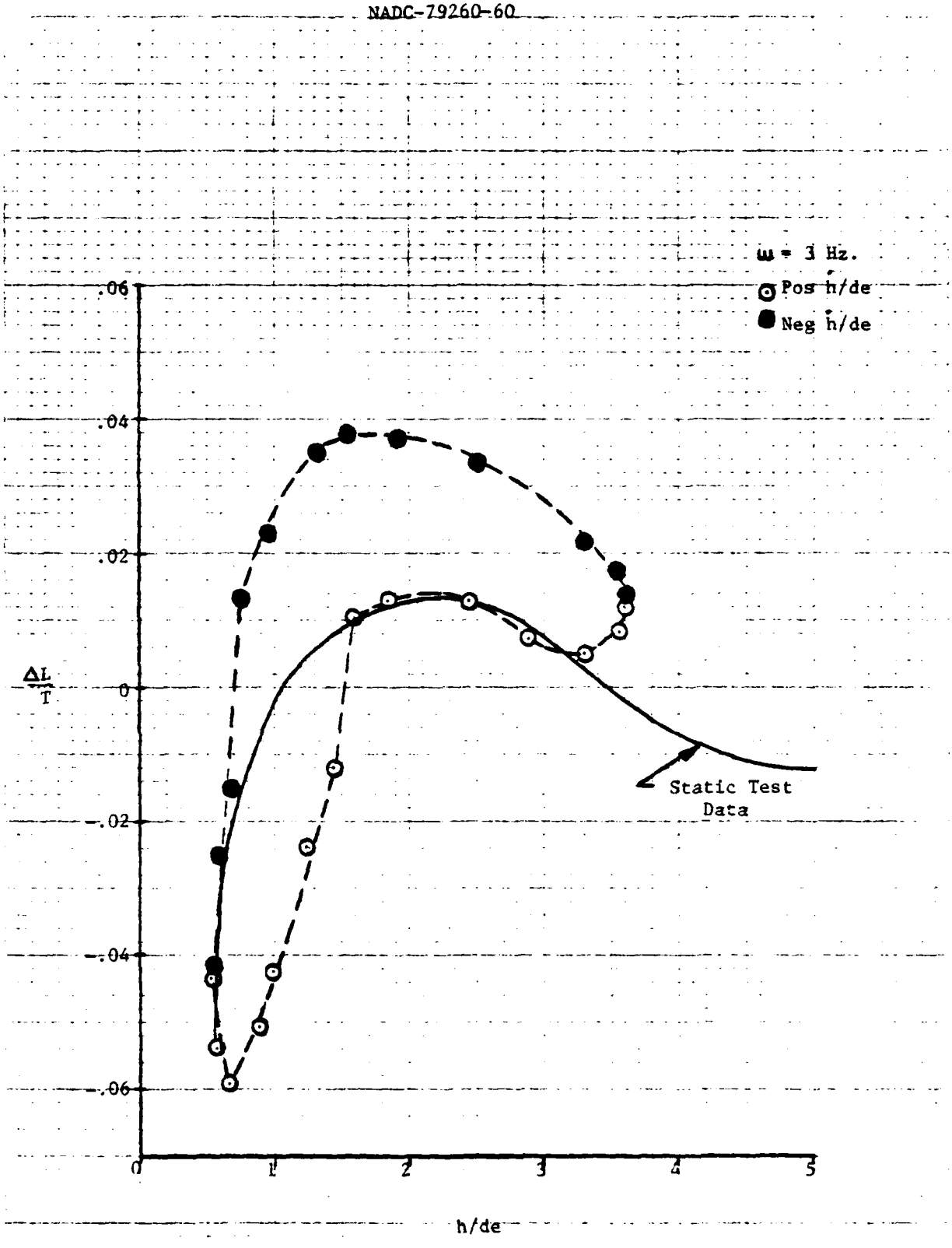

Figure 6. Static and Dynamic Induced Lift in Heave, ω = 3 Hz

In Figure 4, ω = 1Hz, the dynamic data differs from the static data for both positive and negative rates. This is also the case for ω = 2Hz and ω = 3Hz as shown in Figure 5 and 6 respectively. In each case the dynamic data shows a hysteresis type of effect depending on the rate being positive or negative. For negative rates, the dynamic results show an increase in the static data over all values of h/de for ω = 1 and ω = 3Hz. As shown for ω = 2Hz for negative rates the dynamic results indicate a decrease in the static $\Delta L/T$ for h/de less than 1.1 and an increase for h/de greater than 1.1. In each case for positive rates the results indicate a decrease in the static $\Delta L/T$ up to a value of h/de between 1.25 and 1.50. After this, an increase is seen up to an h/de of 3.5 which was the maximum value tested. This increase gets smaller as the frequency increases from ω = 1 to 3 Hz with values close to static value at ω = 3Hz. The hysteresis effect described is consistent with the findings of reference (a) and is attributed to the compression effect associated with the fountain. In the case of a positive rate, where the deck is heaving away from the model, a larger value of $\Delta L/T$ is evident as compared to a negative deck rate with the same magnitude. This indicates that positive rates amplify the suckdown while negative rates amplify the fountain force.

Data from Figures 4, 5, and 6 along with data for the amplitudes which are not plotted were used to develop a curve of induced lift versus height-over-deck for a zero value of deck rate. This curve is shown as Figure 7 along with the static test data. As seen in this figure, from an h/de of 0.5 to 1.0 the curve indicates a decrease in $\Delta L/T$ as compared to the static data. Above h/de = 1.0, the curve shows an increase in $\Delta L/T$ for all values up to the maximum of h/de = 3.5.

This curve of zero deck rate was used to estimate the induced lift as a function of h/de. By comparing these estimates with actual time history data the dynamic effects could be examined. These time histories are shown in Figures 8a through 8h with the neutral point, amplitude, and frequency indicated. Also shown are the estimated values from Figure 7 as indicated by the dotted lines. Figures 8a through 8d (ω = 2Hz) are presented first since a more complete data base was available for this frequency. Very good agreement is seen for an h_o/d_e = 0.8 over the time segment shown with peak values matching very well and no apparent time shift.

For h_o/d_e = 2.0, Figures 8b through 8d, the predicted values are within 1.2% of the actual data. As the amplitude, $\Delta h/de$, is increased the response shows a larger suckdown effect. For $\Delta h/de$ = 1.0 the smallest value of $\Delta L/T$ is 1.0% while at $\Delta h/de$ = 3.0 a value of -6.0% is obtained. Also, the response becomes smoother and more sinusoidal as $\Delta h/de$ is increased.

Figures 8e and 8f show time histories for ω = 1Hz and 3Hz at an h_o/d_e = 0.8 and $\Delta h/de$ = 0.6 respectively. In Figure 8e a good correlation is shown which is within 1.0% of the actual values for the time segment presented. It should be noted that these time histories are representative responses form the original 5 second data runs of reference (a). For

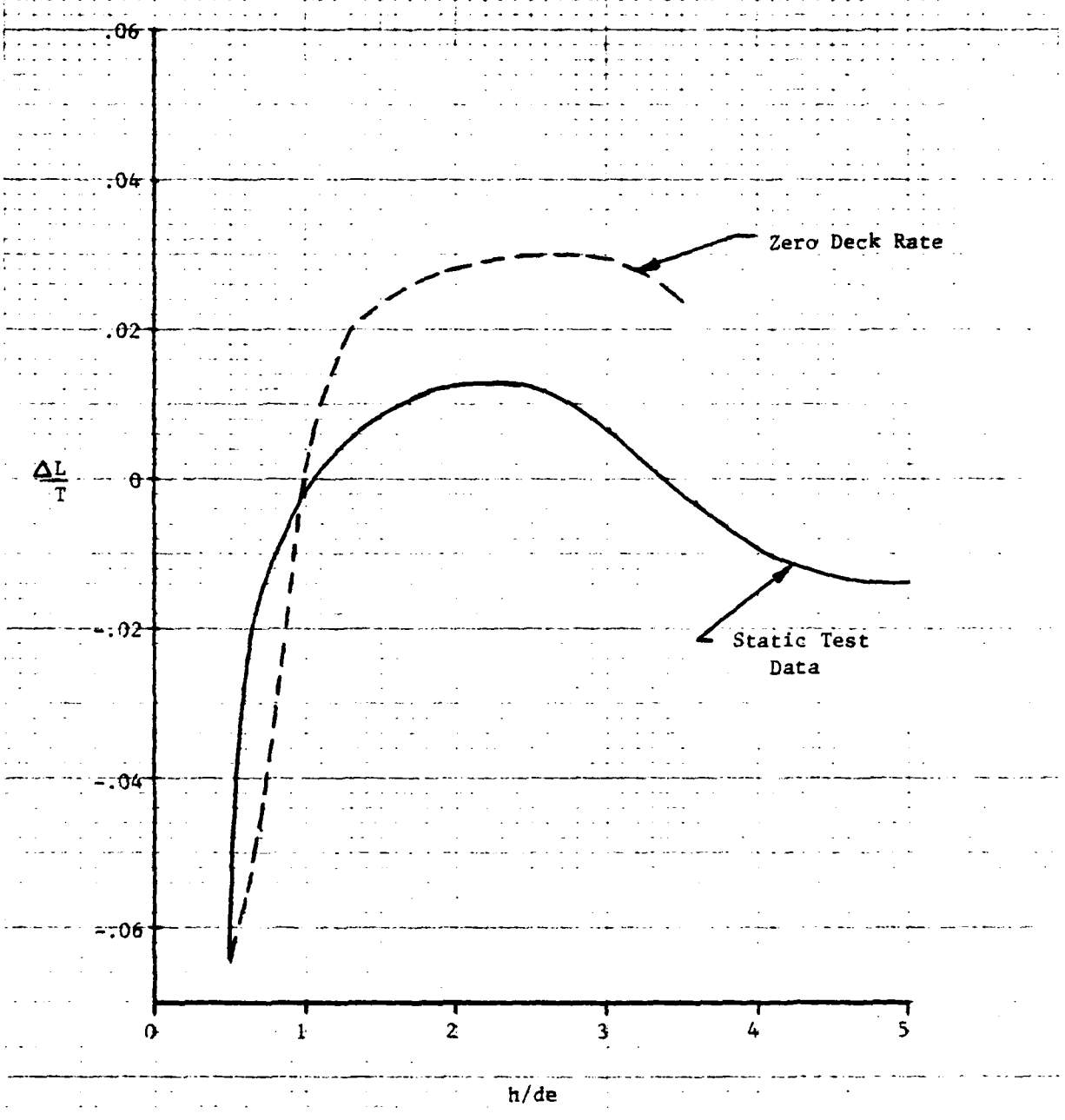

Figure 7. Induced Lift vs. Height Over Deck for Zero Deck Rate

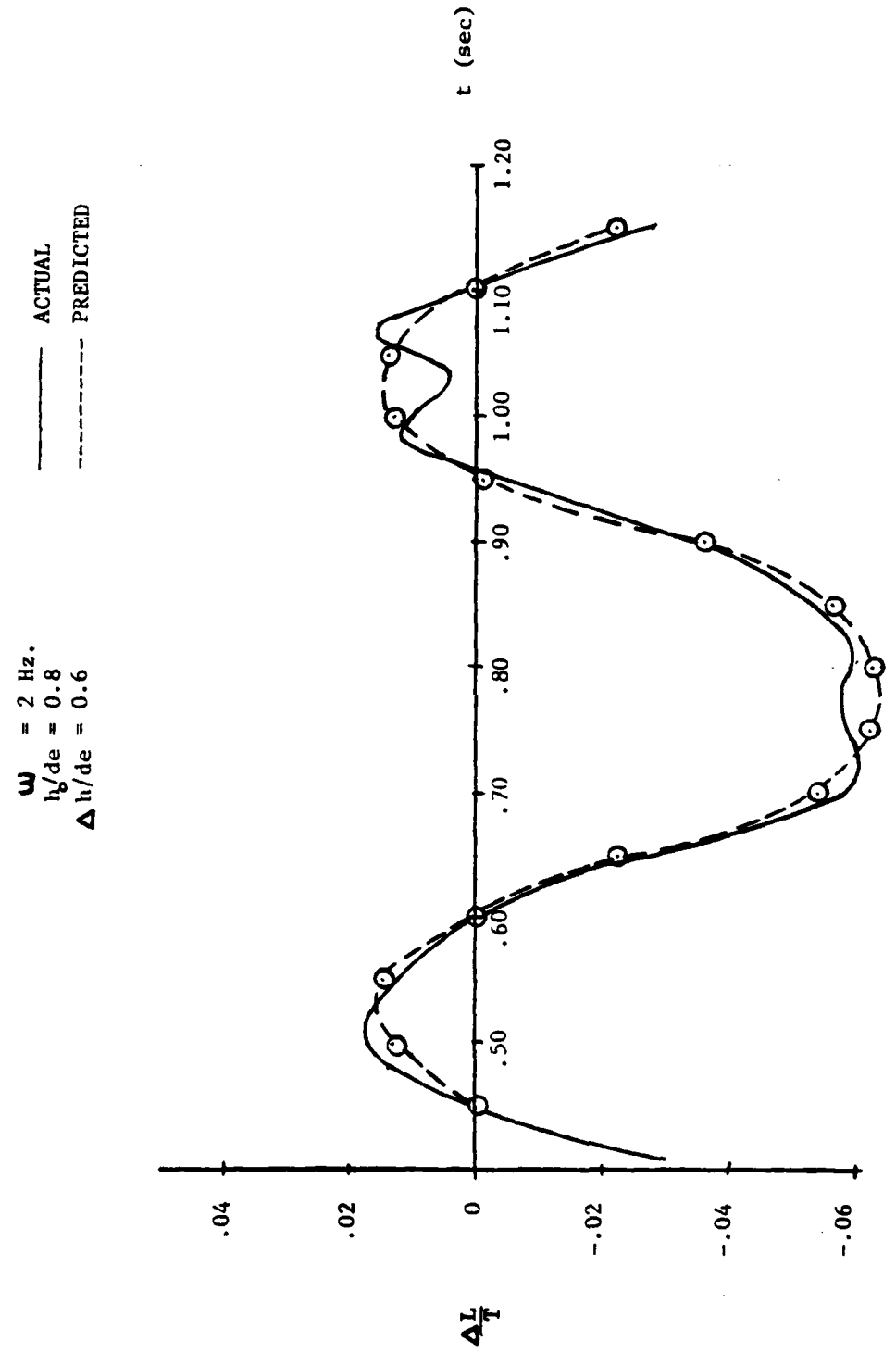

Figure 8a. Induced Lift Time History Comparison (Run 89.2)

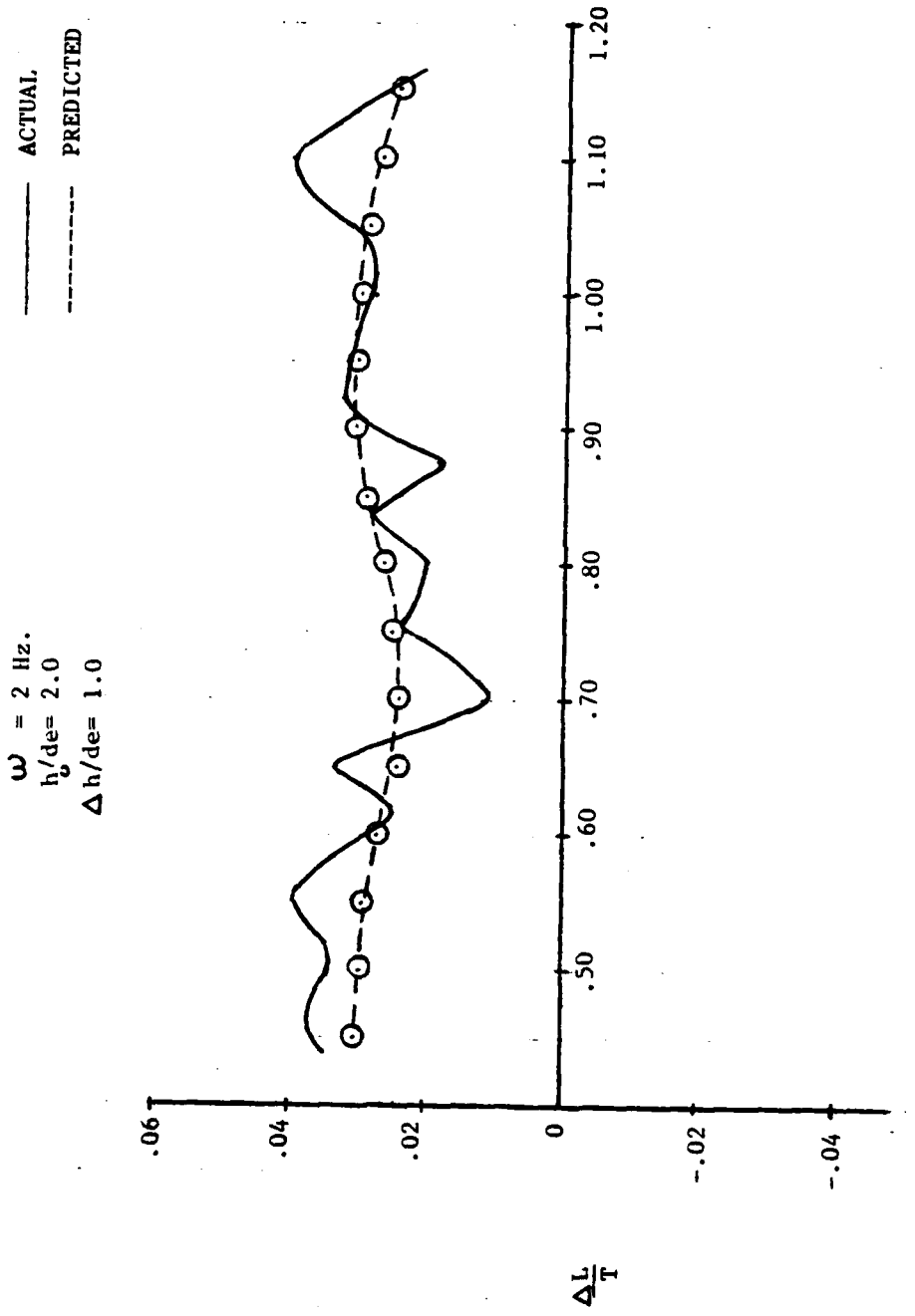

Figure 8b. Induced Lift Time History Comparison (Run 90.5)

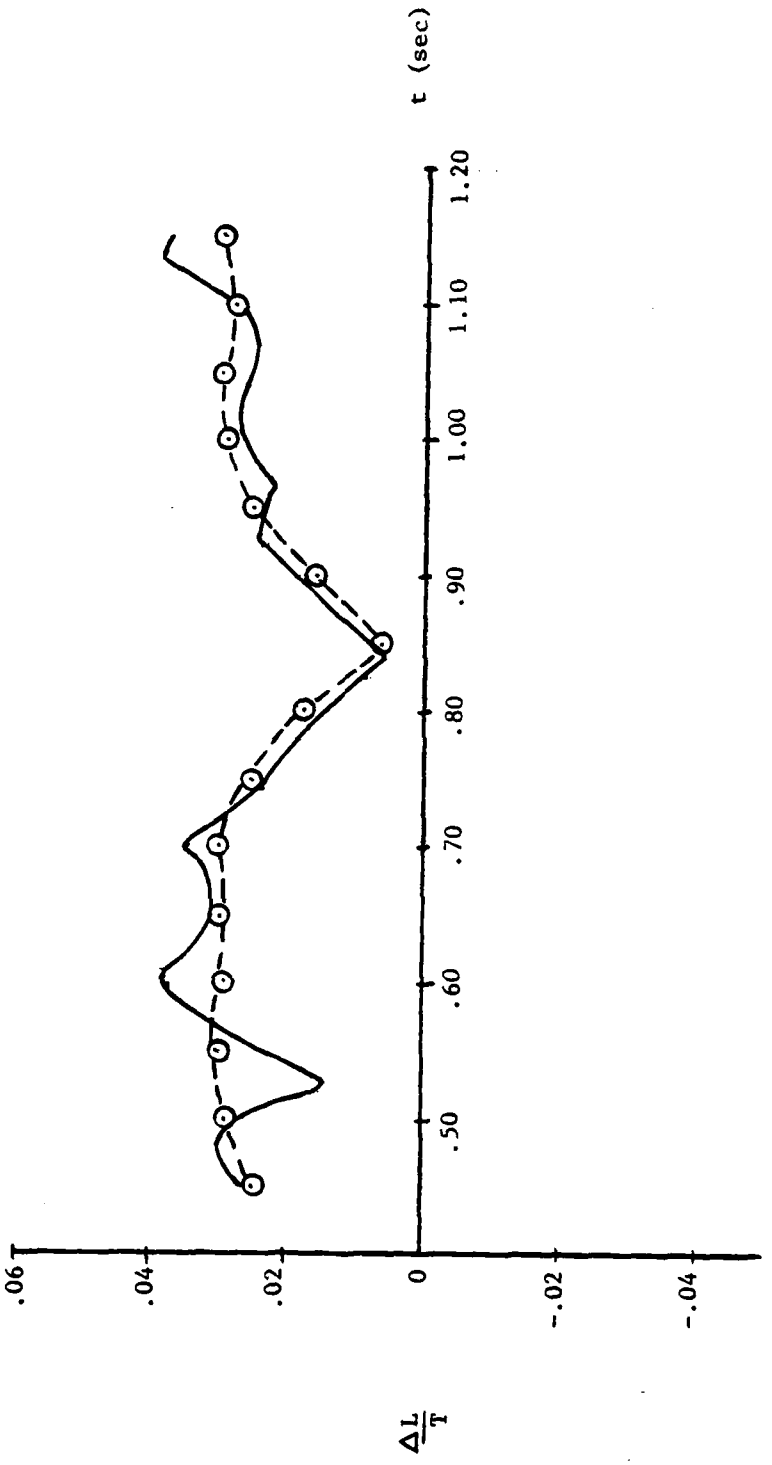

Figure 8c. Induced Lift Time History Comparison (Run 90.4)

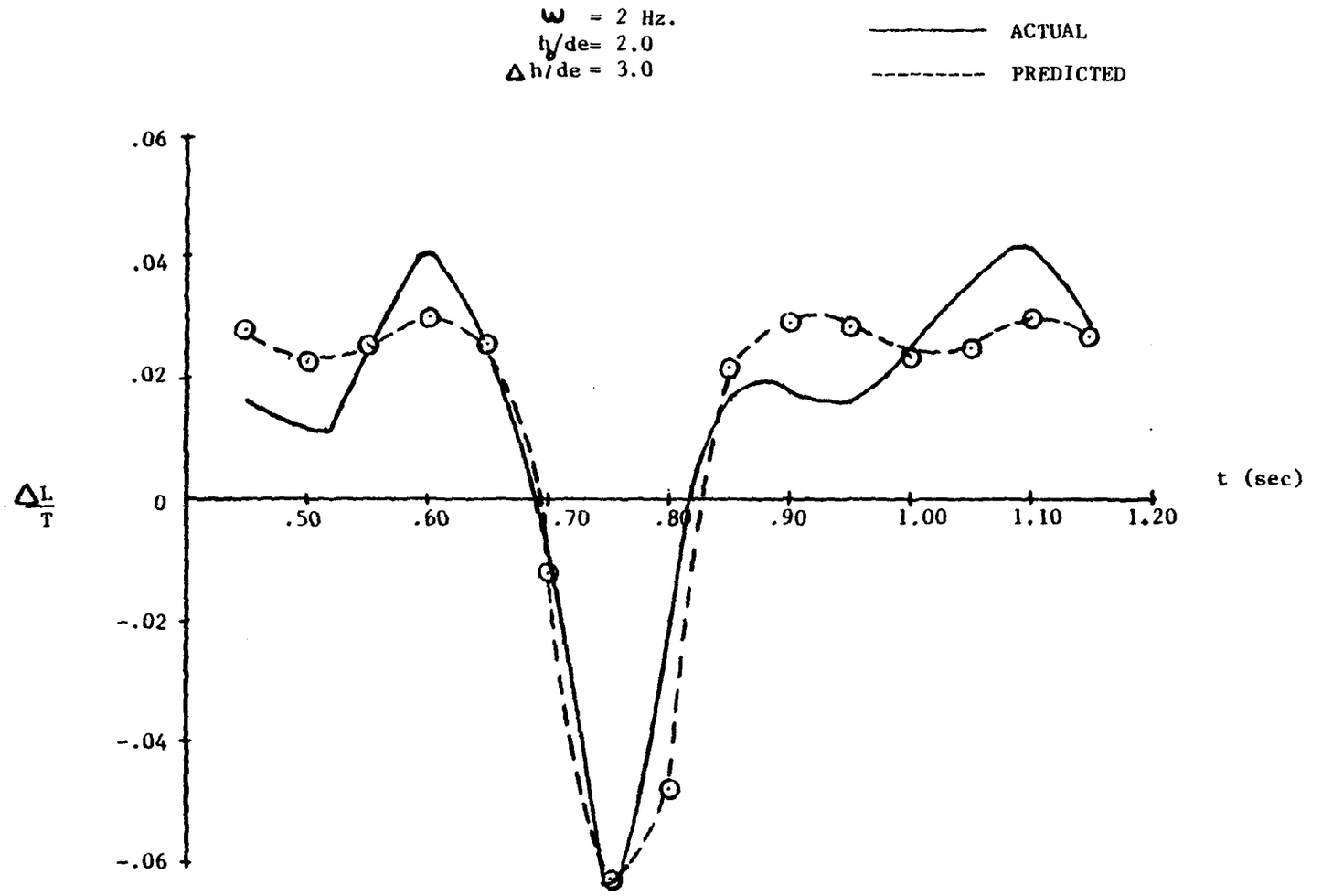

Figure 8d. Induced Lift Time History Comparison (Run 90.2)

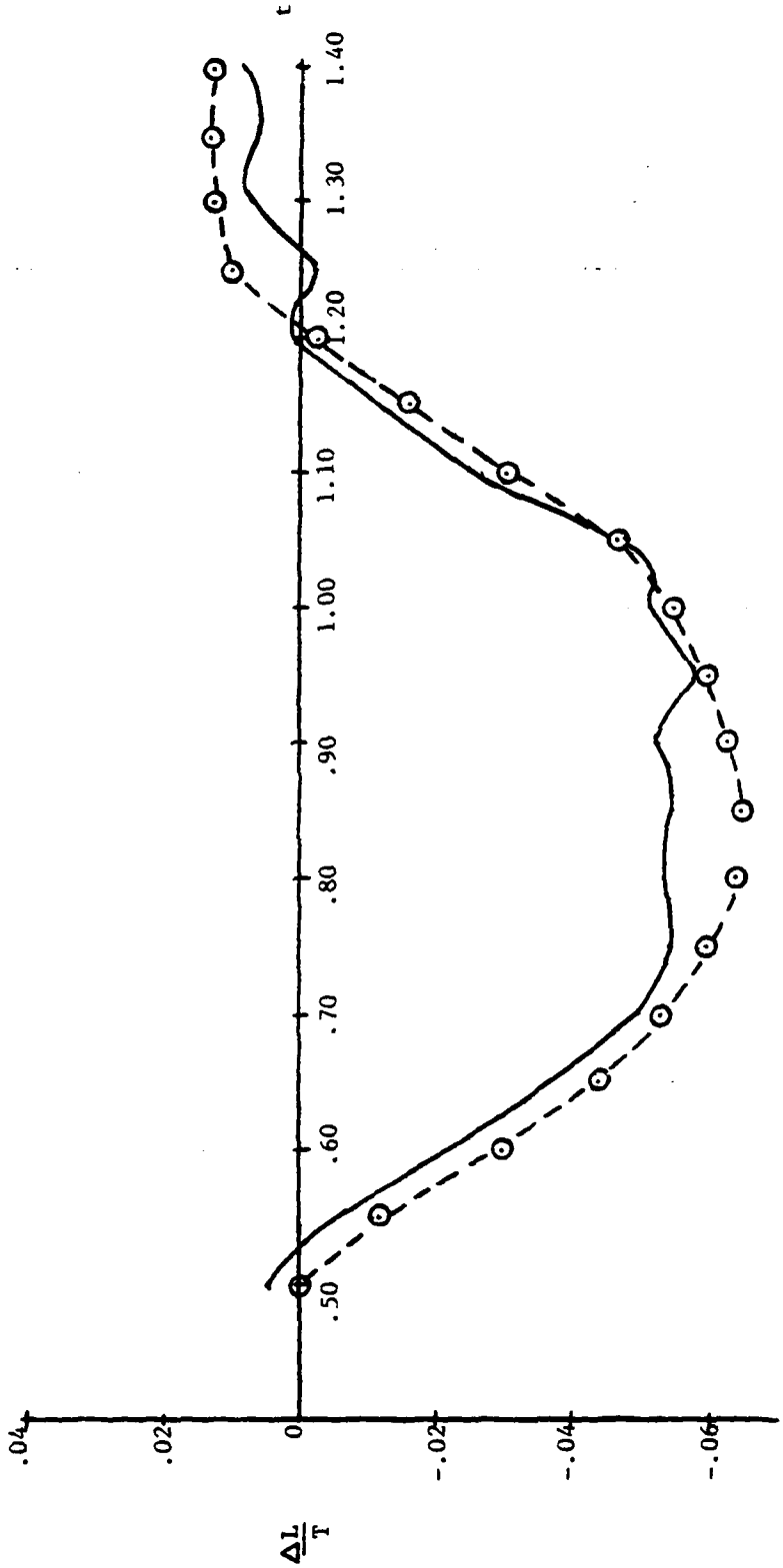

Figure 8e. Induced Lift Time History Comparison (Run 89.1)

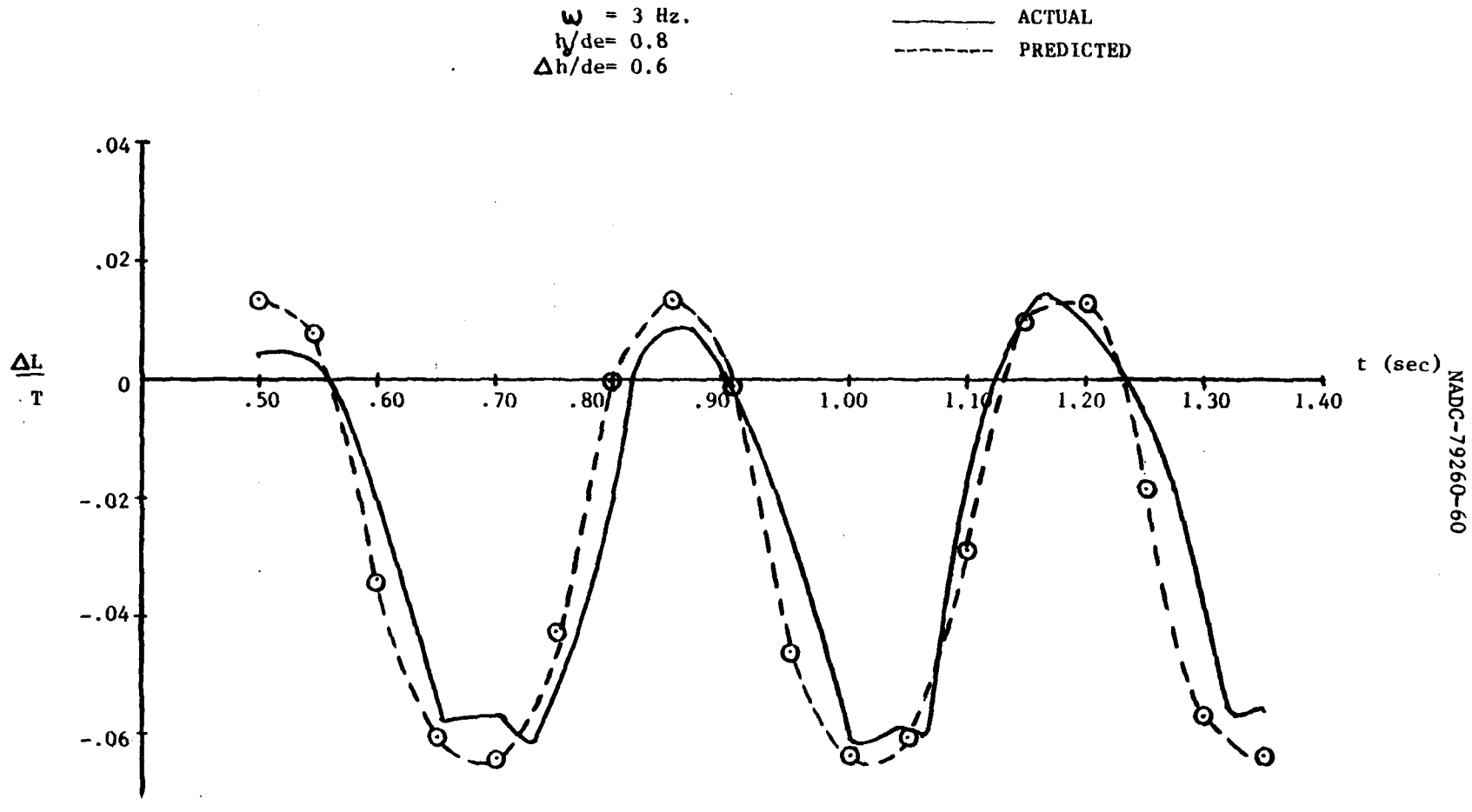

Figure 8f. Induced Lift Time History Comparison (Run 89.3)

ω = 3Hz, figure 8f, good agreement is seen with the actual data where peak values are within 1.0%. For increasing values of $\Delta L/T$ and time the predicted values are within 1.0% while a maximum difference of 2.0% is seen for decreasing values of $\Delta L/T$ and increasing time.

As indicated by figures 8e and 8f for ω = 1 and 3Hz respectively and figure 8a for ω = 2Hz, frequency does not appear to effect induced lift at a neutral point of ho/de = 0.8. In each case the maximum positive value of $\Delta L/T$ is approximately 1.4% while maximum negative values are about -6.0% $\Delta L/T$.

A slight phase shift is evident for frequencies of ω = 1 and 3Hz although peak values show fair correlation as indicated in figures 8g and 8h. These data correspond to a neutral point of ho/de = 2.0 and an amplitude of $\Delta h/de$ = 3.0 as does the data of figure 8d for a frequency of ω = 2Hz. However, no phase shift is evident for this frequency (ω = 2Hz) or any of the other data runs except the two previously mentioned cases (figures 8g and 8h). This indicates that the phaseshift probably resulted from the inability to precisely define the initial time used for plotting these data runs.

Several observations can be summarized with regard to the heaving motion results described above. First, a hysteresis effect is evident dependent upon the direction of the motion. For a positive deck rate, a larger value of $\Delta L/T$ is evident as compared to a negative rate with the same magnitude. Second, developing a curve of induced lift versus height-above-deck for a zero deck rate to estimate the dynamic response correlates reasonably well. Third, increasing the amplitude from 1.0 to 3.0 showed an increase in suckdown of nearly 7.0% indicating that amplitude can have a large effect. Fourth, frequency showed only a small increase in suckdown for a given amplitude and neutral point. Fifth, a slight phase shift was evident for frequencies of ω = 1 and 3Hz at a neutral point of ho/de = 2.0 and is attributed to the difficulty in precisely identifying an initial time for plotting these data runs.

PITCH

For the pitching deck motion, the induced pitching moment is the parameter examined. Figures 9 through 12 show induced pitching moment ($\Delta M/T\bar{c}$) plotted versus pitch angle (θ) for ω = 2Hz at various heights and amplitudes. Positive and negative rates ($\dot{\theta}$) are shown on these figures by open and closed symbols respectively, along with the static test data indicated by the solid line. The effect of frequency could not be determined from the available data since only ω = 2Hz was tested.

At an h/de = 0.8, figure 9 shows significantly larger negative values of pitching moment for the dynamic data where the magnitude is approximately twice the static value. For $\Delta\theta$ = 4° a small hysteresis effect is present while $\Delta\theta$ = 12° does not show this effect. The most pronounced hysteresis effect is shown for the case of $\Delta\theta$ = 20° where differences between positive and negative rates are as much as 2.0%. It is interesting to note that for negative pitch angles the positive rates

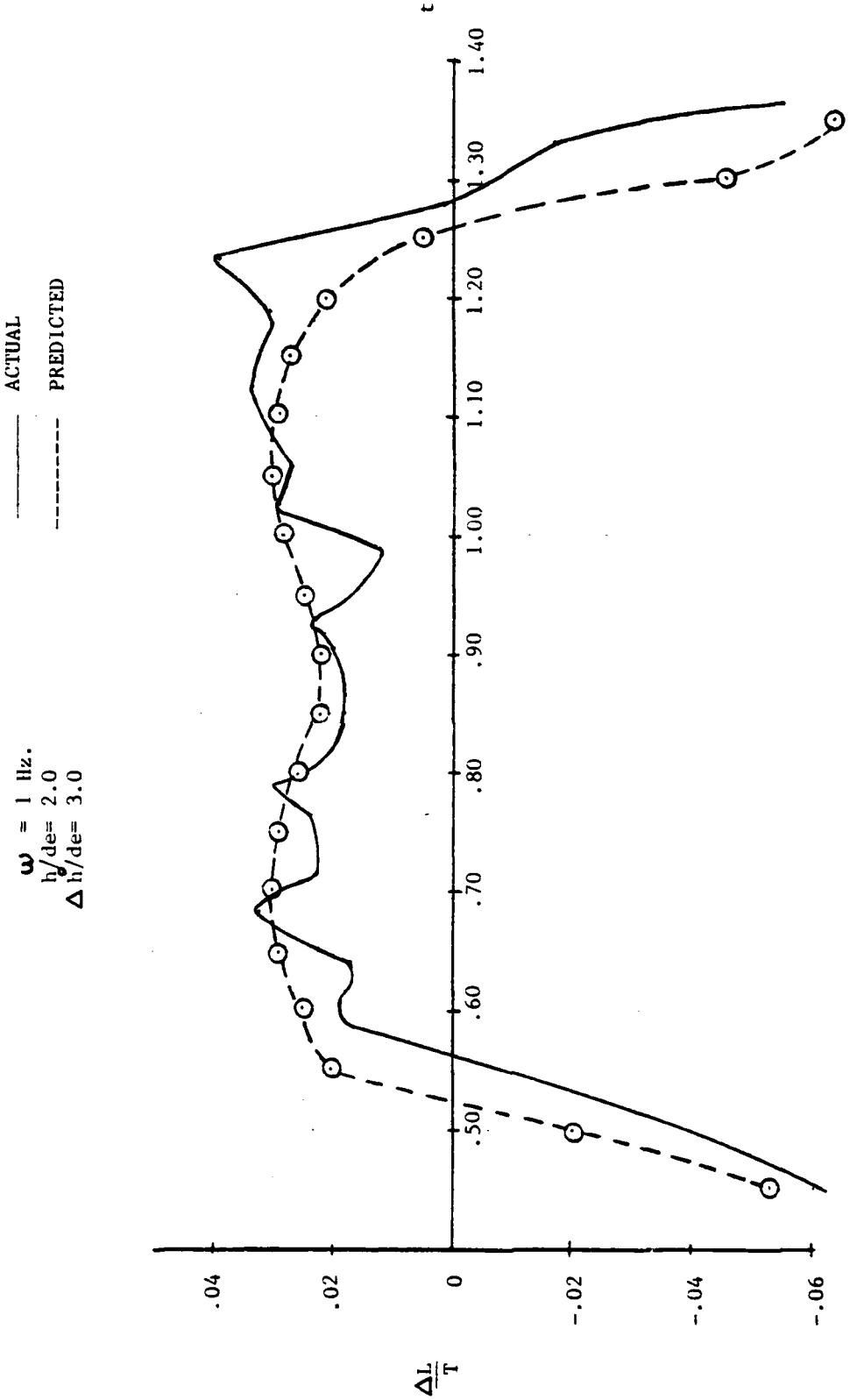

Figure 8g. Induced Lift Time History Comparison (Run 90.1)

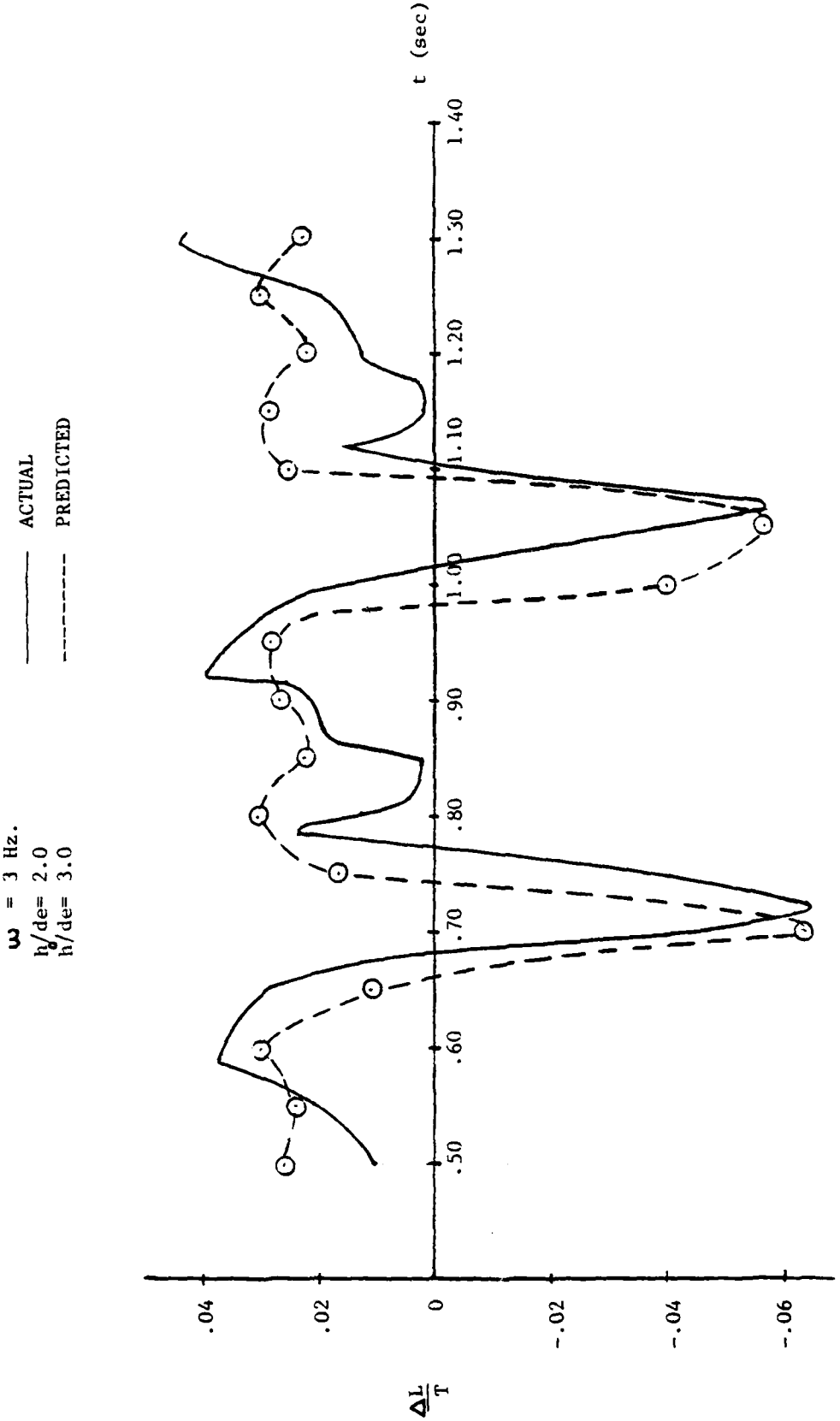

Figure 8h. Induced Lift Time History Comparison (Run 90.3)

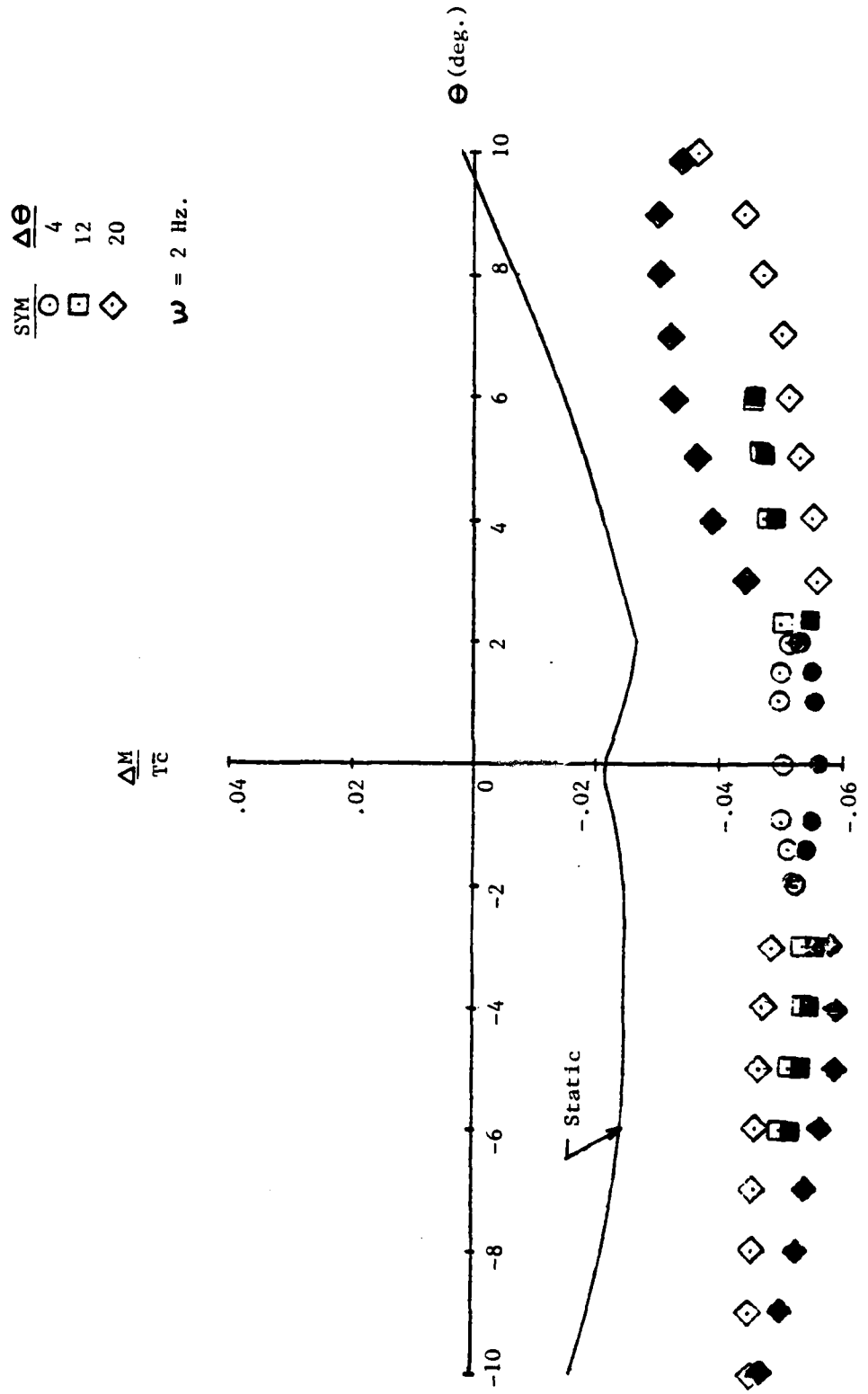

Figure 9. Static and Dynamic Induced Pitching Moment, h/de = 0.8

show a more positive value while the reverse is true for positive pitch angles. Increasing amplitude does not show a significant effect on the pitching moment for this h/de as the data falls within a small band for the three amplitudes shown.

Figure 10 shows the induced pitching moment at h/de = 2.0 for the three amplitudes of 4°, 12°, and 20°. As expected, the hysteresis effect is very pronounced since the fountain is the strongest at this height. At $\Delta\theta = 4°$ positive rates show more positive values over all pitch angles than do the negative rates. The reverse is true for amplitudes of 12° and 20° with differences as much as 4.0 $\Delta M/T\bar{c}$ evident. For this height the static data shows a significant increase over the values at h/de = 0.8 where all values shown are negative. The dynamic data also shows an increase on the order of 3.0% as the height is increased from 0.8 to 2.0 as indicated in figures 9 and 10. It should also be pointed out that for an h/de = 2.0 the static values become positive over almost the entire range of pitch angles shown.

As indicated in figure 11, increasing h/de to 5.0 produces significant changes in pitching moment. The static data is positive for both positive and negative pitch angles while the dynamic data shows an unexpected increase at $\Delta\theta = 20°$. This is also the case for an h/de = 8.0 as indicated in figure 12. At heights of 5.0 and 8.0 the induced pitching moment should be very small in magnitude and close to the static values since the model is essentially out of ground effect. For $\Delta\theta = 4°$ and 12° these data show an almost constant value of -0.025 for induced pitching moment. This fact, along with the data for $\Delta\theta = 20°$ being so close to the static value at both h/de = 5.0 and 8.0 indicates a zero shift in the data. This shift may also apply to figures 9 and 10 where large differences are seen between the static and dynamic responses. In order to develop a curve for a zero value of pitch rate to estimate the dynamic response it is necessary to account for this zero shift. To accomplish this the response for $\Delta\theta = 20°$ at both h/de = 5.0 and h/de = 8.0 was assumed to fall at a constant level of -0.025 to be consistent with the data for $\Delta\theta = 4°$ and $\Delta\theta = 12°$. Also, the effect of height must be included since significant differences in pitching moment are seen at various values of h/de. Figure 13 presents the curves developed for the four values of h/de which were tested. The height effect was accounted for in this way to show that at lower values of h/de this effect is much stronger than at the higher values.

Figure 13 was used to predict the induced pitching moment as a function of pitch angle and height. These predictions were compared with actual time history data and are shown in figures 14a through 14l with predicted values indicated by the dotted line.

Figures 14a through 14c present induced pitching moment versus time for h/de = 0.8 and amplitudes of 4, 12, and 20° respectively. Good correlation is seen between the actual and predicted values for each amplitude with differences of less than 1.0% $\Delta M/T\bar{c}$. As the amplitude is increased the magnitude of the dynamic response shows larger fluctuations of induced pitching moment.

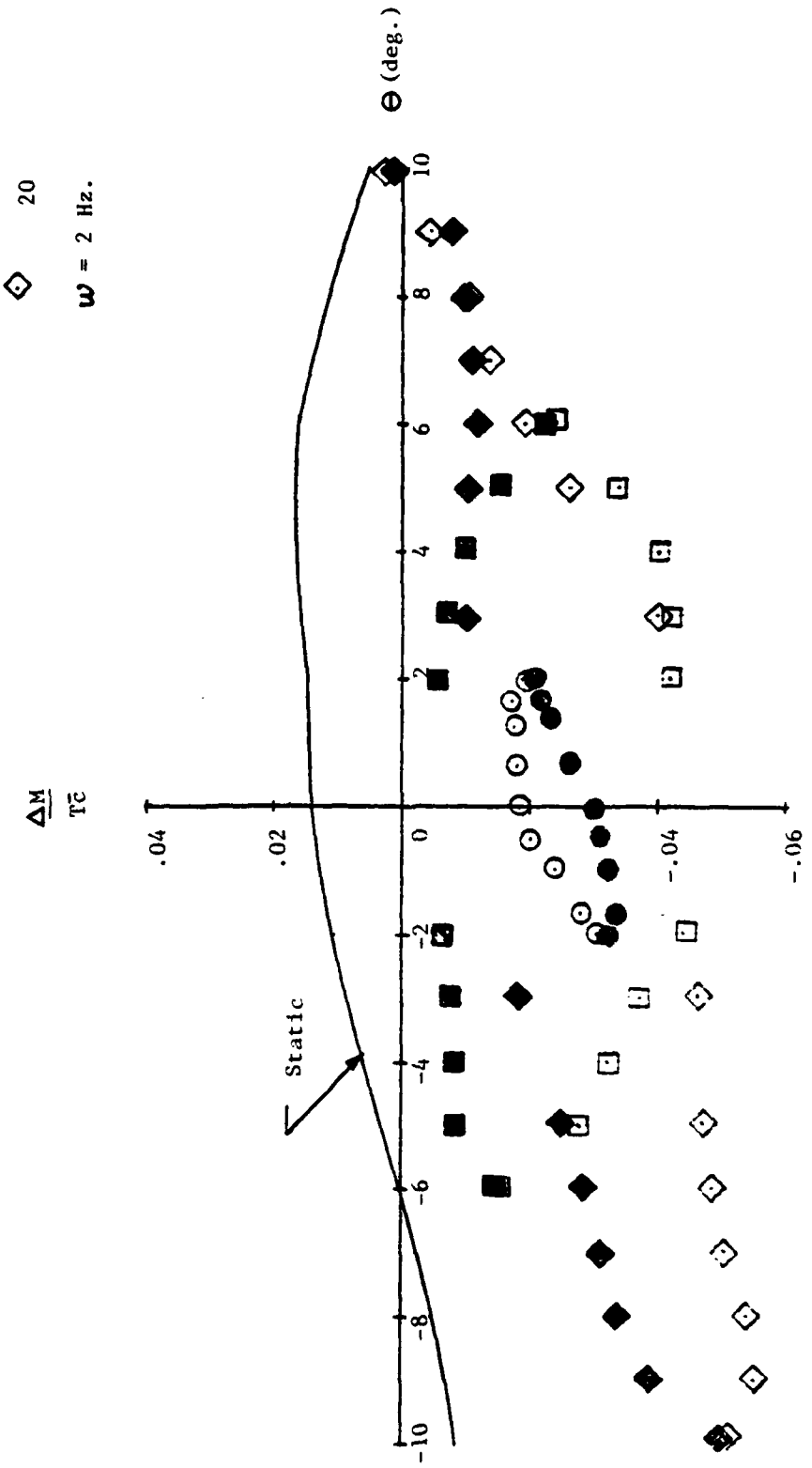

Figure 10. Static and Dynamic Induced Pitching Moment, h/de = 2.0

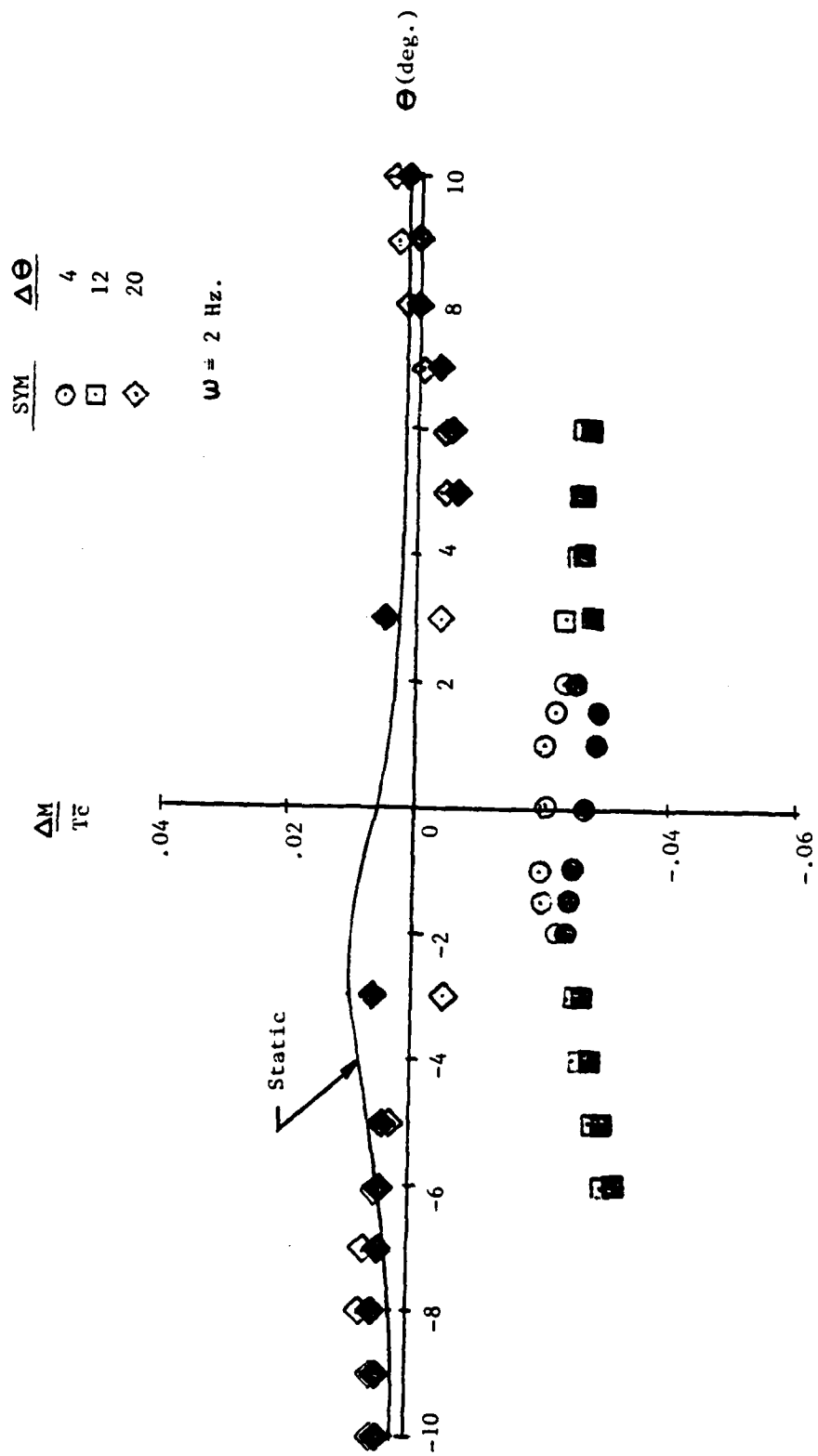

Figure 11. Static and Dynamic Induced Pitching Moment, h/de = 5.0

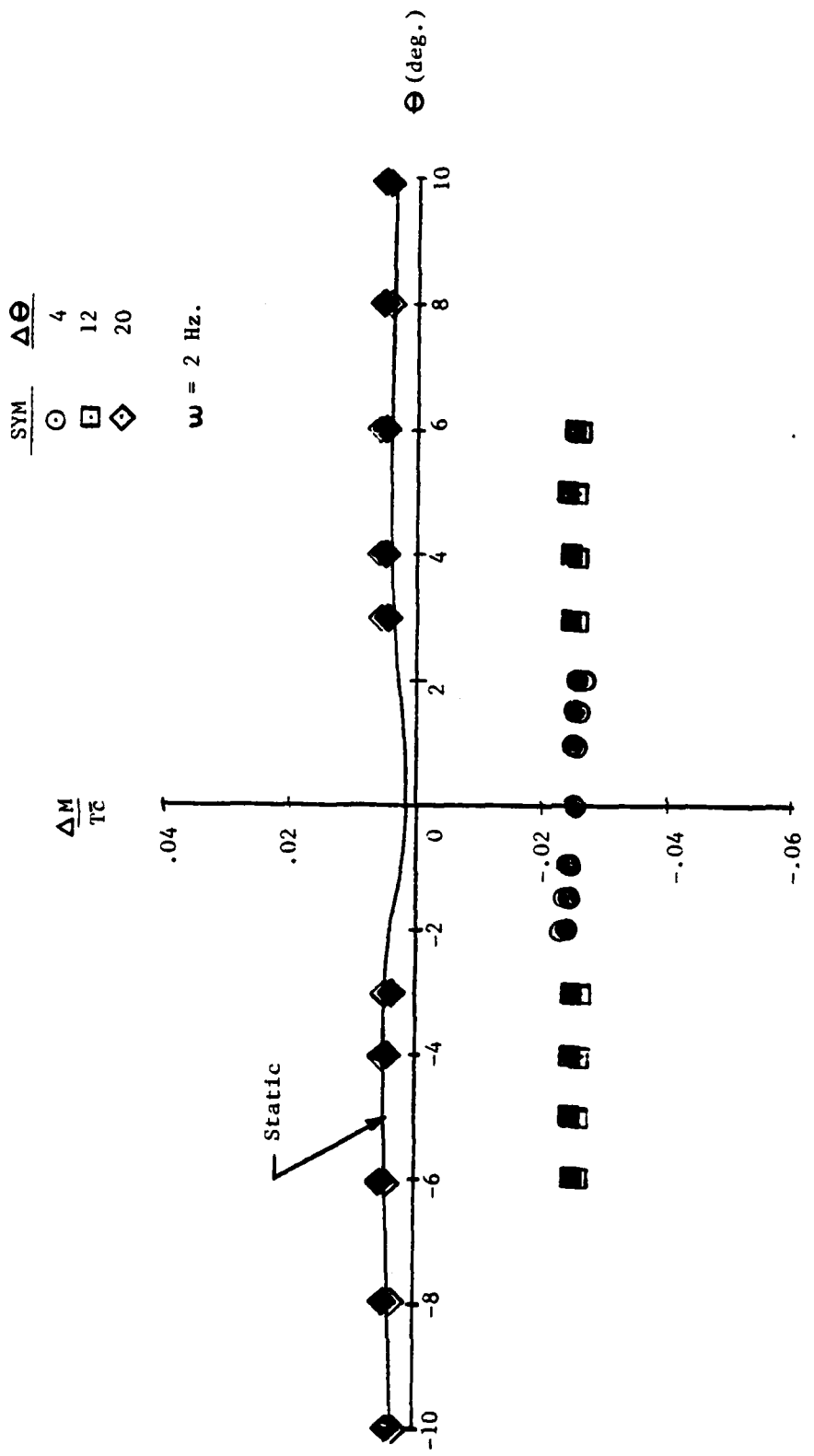

Figure 12. Static and Dynamic Induced Pitching Moment, h/de = 8.C

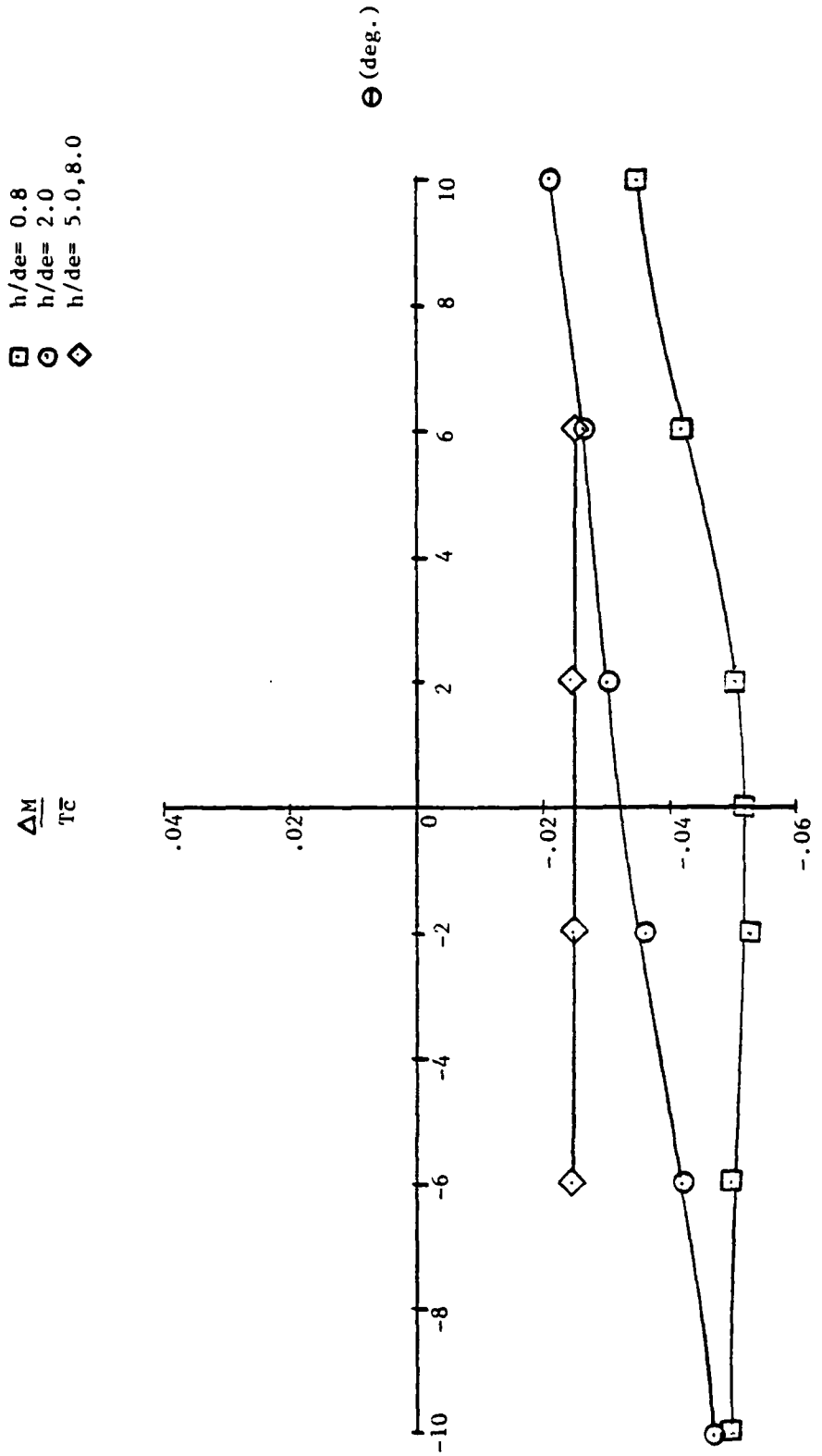

Figure 13. Induced Pitching Moment vs. Pitch Angle for Zero Deck Rate

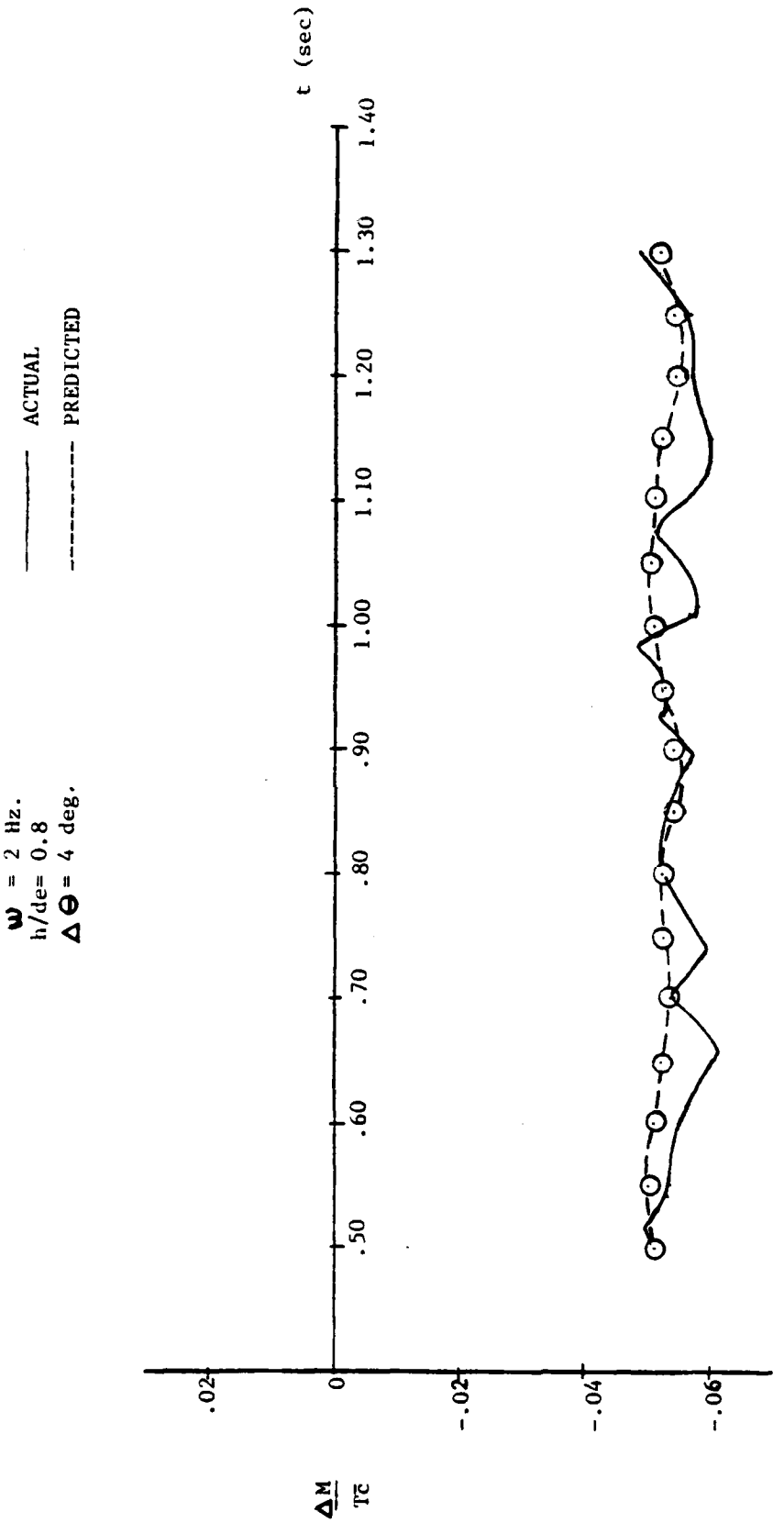

Figure 14a. Induced Pitching Moment Time History Comparison (Run 82.1)

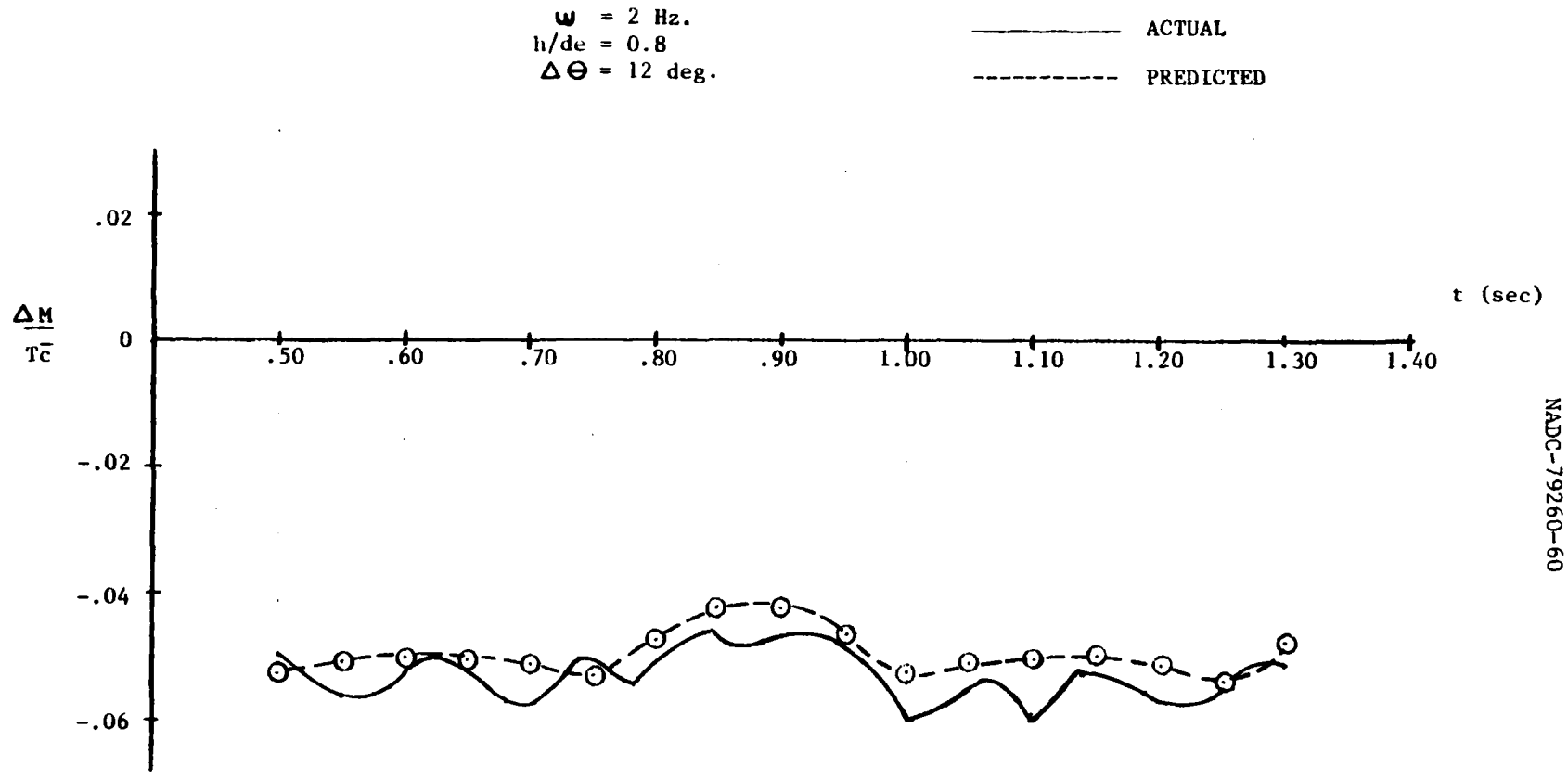

Figure 14b. Induced Pitching Moment Time History Comparison (Run 82.2)

NADC-79260-60

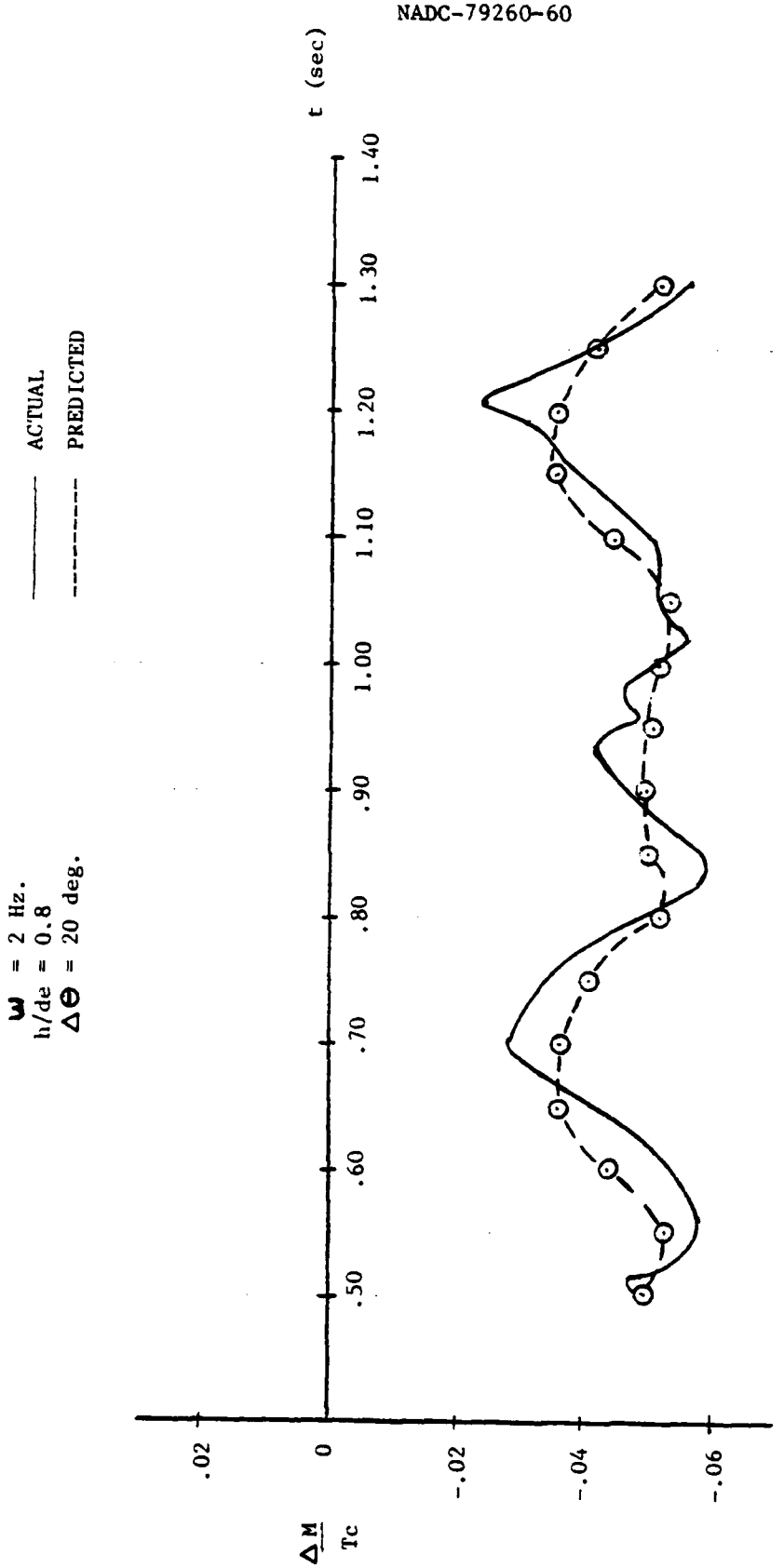

Figure 14c. Induced Pitching Moment Time History Comparison (Run 82.3)

For h/de = 2.0, figures 14d through 14f show induced pitching moment versus time for the three amplitudes tested. A fair correlation is shown between the predicted and actual responses at each amplitude. At $\Delta\theta$ = 4° differences of up to 1.5% are evident while at $\Delta\theta$ = 20° an error of 2.5% can be seen. These figures also show that increasing amplitude has the same effect on induced pitching moment at this h/de as it did at h/de = 0.8, where larger fluctuations in the magnitude of the dynamic response are seen for increasing amplitudes.

Induced pitching moment versus time for an h/de = 5.0 is shown in figures 14g through 14i. The dynamic response at this height should be nearly zero since the model is essentially out of ground effect. Figures 14g and 14h show good agreement between predicted and actual values although the magnitudes are on the order of $-0.025\ \Delta M/T\bar{c}$. These values are not zero due to the zero shift which has been previously discussed. Another result of this shift is seen in figure 14i where a poor correlation exists between the predicted and actual values even though the actual response is very small as expected.

In figures 14j through 14l, for an h/de = 8.0, characteristics similar to those just discussed for an h/de = 5.0 are present. A good correlation is seen for amplitudes of 4° and 12° although the magnitudes are again on the order of $-0.025\ \Delta M/T\bar{c}$. For $\Delta\theta$ = 20° (figure 14l) a poor correlation is seen even though the magnitude of the actual response is nearly zero as anticipated.

Several observations can now be summarized with regard to the pitching motion results described above. First, reasonably good correlation is seen between the actual data and the predicted values using a curve of $\Delta M/T\bar{c}$ versus pitch angle for a zero pitch rate. Second, a hysteresis effect is present in the data which is most pronounced at an h/de = 2.0 where the fountain is the strongest. Third, height shows a large effect on $\Delta M/T\bar{c}$ at the lower values of h/de, 0.8 and 2.0, while at heights greater than 5.0 little or no effect is seen. Fourth, frequency effects could not be determined from these data since ω = 2Hz was the only frequency tested. Fifth, increasing the amplitude for a given height produces larger fluctuations in the magnitude of the actual response. Sixth, a zero shift is apparent in the data for h/de = 5.0 and 8.0 which causes large differences between actual and predicted values at an amplitude of $\Delta\theta$ = 20°.

ROLL

For the rolling deck motion the parameter examined is the induced rolling moment, $\Delta\mathcal{L}/Tb$. Figures 15 and 16 show induced rolling moment versus roll angle for the various amplitudes, frequencies, and height-above-deck conditions which were tested. The open symbols indicate a positive roll rate ($\dot{\phi}$), while negative rates are shown as closed symbols. The static data for each figure is indicated by the solid line.

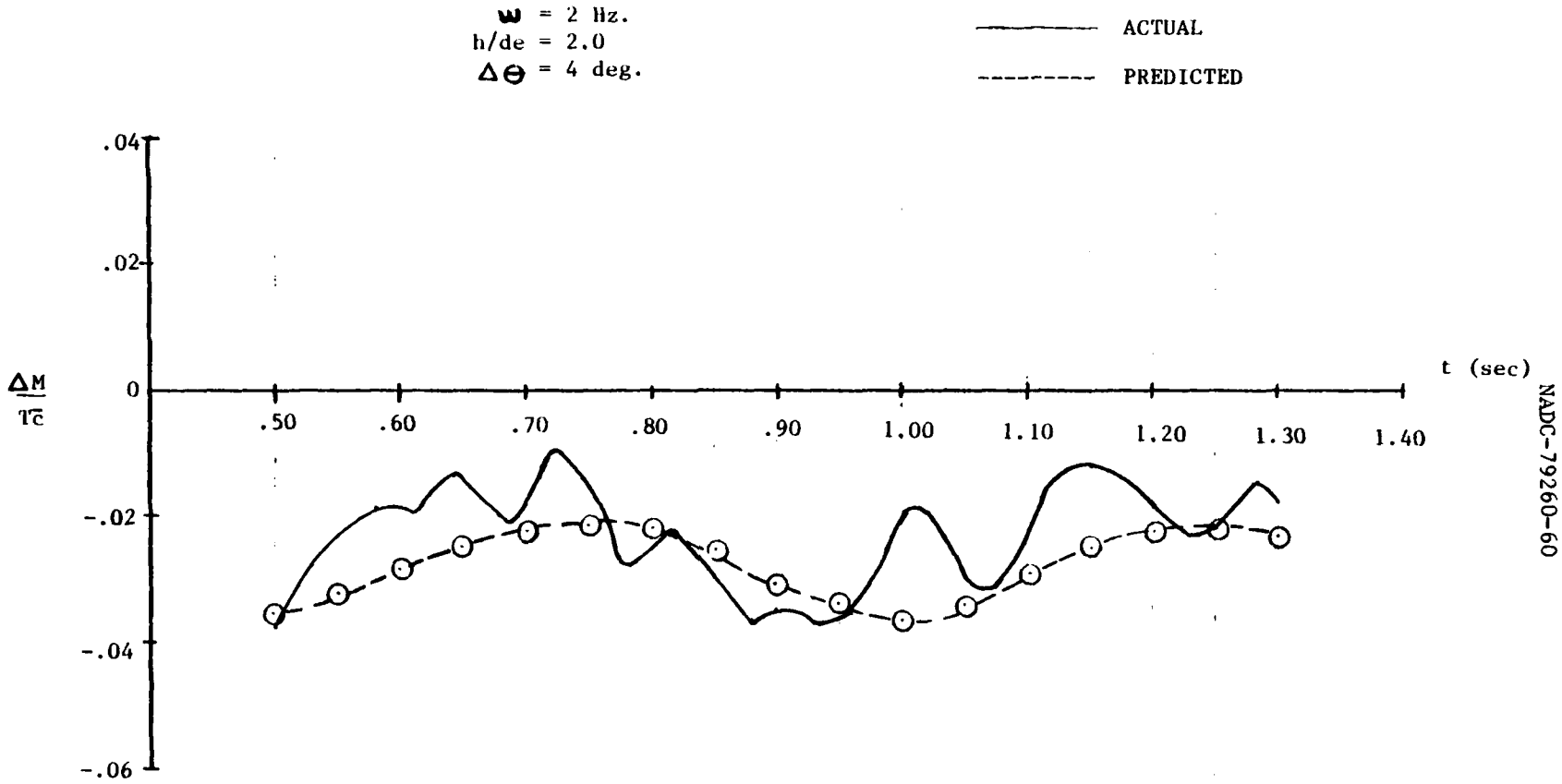

Figure 14d. Induced Pitching Moment Time History Comparison (Run 82.6)

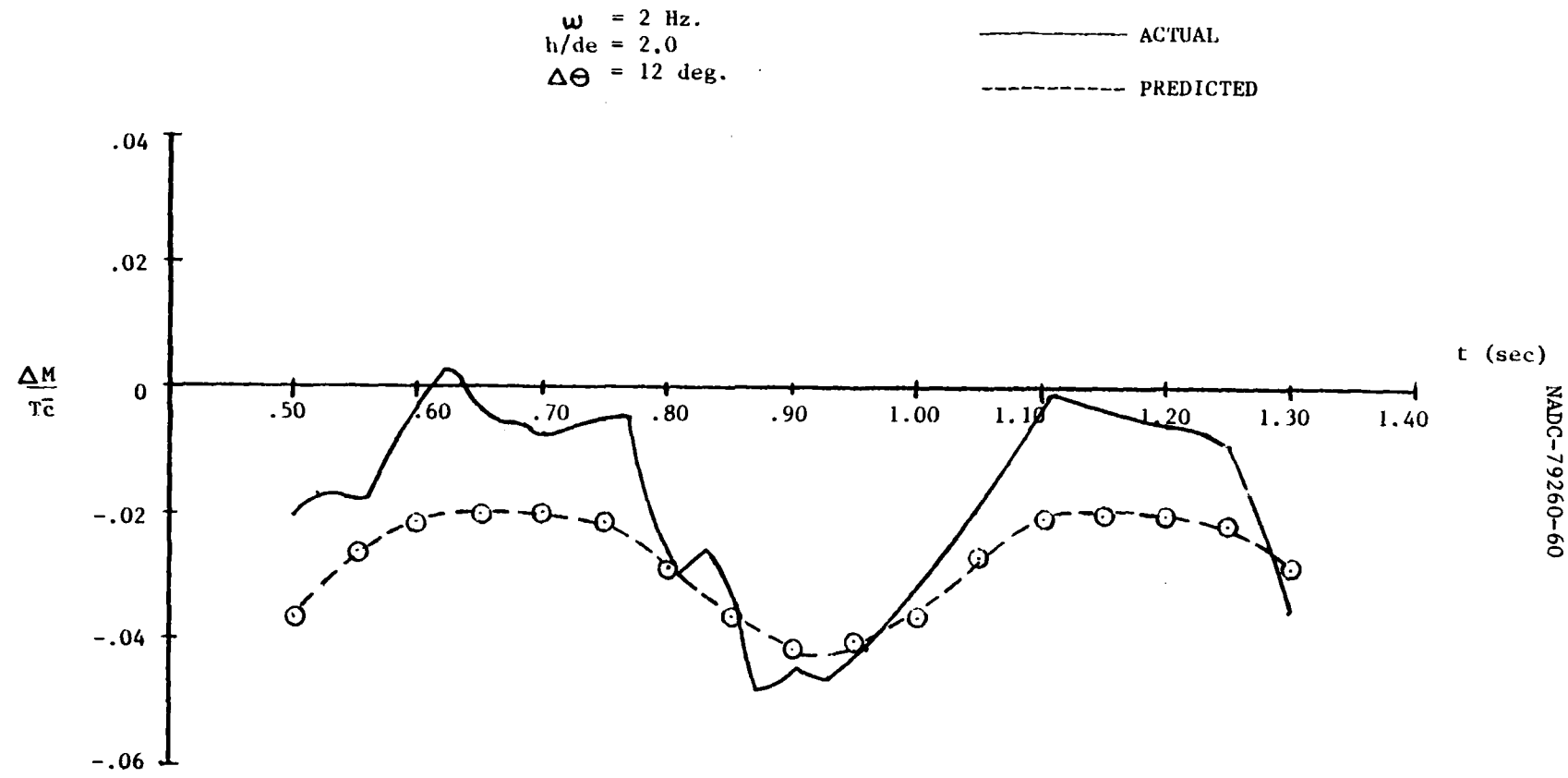

Figure 14e. Induced Pitching Moment Time History Comparison (Run 82.5)

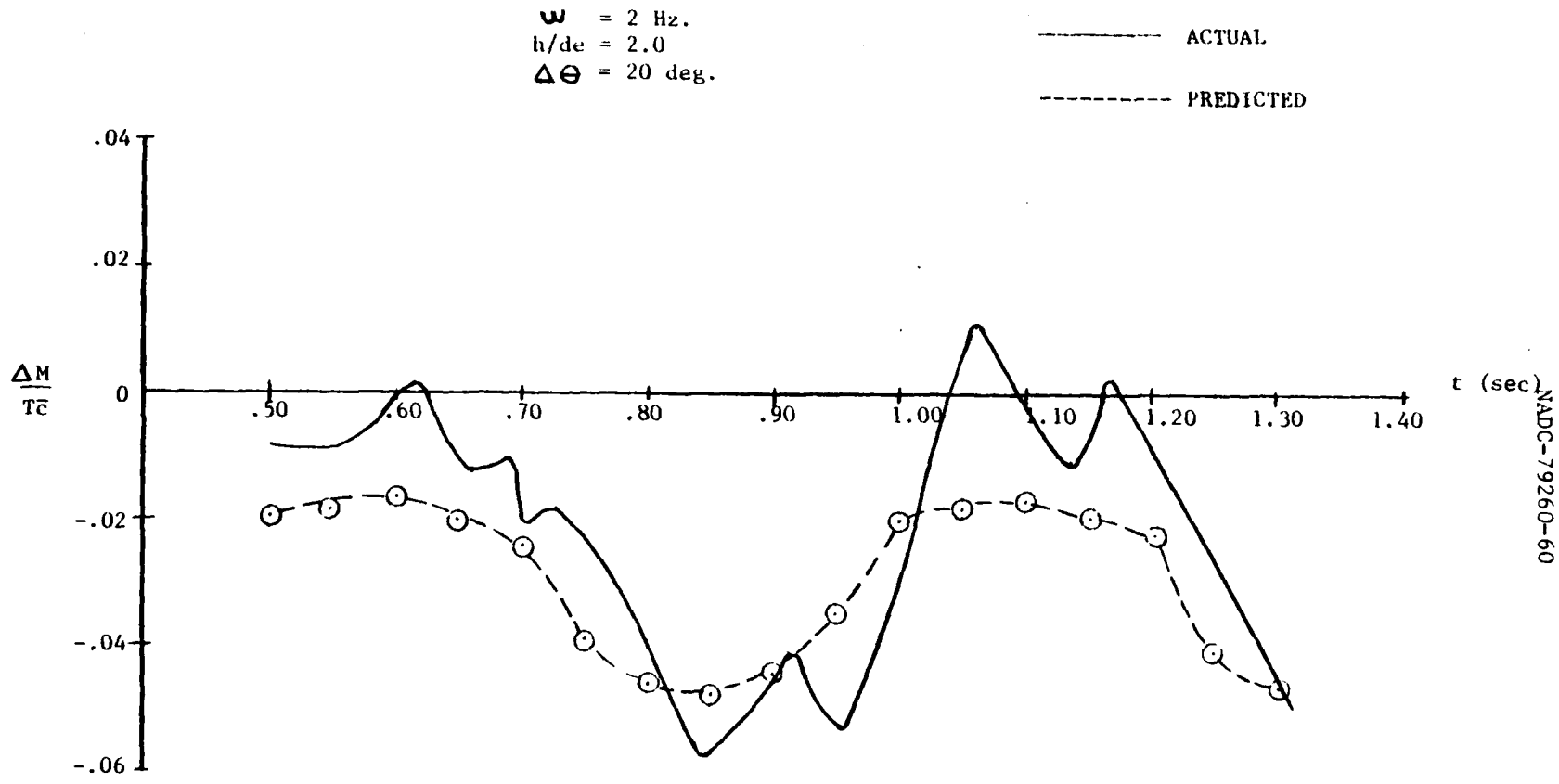

Figure 14f. Induced Pitching Moment Time History Comparison (Run 82.4)

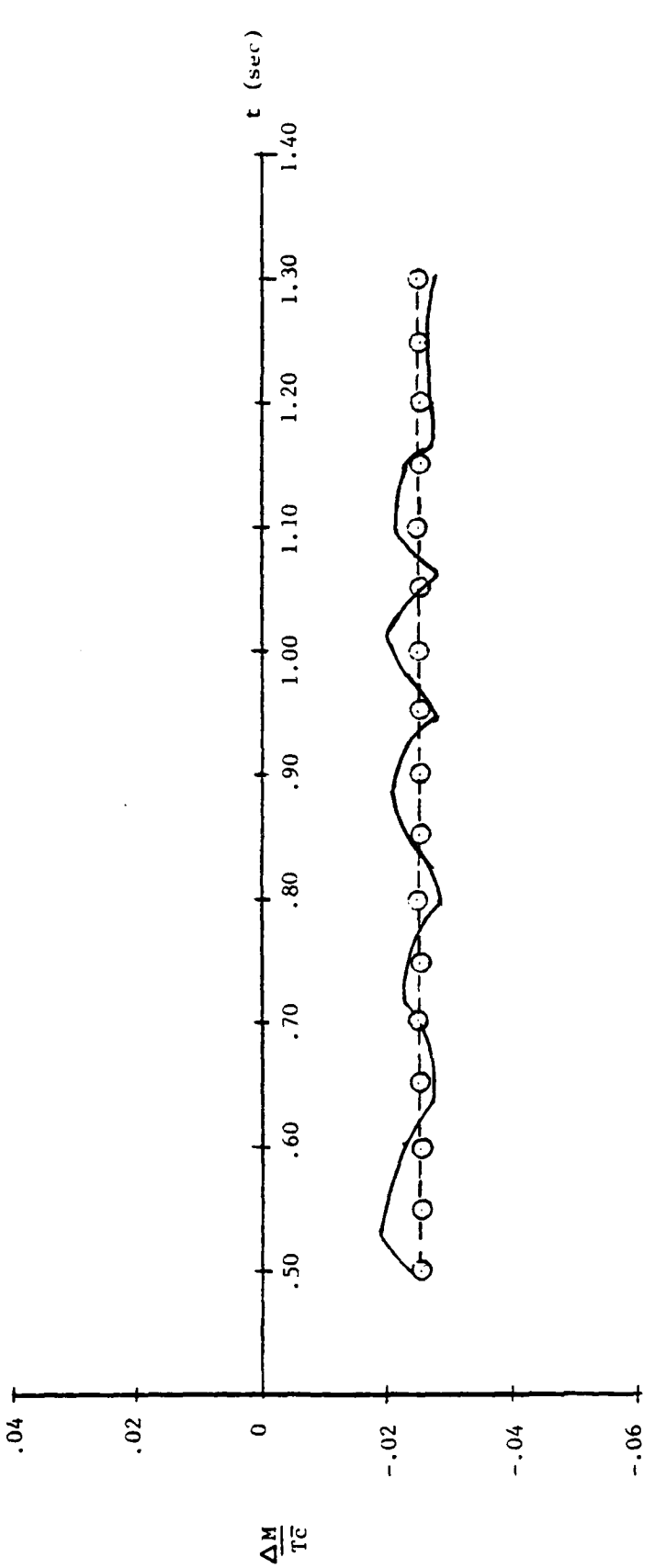

Figure 14g. Induced Pitching Moment Time History Comparison (Run 85.1)

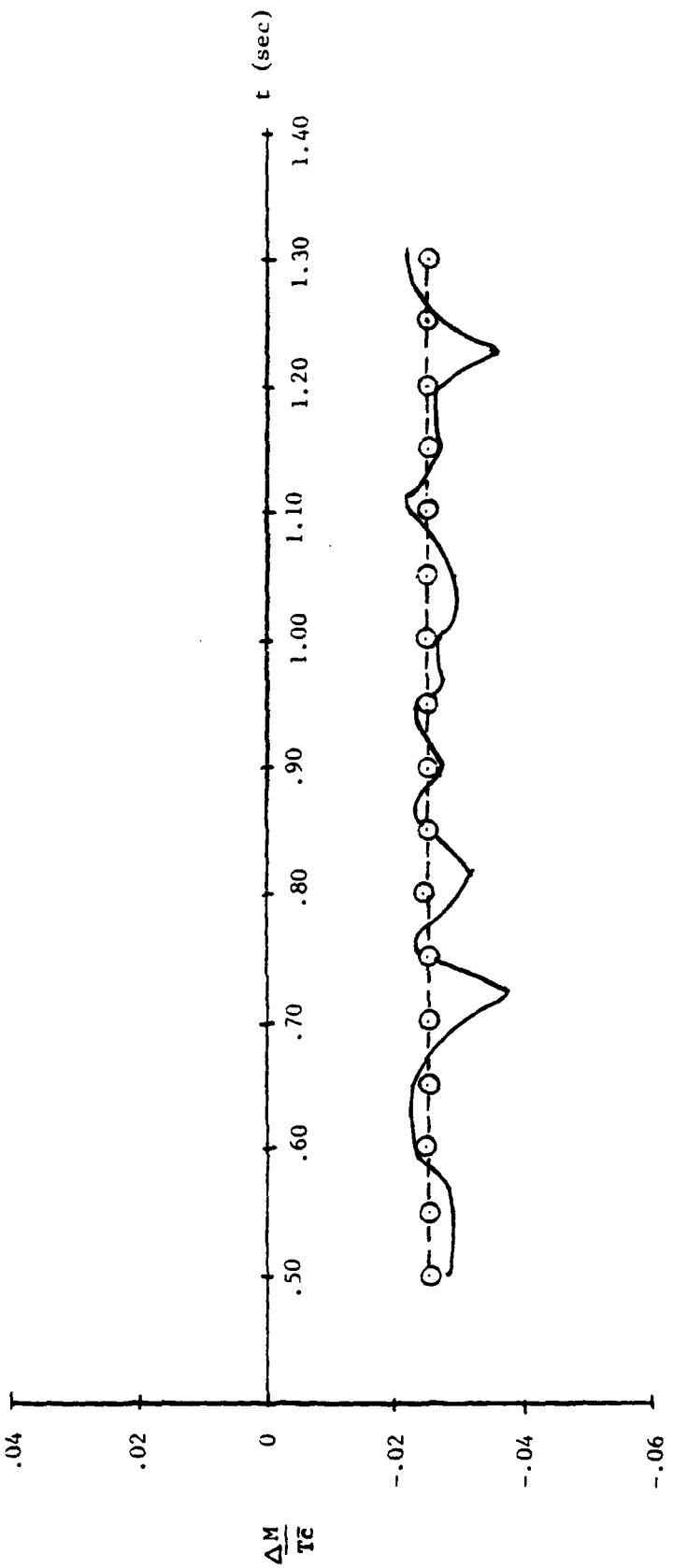

Figure 14h. Induced Pitching Moment Time History Comparison (Run 85.2)

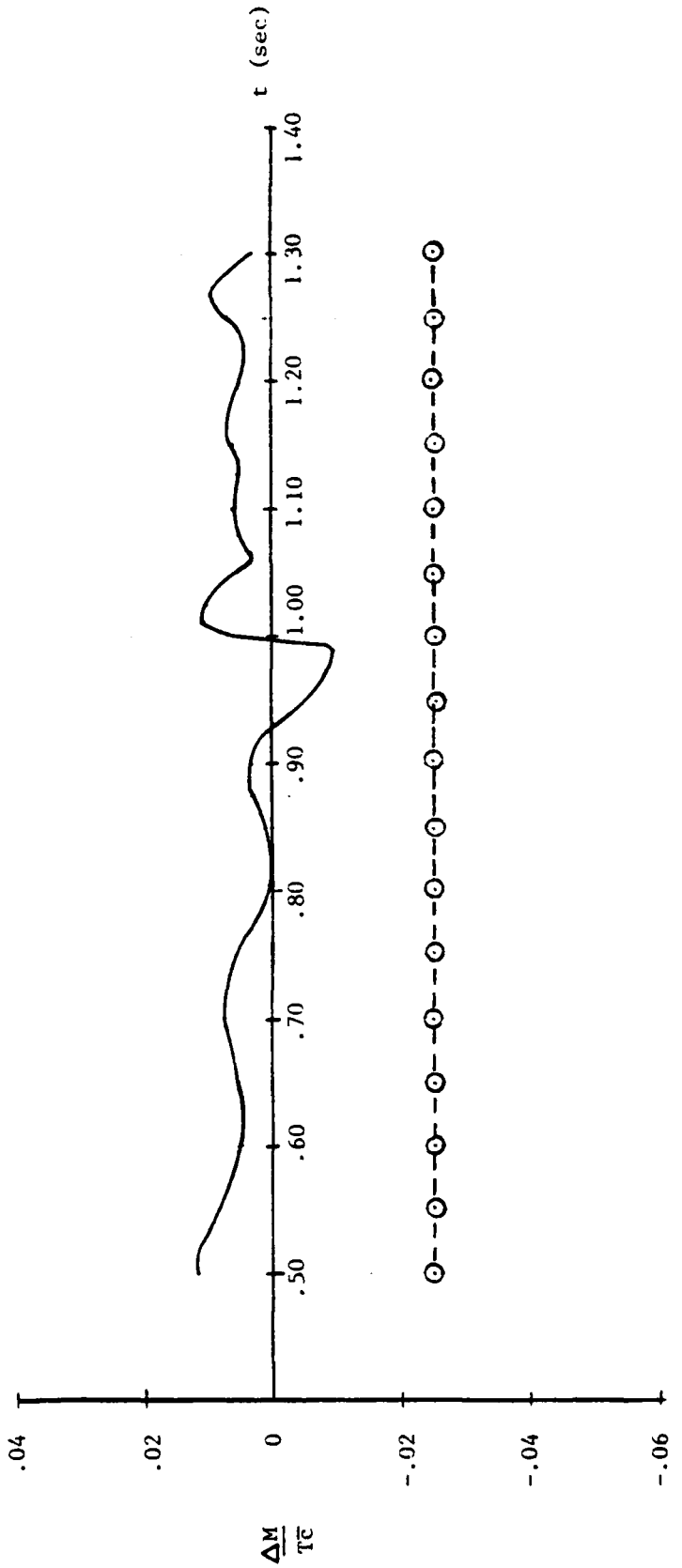

Figure 141. Induced Pitching Moment Time History Comparison (Run 85.3)

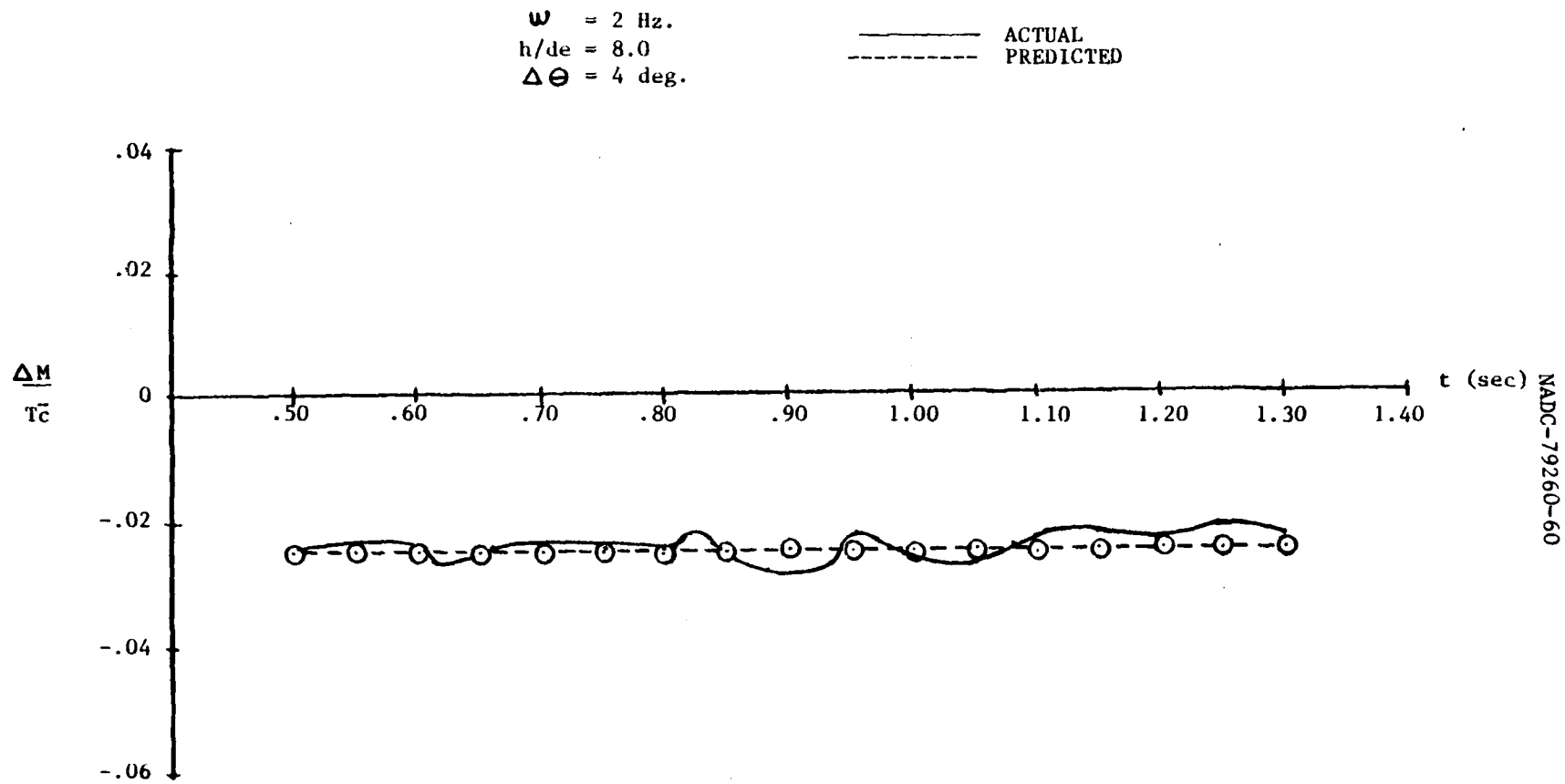

Figure 14j. Induced Pitching Moment Time History Comparison (Run 87.1)

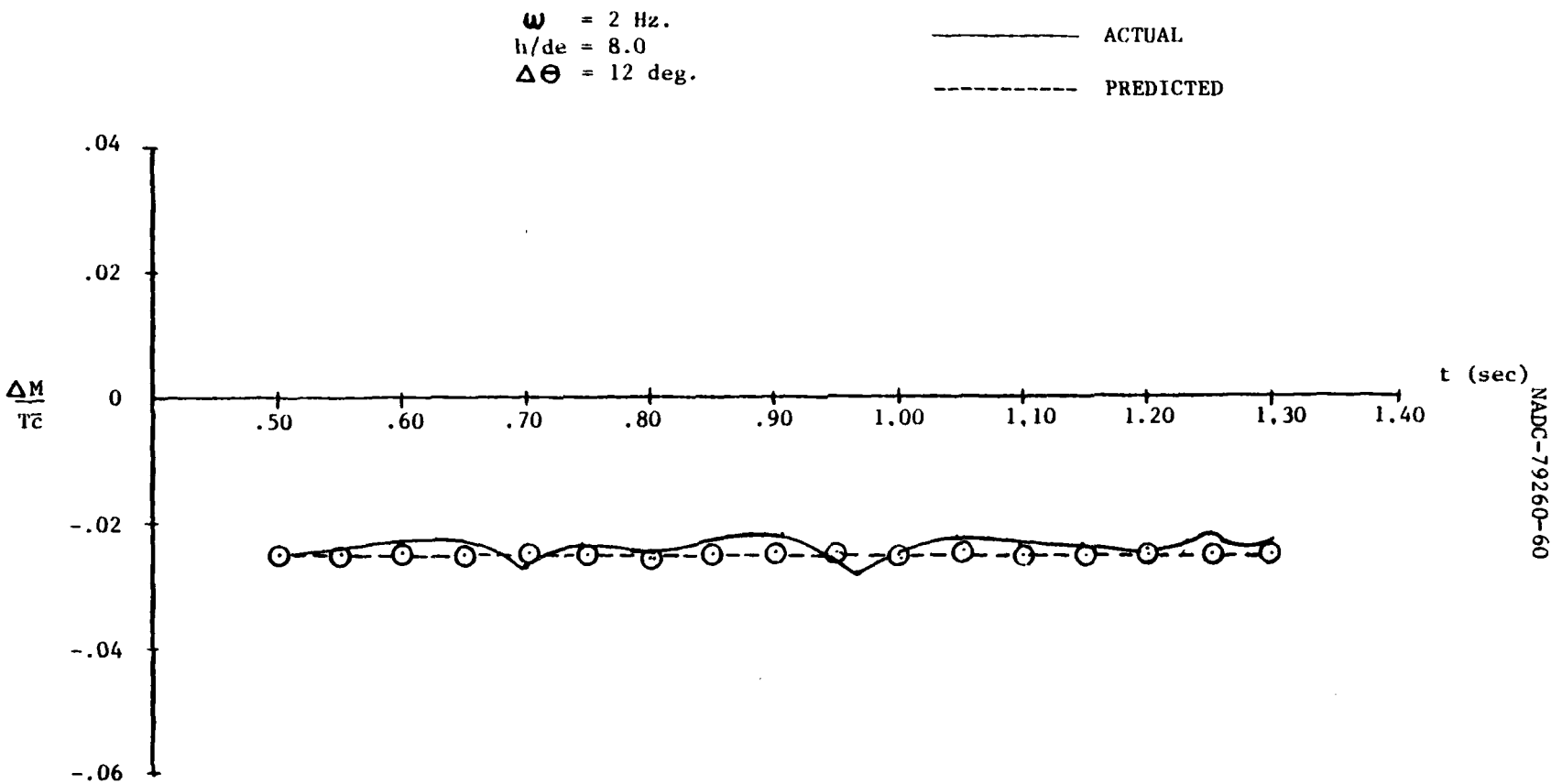

Figure 14k. Induced Pitching Moment Time History Comparison (Run 87.2)

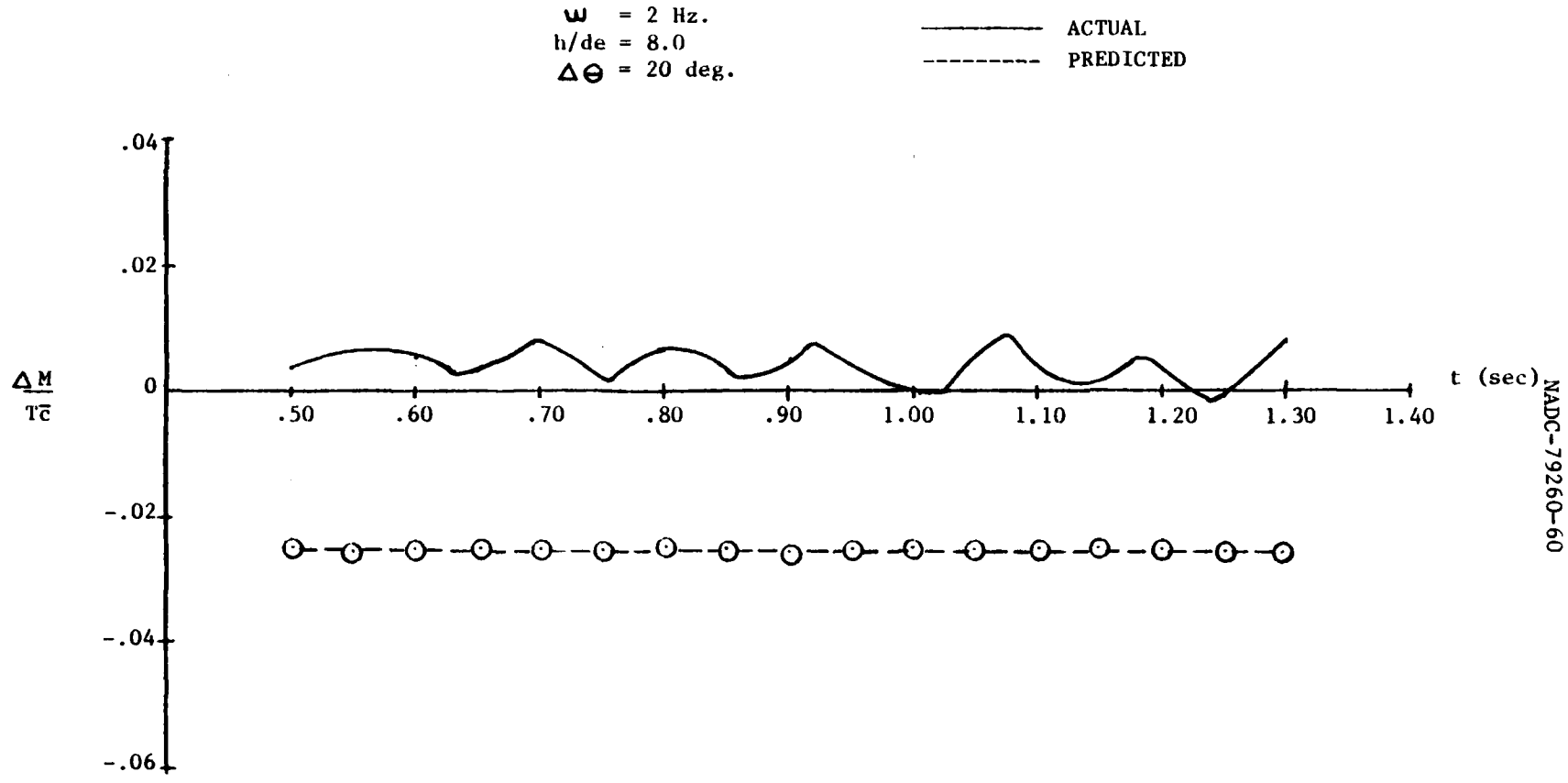

Figure 141. Induced Pitching Moment Time History Comparison (Run 87.3)

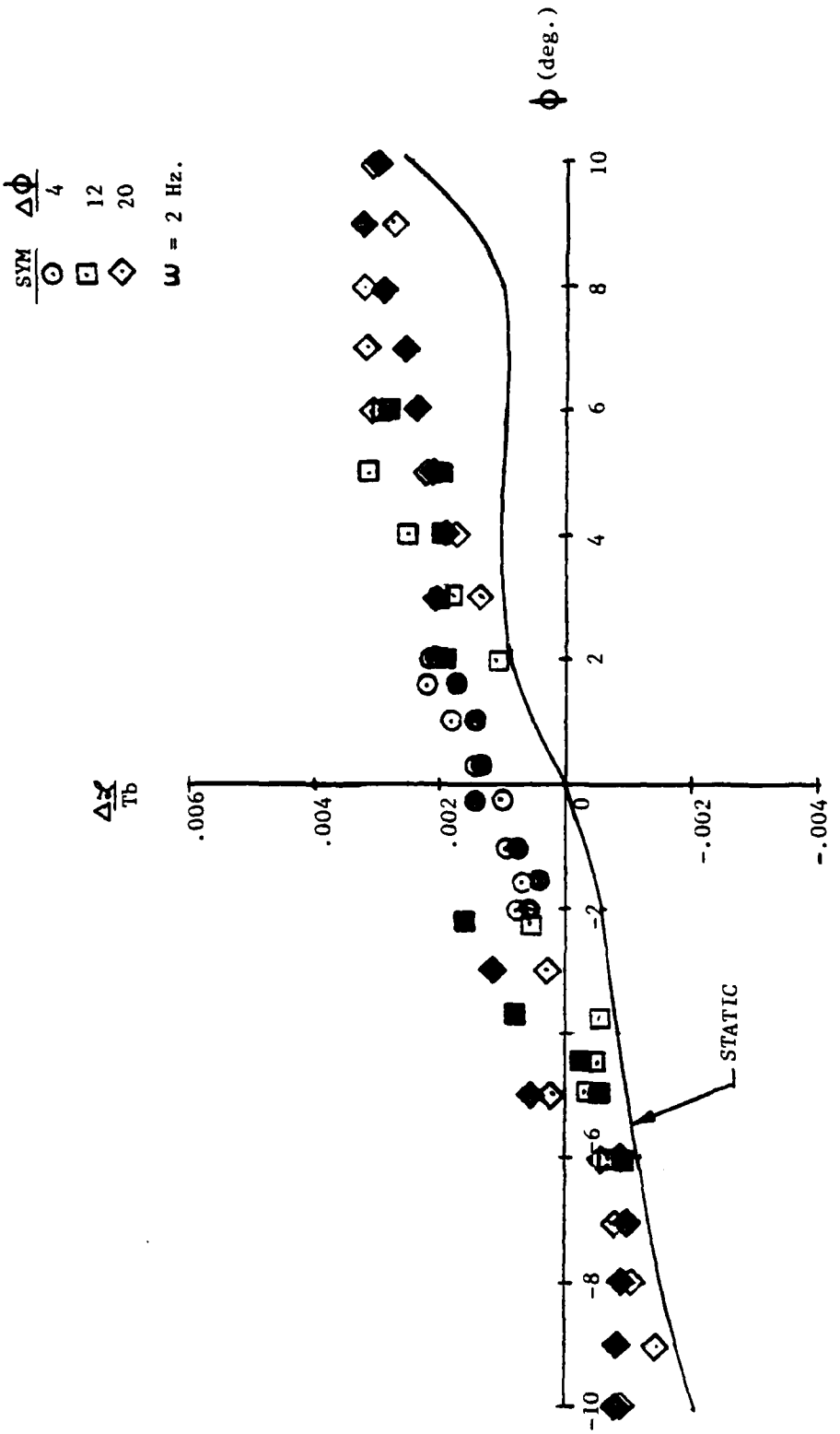

Figure 15. Static and Dynamic Induced Rolling Moment, h/de = 0.8

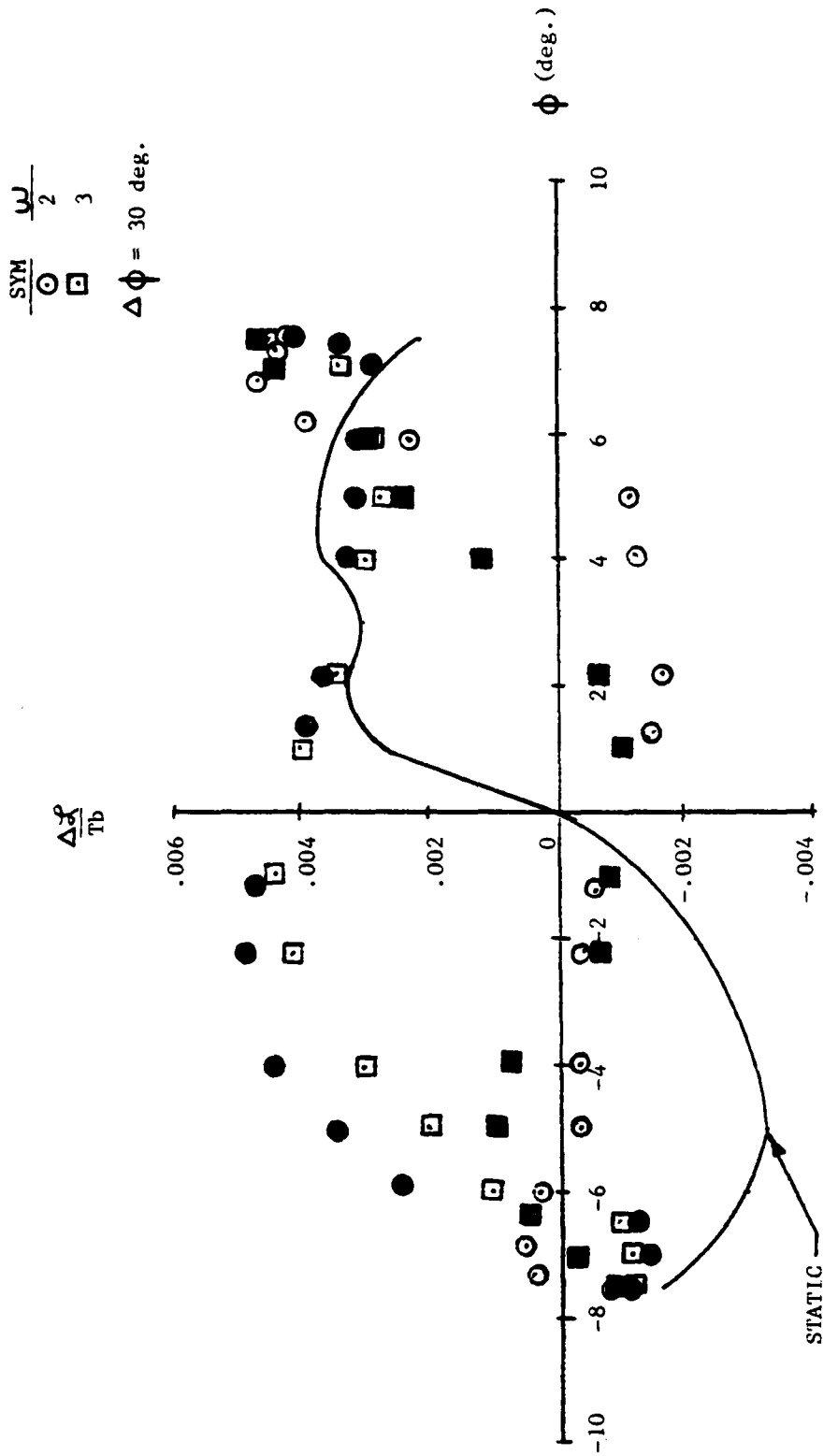

Figure 16. Static and Dynamic Induced Rolling Moment, h/de = 2.0

Figure 15 shows the variation of induced rolling moment with changes in roll angle ($\Delta\phi$) for ω = 2Hz at an h/de = 0.8. The dynamic data differs from the static data for each angular displacement at both positive and negative rates as shown. For ϕ = 0° the static value of $\Delta\mathcal{L}$/Tb is zero while the dynamic value shows a shift of about 0.15%. Both static and dynamic data appear fairly symmetric about ϕ = 0° as expected for this motion. Varying $\Delta\phi$ from 4° through 20° does not show a large effect on rolling moment as indicated. The data for $\Delta\phi$ = 4°, 12°, and 20° fall within a relatively small band similar in shape to the static curve but shifted up 0.15% for both positive and negative roll angles. Although there are differences in rolling moment for positive and negative rates, these differences are small in magnitude. A small hysteresis effect is present in this figure, but is not a pronounced effect at this h/de. For h/de = 2.0 and $\Delta\phi$ = 30°, as shown in figure 16, the hysteresis effect is very pronounced at both frequencies indicated. It should be noted that for ω = 2Hz the negative rates indicated by the closed symbols show a higher value of induced rolling moment than do the positive rates. This is true except at the extreme roll angles where a slight reversal is indicated. For ω = 3Hz the opposite trend is indicated where the positive rates show a higher rolling moment than do the negative rates. The difference in magnitude for positive and negative rates at this h/de is much larger than for an h/de = 0.8. This is due to the fact that for this configuration the fountain is strongest at an h/de = 2.0 and therefore the largest variations should be seen at this height. The results for pitching moment also showed the largest variation at an h/de = 2.0, although the overall magnitudes are on the order of $\pm$0.35% which is very small.

By combining figures 15 and 16 for rolling moment at the various amplitudes, frequencies, and heights indicated, a curve of induced rolling moment versus roll angle was obtained corresponding to a Zero value of deck roll rate. Figure 17 shows this curve indicated by the dotted line along with the static test data for both h/de = 0.8 and 2.0. As indicated in this figure the dotted curve does not pass through the origin. For this rolling motion a symmetry about the origin was expected as shown for the static data, but a shift of about 0.15% is indicated. This shift was investigated and the probable cause is a bias in setting the neutral point statically and dynamically. Assuming this shift is due to measurement error, the zero curve can be lowered 0.15% to pass through the origin and compared to the static data at h/de = 0.8 and 2.0. This shifted zero curve was used to predict the rolling moment as a function of roll angle and compared with actual time history data. These comparisons are shown in figures 18a through 18e with predicted values indicated by the dotted line. Since the values for rolling moment are very small the discussion of these figures will focus on trends and not on percent differences between predicted and actual values. It should be noted that the effect of frequency on the induced rolling moment at this h/de cannot be determined since only one frequency was tested.

Figures 18a through 18c show induced rolling moment versus time for ω = 2Hz, h/de = 0.8, and at amplitudes of 4°, 12° and 20°. The predicted

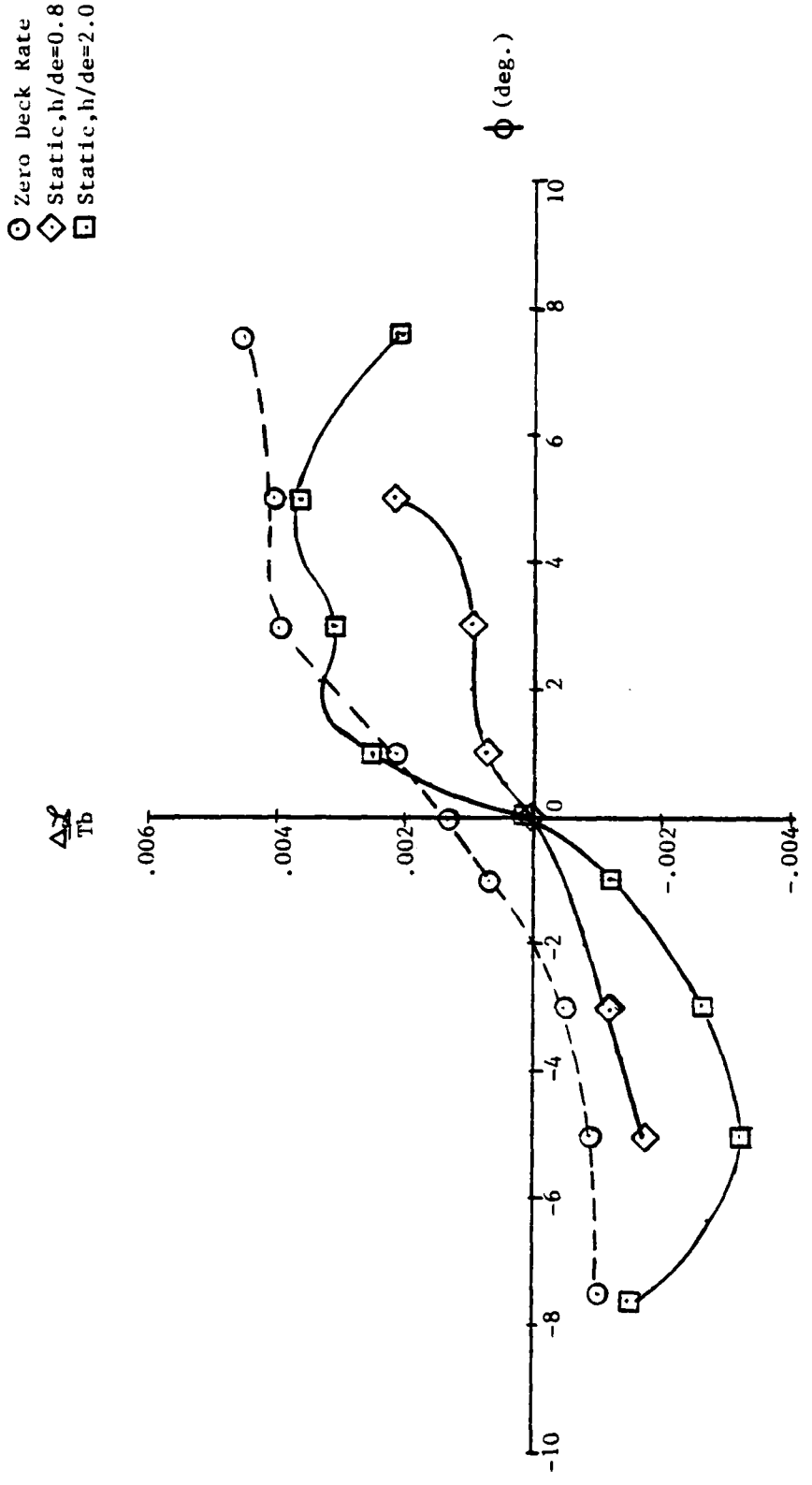

Figure 17. Induced Rolling Moment vs. Roll Angle for Zero Deck Rate

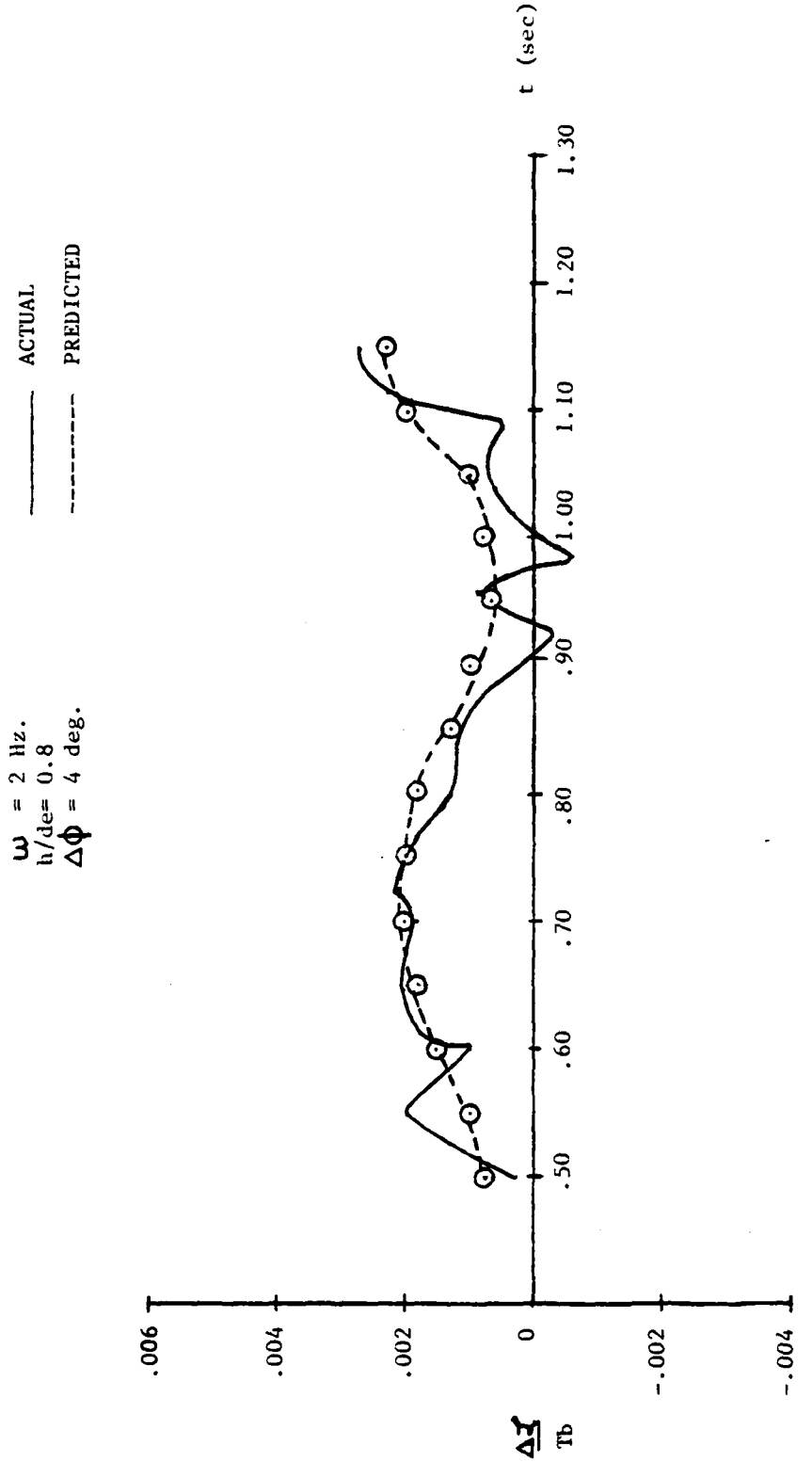

Figure 18a. Induced Rolling Moment Time History Comparison (Run 92.1)

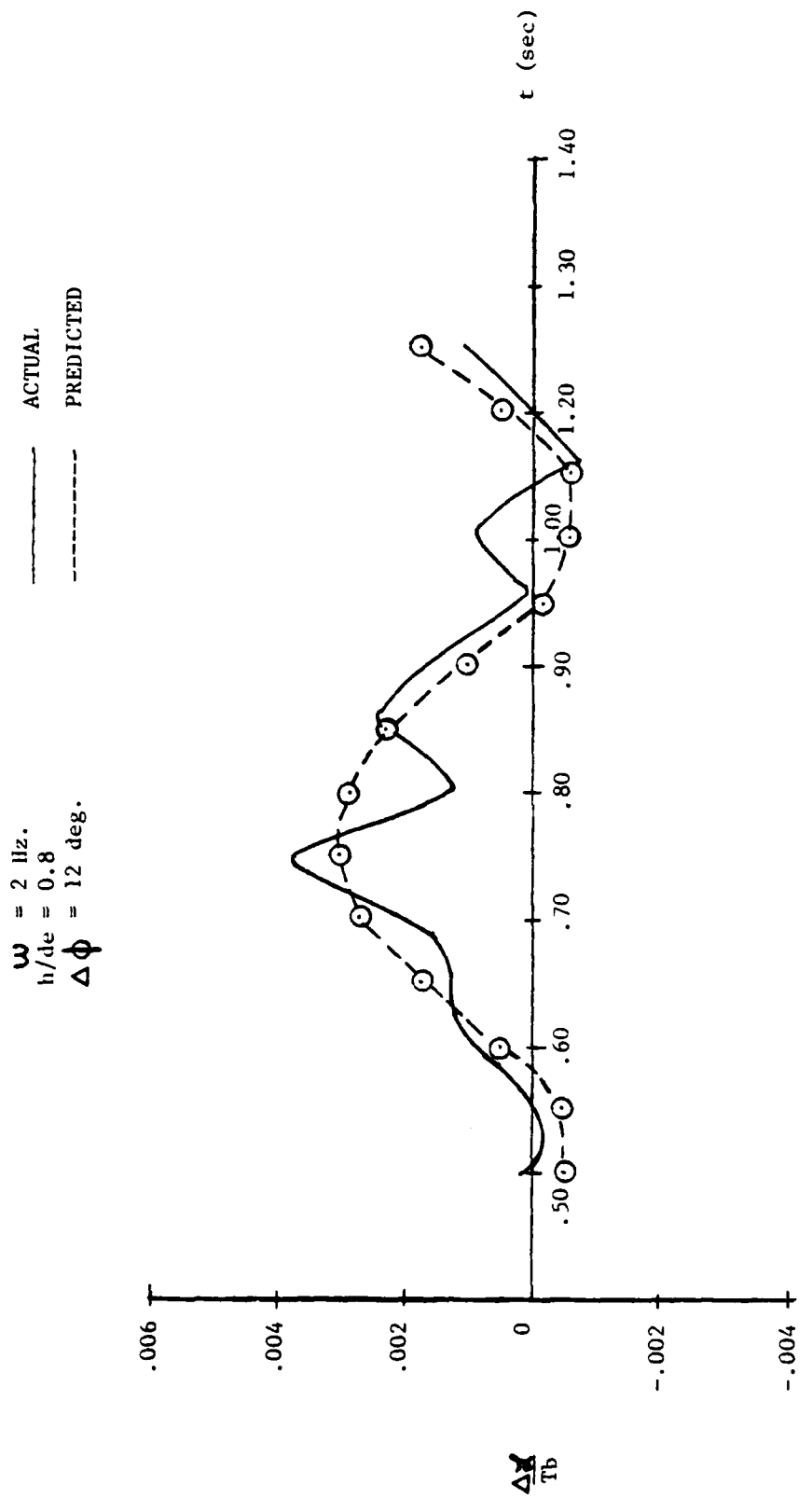

Figure 18b. Induced Rolling Moment Time History Comparison (Run 92.2)

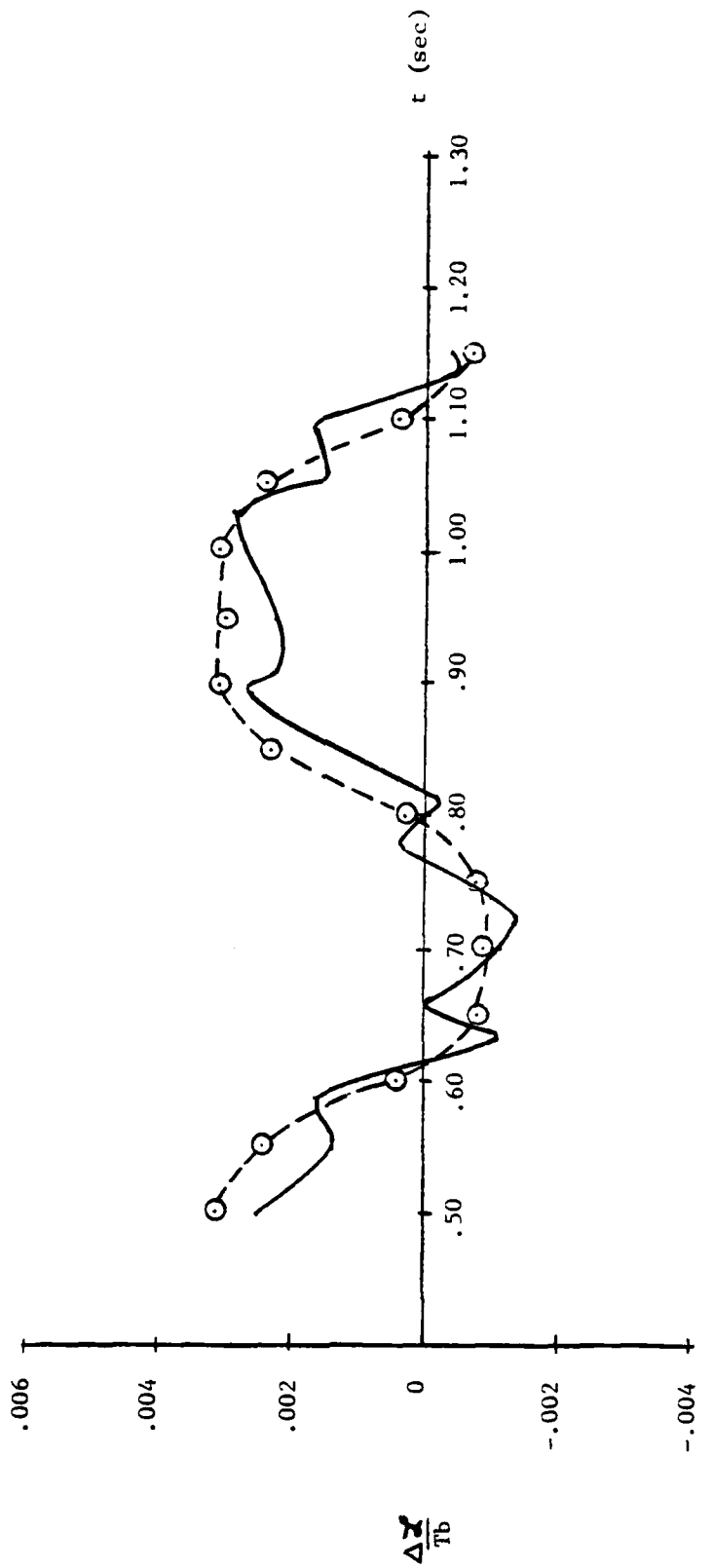

Figure 18c. Induced Rolling Moment Time History Comparison (Run 92.3)

values correlate reasonably well with the actual response for each amplitude. As the amplitude is increased from 4° to 12° the positive peak values show a large increase while negative peak values remain fairly constant. A further increase from 12° to 20° only shows an increase in negative peak value.

Figures 18d and 18e show induced lift for h/de = 2.0, $\Delta\phi$ = 30°, and for two frequencies (ω = 2 and 3Hz). In both cases a slight time shift seems apparent, however this shift is attributed to the difficulty in precisely identifying an initial time used to plot the time history. Peak values correspond well with the actual data and frequency changes show little or no effect on rolling moment. Although the fountain is the strongest at h/de = 2.0, no appreciable difference in magnitude is seen between the response at h/de = 0.8, $\Delta\phi$ = 20° and at h/de = 2.0, $\Delta\phi$ = 30°. Based on this limited data base, height does not seem to have a large effect on induced rolling moment.

Several observations can be summarized in regard to the rolling deck motion results described above. First, the magnitude of the response for any of the conditions tested is very small (less than 0.5%). Second, the dynamic response showed a shift of approximately 0.15% above the static data and is attributed to a bias in setting the neutral point. Third, based on the limited amount of data available, frequency and height do not appear to have a large effect on induced rolling moment. Fourth, an increase in amplitude does not have a large effect for the various amplitudes, frequencies, and heights which were tested. Fifth, a slight time shift was observed in several of the figures and is attributed to the difficulty in identifying precisely an initial time from the data.

CONCLUSIONS AND RECOMMENDATIONS

Transient induced aerodynamic data for a 3-fan subsonic VSTOL model operating in a moving deck environment have been analyzed in terms of single axis deck motions. These include heaving, pitching, and rolling motions only. Combined deck motions, such as heave and pitch, were not considered for this first correlation analysis due to the added complexity that they introduce.

A method has been developed to predict the dynamic response of induced forces and moments based upon a zero value of deck rate for each motion. In general, good correlation is seen between the actual and predicted values. The following represent the more pertinent conclusions which have been reached as a result of this analysis.

HEAVE

- A hystersis effect is present for this motion where the induced lift loss, $\Delta L/T$, is greater for the deck heaving away from the model as compared to the deck heaving towards the model.

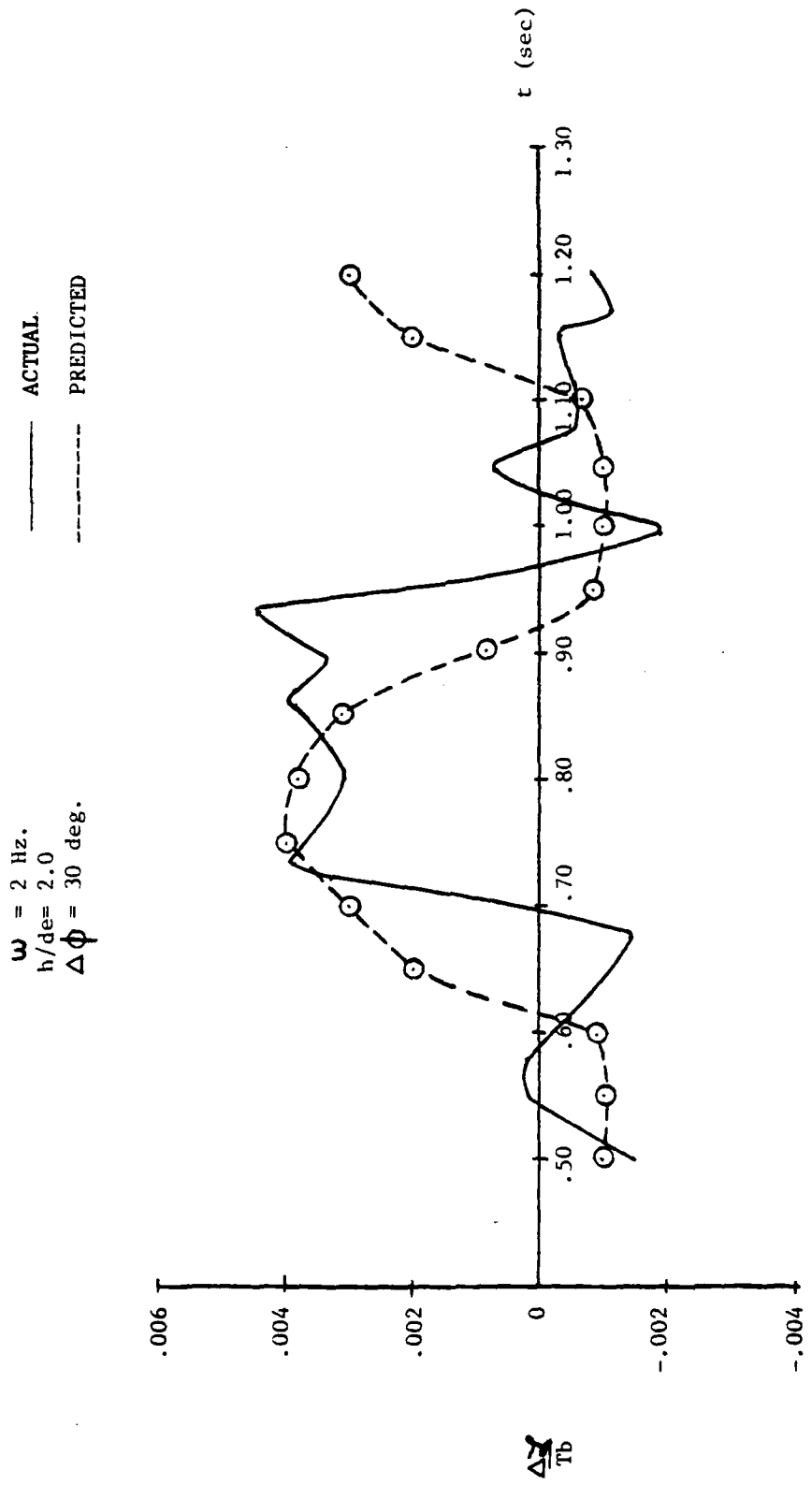

Figure 18d. Induced Rolling Moment Time History Comparison (Run 163.1)

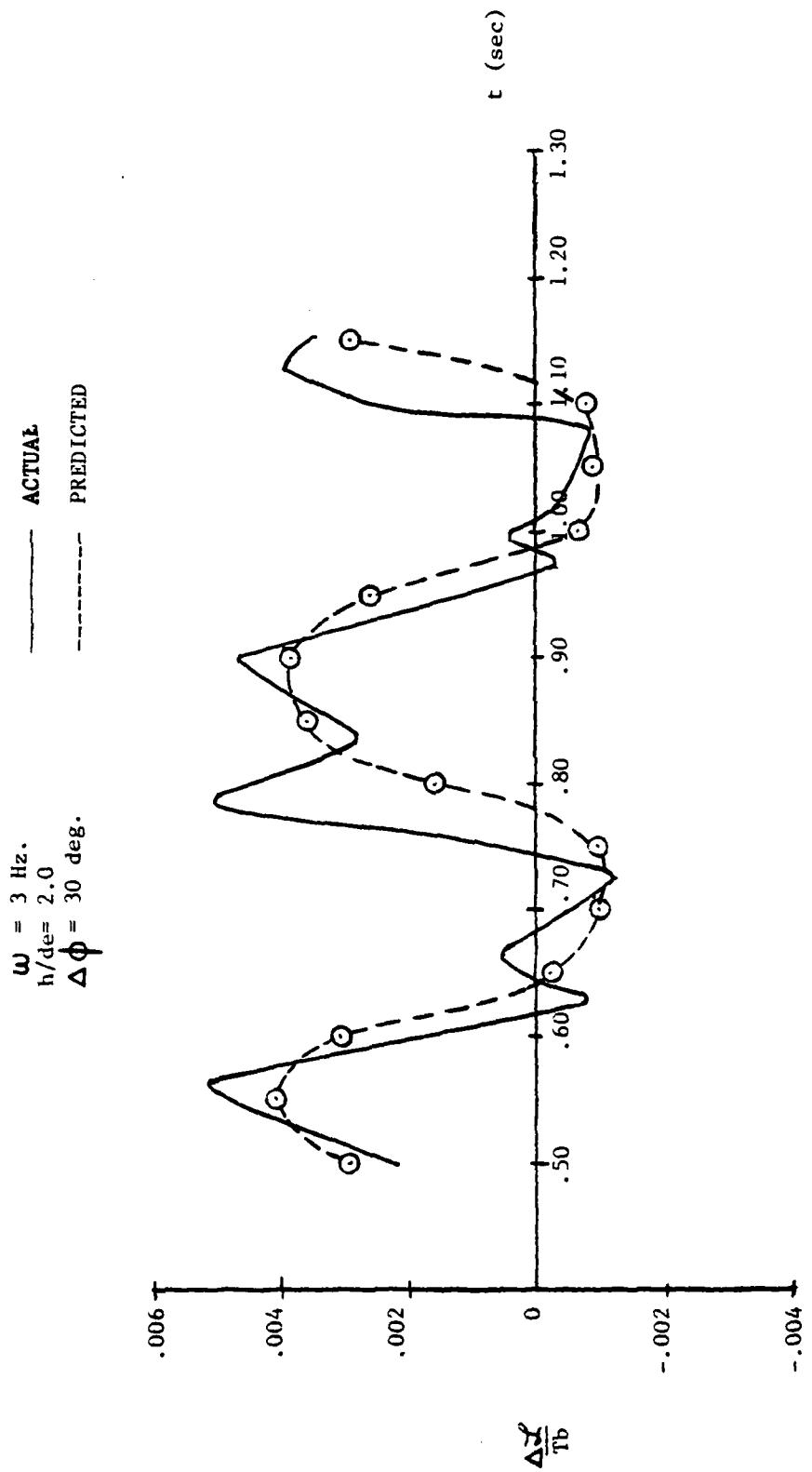

Figure 18e. Induced Rolling Moment Time History Comparison (Run 163.2)

- For a given amplitude and neutral point, frequency did not have a large effect on the induced lift.

- Increasing the amplitude increased significantly the suckdown effect. As much as 7.0% suckdown was seen for an increase of amplitude from 1.0 to 3.0 h/de.

- Predictions of transient lift variations based on a quasi-static (zero deck rate) assumption correlate within about 1.5% of actual test results.

PITCH

- Height has a significant effect on induced pitching moment at lower values of h/de. At values of h/de = 5.0 and 8.0, height effects become negligible because the model is out of ground effect.

- A hysteresis is present and most noticeable at h/de = 2.0 where the fountain is the strongest.

- Frequency effects could not be determined because of the limited data available.

- Increasing the amplitude of the sinusoidal motion increases the magnitude of the actual response by up to 1.5% $\Delta M/T\bar{c}$.

- For h/de = 5.0 and 8.0 a zero shift is apparent in the data and is on the order of about -0.025 $\Delta M/T\bar{c}$.

ROLL

- The magnitude of induced rolling moment for any of the heights, amplitudes, and frequencies tested was less than 0.5%.

- A shift of approximately 0.15% was observed between the dynamic response and the static data at both heights tested due to a bias in setting the neutral point (ϕ_o).

- Amplitude did not have a large effect on induced rolling moment for any of the conditions tested.

- Frequency did not have a significant effect on the induced rolling moment based on the limited amount of data available.

These conclusions show that a moving deck can produce substantial changes in induced lift and pitching moment for this configuration. The major contribution for heaving motion is the amplitude where as much as a 7.0% difference in induced lift was seen for two different values of $\Delta h/de$. In the case of pitching motion, the driving factor is height over deck with a 3.0% difference in pitching moment evident between an h/de = 0.8 and 2.0. This 3.0% difference can be important to a pilot in hover who is trying to maintain trim.

This analysis has shown that a quasi-static curve, as developed for each deck motion described, can provide a reasonable estimate of the dynamic response. As more data becomes available it is recommended that this approach be modified as required to improve estimation accuracy at the preliminary design stage.

It is also recommended that the data of reference (a) for the supersonic configuration be examined in a similar manner to facilitate a comparison of the subsonic and supersonic configurations. This comparison would be especially valuable since the supersonic configuration is dominated by suckdown and the subsonic configuration is more fountain dominated.

R E F E R E N C E S

(a) Kamman, J. H., and Hall, C. L., "Lift System Induced Aerodynamics of V/STOL Aircraft in a Moving Deck Environment", NADC-77-107-30, 29 Sep 1978.

(b) Caddy, M. J., "TIGS-An Interactive Graphical System for the Creation and Correction of Tabular Data Sets", NADC-78229-60, unpublished.

(c) Caddy, M. J., "TREAD/TLOOK-Multipurpose Computer Routine for Interpolation and Extrapolation of Tabular Data", NADC-76366-30, 11 Jan 1977.

LIST OF SYMBOLS

Symbol		Units
de	Equivalent nozzle exit diameter	m(ft.)
f	Arbitrary function	-
g	Arbitrary function	-
h	Height-above-deck	m(ft.)
Δh	Heave amplitude	m(ft.)
h_o	Neutral height-over-deck	m(ft.)
K	Arbitrary function	-
$\frac{\Delta L}{T}$	Induced lift	-
$\frac{\Delta \mathcal{L}}{Tb}$	Induced rolling moment	-
$\frac{\Delta M}{Tc}$	Induced pitching moment	-
RMS	Root-mean-square	-
t	Time	sec.
θ	Pitch angle	deg
$\Delta\theta$	Angular amplitude - pitch	deg
θ_o	Neutral pitch angle	deg
ϕ	Roll angle	deg
$\Delta\phi$	Angular amplitude - roll	deg
ϕ_o	Neutral roll angle	deg
ω	Frequency	Hz
(°)	Degrees	-

APPENDIX A

GOVERNING EQUATIONS AND COMPUTER PROGRAMS

A P P E N D I X A

This appendix outlines the formulation of the governing equations for sinusoidal deck motions. The reduction of the reference (a) data into a form suitable for analysis as well as the computer program developed to analyze the data will also be discussed.

GOVERNING EQUATIONS

In the heaving direction, induced lift was assumed to be a function of deck position and rate,

$$\frac{\Delta L}{T} = f_1(h) + f_2(\dot{h}) \tag{1}$$

Since the deck motion is sinusoidal, the position of the aircraft at any time (t) can be obtained by the neutral point plus a value determined by the sinusoidal motion. This can be written in equation form as follows:

$$h = h_o + \frac{\Delta h}{2} \sin(\omega t) \tag{2}$$

The equivalent nozzle jet exit diameter, de, was used to nondimensionalize equation (2) in order to be consistent with the data of reference (a),

$$\frac{h}{de} = \frac{h_o}{de} + \frac{\left(\frac{\Delta h}{de}\right)}{2} \sin(\omega t) \tag{2a}$$

Using equation (2a) the deck rate was computed as a function of frequency, amplitude, and neutral point which are the parameters varied in the reference (a) data. Differentiating with respect to time yields,

$$\frac{\dot{h}}{de} = \omega \frac{\left(\frac{\Delta h}{de}\right)}{2} \cos(\omega t) \tag{3}$$

Rewriting equation (2a),

$$\sin(\omega t) = 2 \frac{\left(\frac{h}{de} - \frac{h_o}{de}\right)}{\frac{\Delta h}{de}} \tag{4}$$

the equation for deck rate is obtained and can be written in the following form,

$$\frac{\dot{h}}{de} = \omega \sqrt{\left(\frac{\frac{\Delta h}{de}}{2}\right)^2 - \left(\frac{h}{de} - \frac{h_o}{de}\right)^2} \tag{5}$$

In the pitch direction, the induced pitching moment was assumed to be a function of pitch angle, pitch rate, and deck position as follows,

$$\frac{\Delta M}{Tc} = g_1(\theta) + g_2(\dot{\theta}) + g_3(h) \tag{6}$$

Pitch angle and rate were computed as follows,

$$\theta = \theta_o + \frac{\Delta\theta}{2} \sin(\omega t) \tag{7}$$

Differentiating equation (7) with respect to time yields an expression for the pitch rate,

$$\dot{\theta} = \omega \frac{\Delta\theta}{2} \cos(\omega t) \tag{8}$$

From this point the pitch rate can be obtained as a function of frequency, amplitude, and neutral angle as follows,

$$\dot{\theta} = \omega\sqrt{\left(\frac{\Delta\theta}{2}\right)^2 - (\theta - \theta_o)^2} \tag{9}$$

The third term of equation (6), $g_3(h)$, represents the effect of deck height on the induced pitching moment and has already been discussed.

For the roll direction, induced rolling moment can be defined in a similar manner. Induced rolling moment is a function of roll angle, roll rate, and deck position as follows,

$$\frac{\Delta \mathcal{L}}{Tb} = k_1(\phi) + k_2(\dot{\phi}) + k_3(h) \tag{10}$$

Roll angle and rate are found using the same approach as was used for pitch angle and rate. This approach yields the following equations,

$$\phi = \phi_o + \frac{\Delta\phi}{2} \sin(\omega t) \tag{11}$$

$$\dot{\phi} = \omega \frac{\Delta\phi}{2} \cos(\omega t) \tag{12}$$

$$\dot{\phi} = \omega\sqrt{\left(\frac{\Delta\phi}{2}\right)^2 - (\phi-\phi_o)^2} \qquad (13)$$

The last term of equation (12), $k_3(h)$, represents the effect of height on the induced rolling moment and has already been discussed.

DATA REDUCTION

This section of the report describes how the data was reduced for analysis so that a computer program could be used for computational purposes. The data selected for analysis, as previously indicated, were obtained from reference (a) for the 3-fan subsonic VSTOL configuration. These data were in the form of time histories for induced lift, pitching moment, and rolling moment. A computer program, reference (b), was used in order to set up a table of digitized values for each data run. Once established, this table was entered and the values at any specified time were determined using a second computer program, reference (c). This second program uses a spline function to interpolate or extrapolate the table data and has been proven to be very accurate. These two computer programs were then used in conjunction with the computer program REDUCE which was developed for this analysis.

DATA ANALYSIS

The computer program REDUCE will not be presented in great detail here but the basic elements used to analyze the data will be discussed. Figure A-1 shows the flow of the data analysis. The two points shown as A and B indicate the portion of the flow for which the computer program REDUCE was used. As shown in this figure REDUCE has five basic elements indicated by (1) through (5). Element (1) is the input of specified rates for any of the deck motions. These values are determined for each data run based on the equations previously developed,

$$\dot{h}/de = \omega\left(\frac{\frac{\Delta h}{de}}{2}\right)\cos(\omega t) \qquad (14)$$

$$\dot{\theta} = \omega\frac{\Delta\theta}{2}\cos(\omega t) \qquad (15)$$

$$\dot{\phi} = \omega\frac{\Delta\phi}{2}\cos(\omega t) \qquad (16)$$

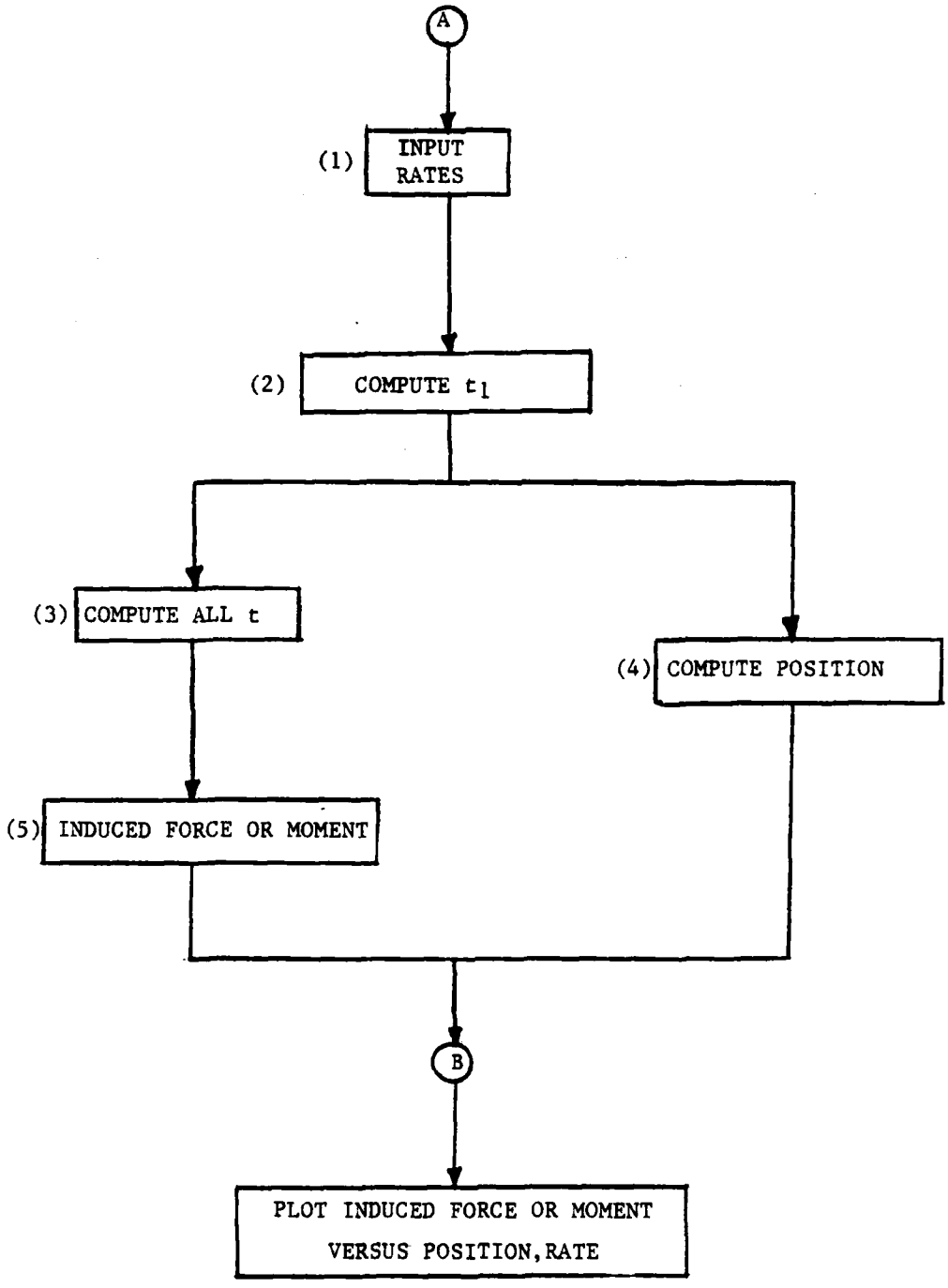

Figure A-1. Data Analysis Flow Chart

The maximum positive and negative rate values are readily obtained from these equations since the cosine has a maximum of ± 1 and the frequency and amplitudes are known.

Element (2) of this flow is the computation of an initial time, t_1, which is used to compute all other times of interest for a given data run. The equations for rate were rearranged as follows to obtain t_1,

$$t_1 = \frac{1}{\omega} \cos^{-1} \left[\frac{2(\dot{h}/de)}{\omega(\Delta h/de)} \right] \tag{17}$$

$$t_1 = \frac{1}{\omega} \cos^{-1} \left[\frac{2\dot{\theta}}{\omega \Delta\theta} \right] \tag{18}$$

$$t_1 = \frac{1}{\omega} \cos^{-1} \left[\frac{2\dot{\phi}}{\omega \Delta\phi} \right] \tag{19}$$

The importance of t_1 is that it corresponds to the first time at which the specified rate occurs on the sine curve. As indicated by element (3), all other times at which a specific rate occurs can be computed knowing t_1. The computation of this value is shown as element (4) of the data flow analysis of figure A-1. Also, the number of times that a given rate will occur in one second must be known and is a function of frequency as indicated in figure A-2. In this figure the term h_1 is the position value (h, θ, ϕ) corresponding to the specified rate.

Element (5) is the last segment of the REDUCE program. For each time computed in element (3), the induced force or moment value was obtained using the computer program described in reference (c). For the entire 5 second data run, an RMS of these values was calculated along with the corresponding position value. These data were then plotted as induced force or moment versus position and rate and have been discussed in the approach section of this report.

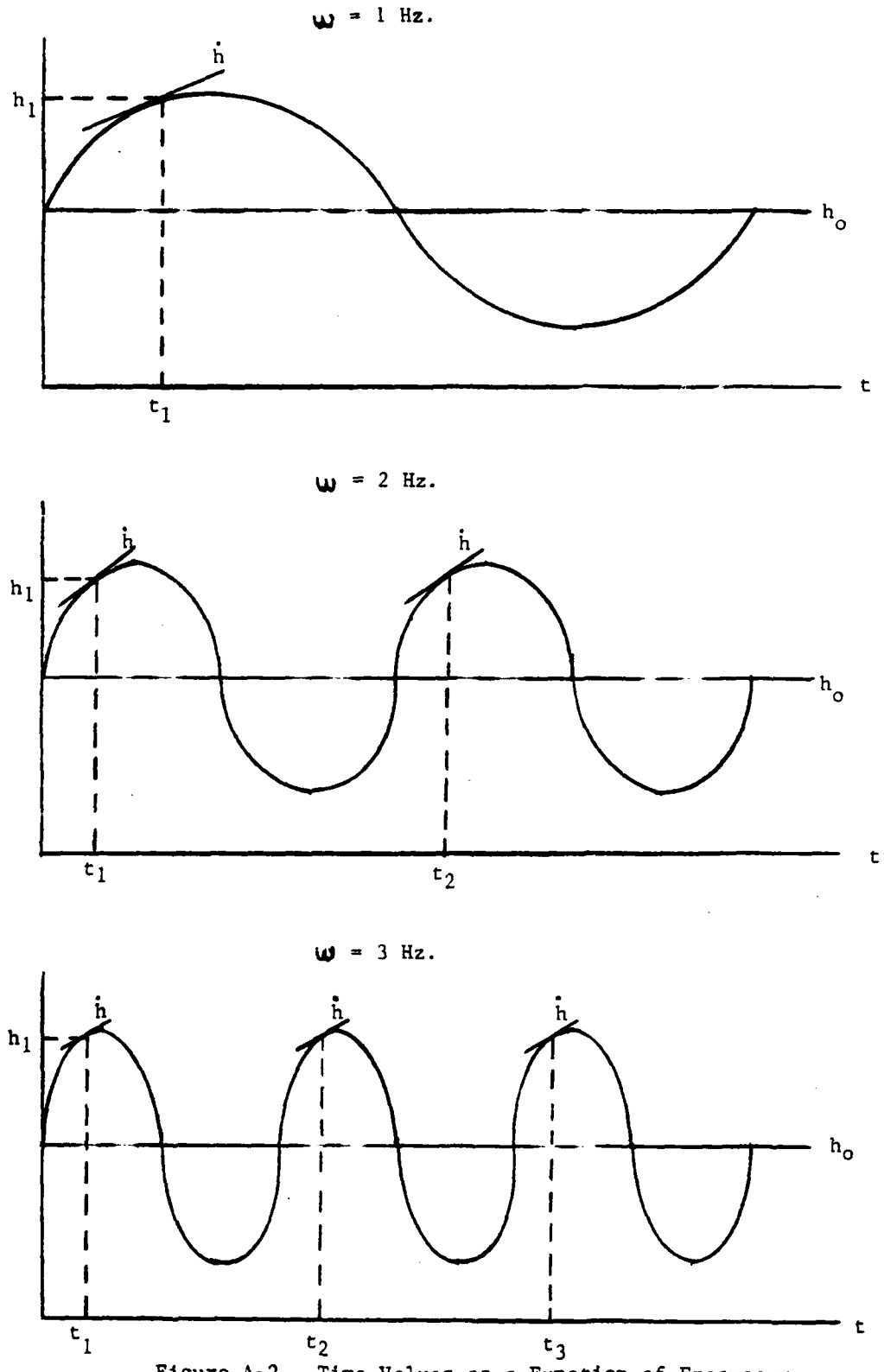

Figure A-2. Time Values as a Function of Frequency

APPENDIX B

SUBSONIC HEAVING MOTION DATA

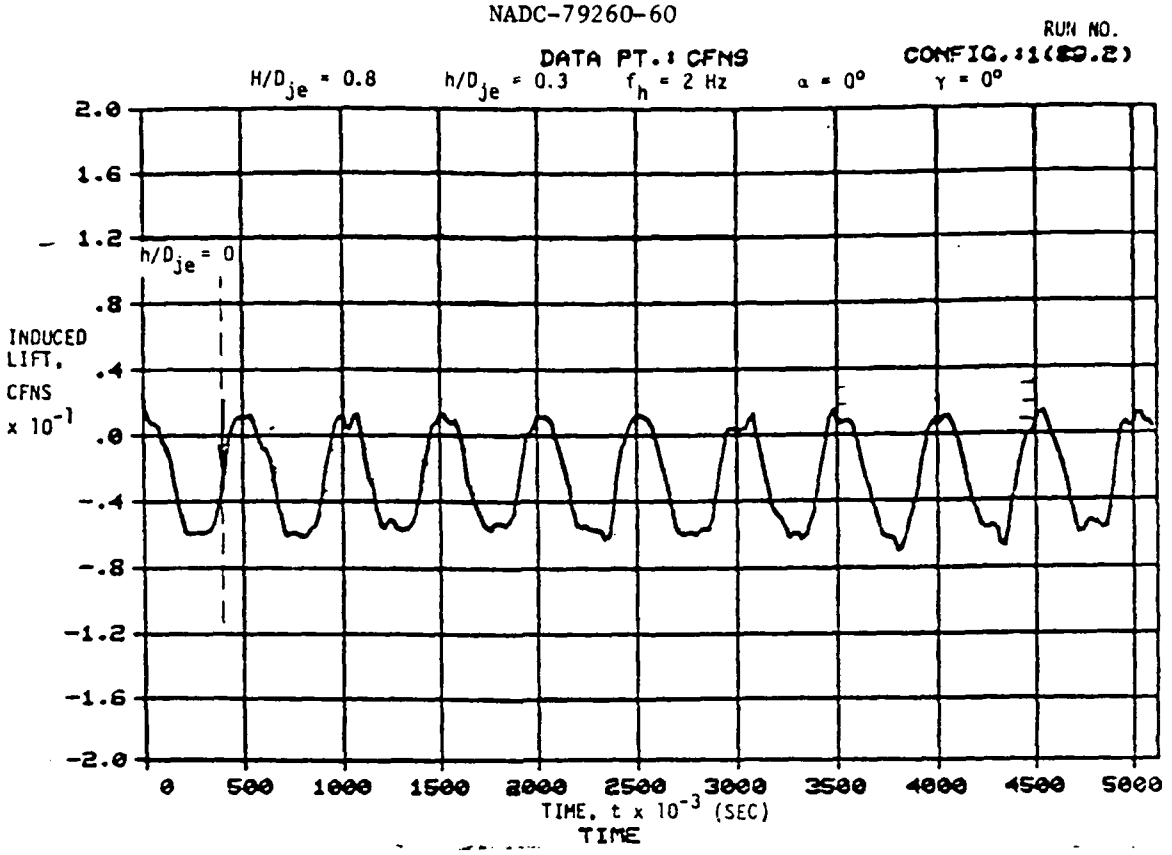

Figure B-1. Subsonic Heaving Motion Data (Run 89.2)

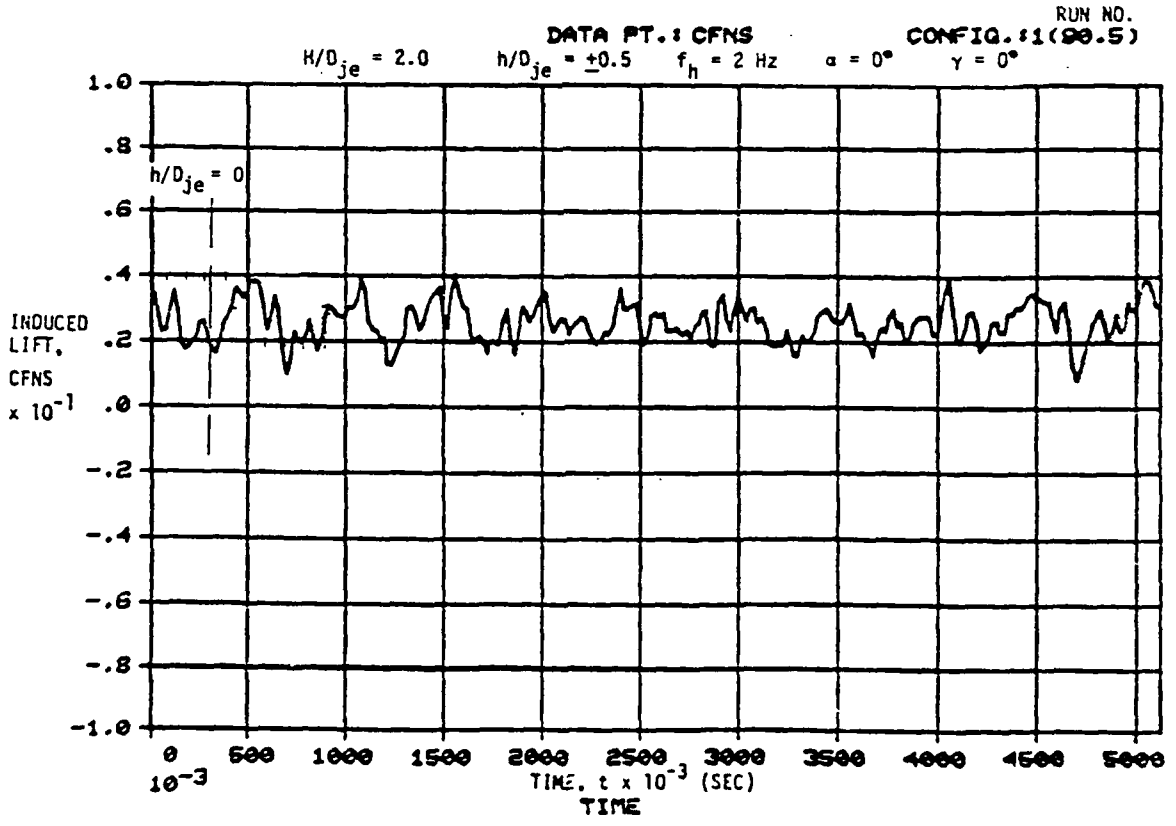

Figure B-2. Subsonic Heaving Motion Data (Run 90.5)

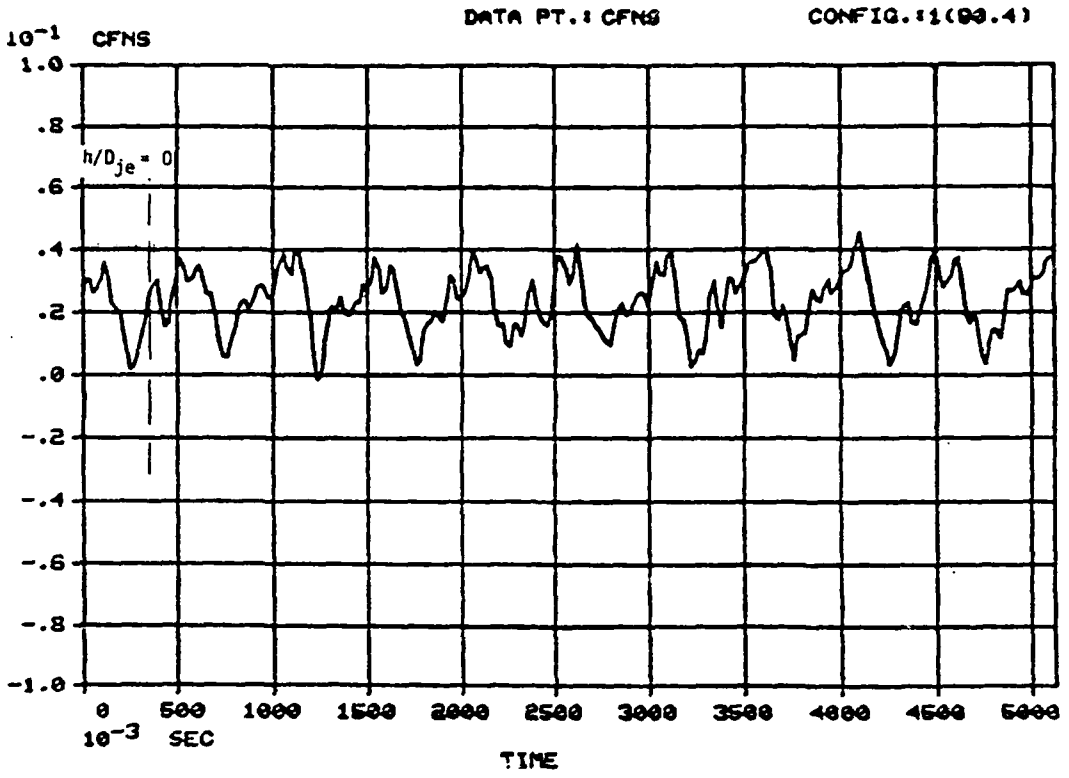

Figure B-3. Subsonic Heaving Motion Data (Run 90.4)

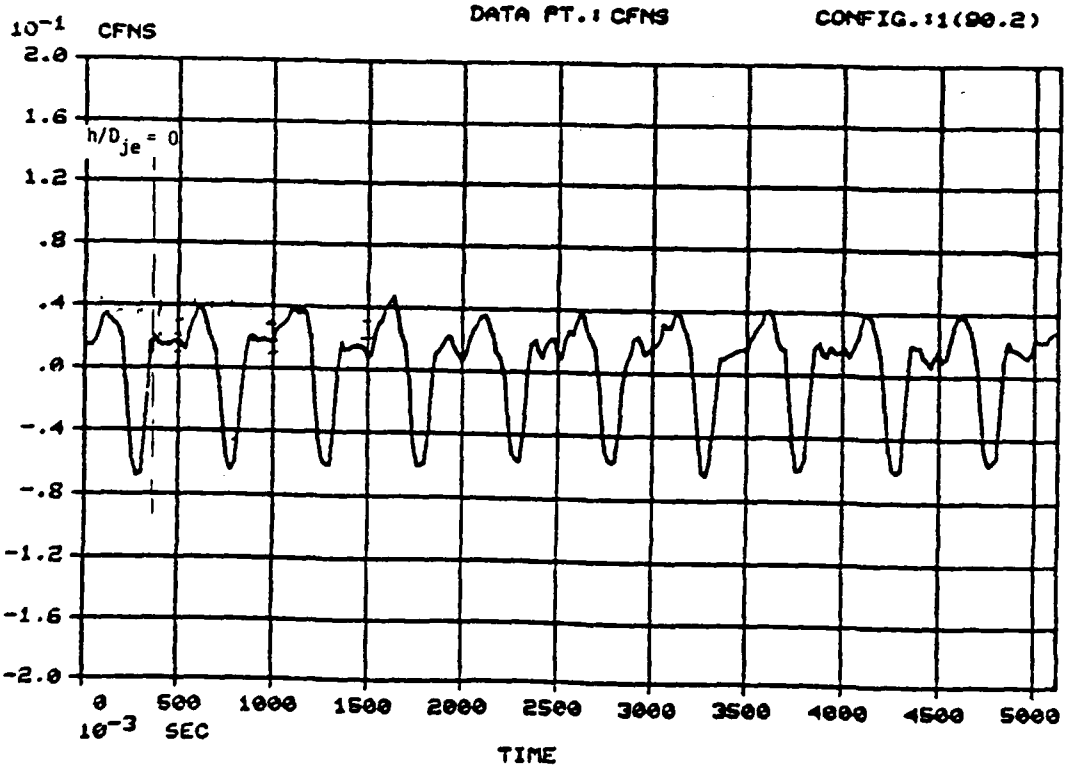

Figure B-4. Subsonic Heaving Motion Data (Run 90.2)

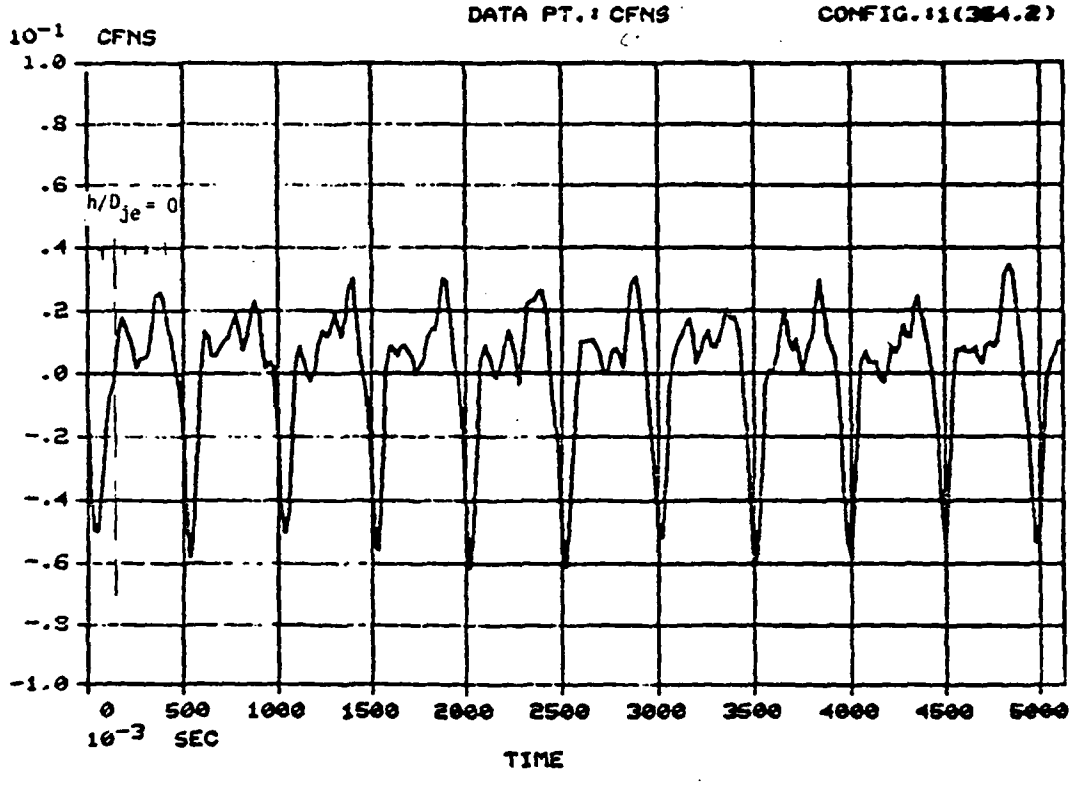

Figure B-5. Subsonic Heaving Motion Data (Run 364.2)

APPENDIX C

SUBSONIC PITCHING MOTION DATA

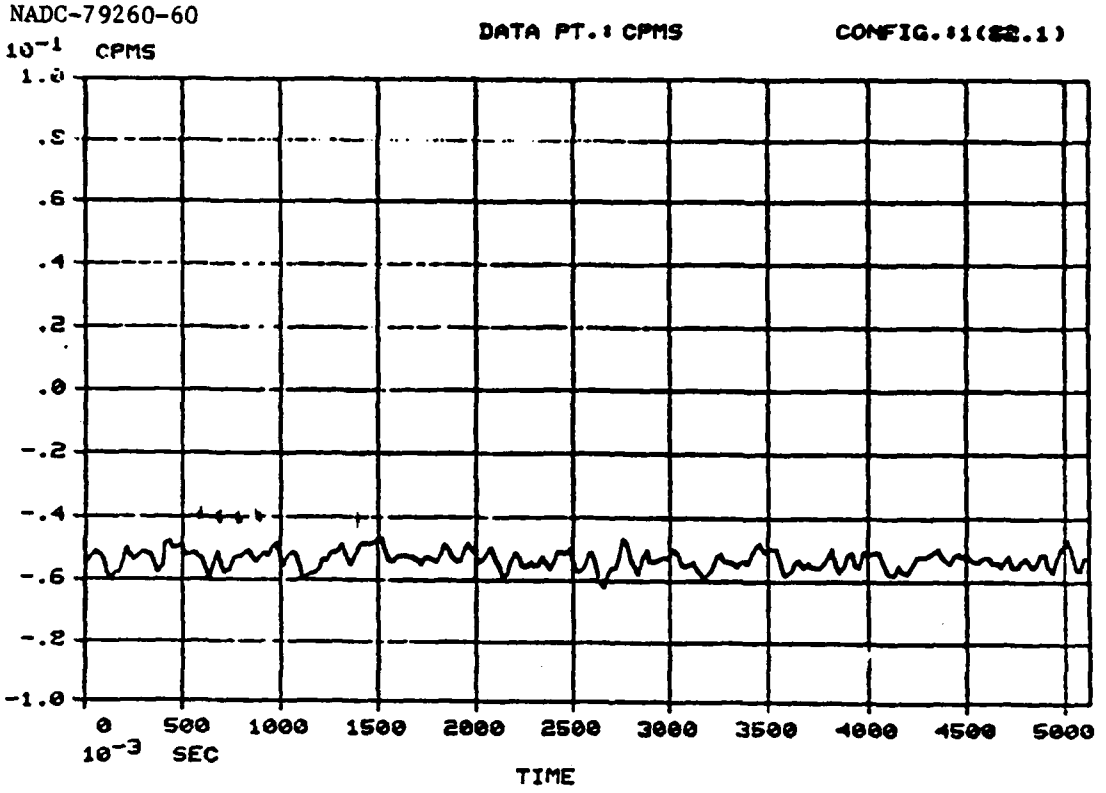

Figure C-1. Subsonic Pitching Motion Data (Run 82.1)

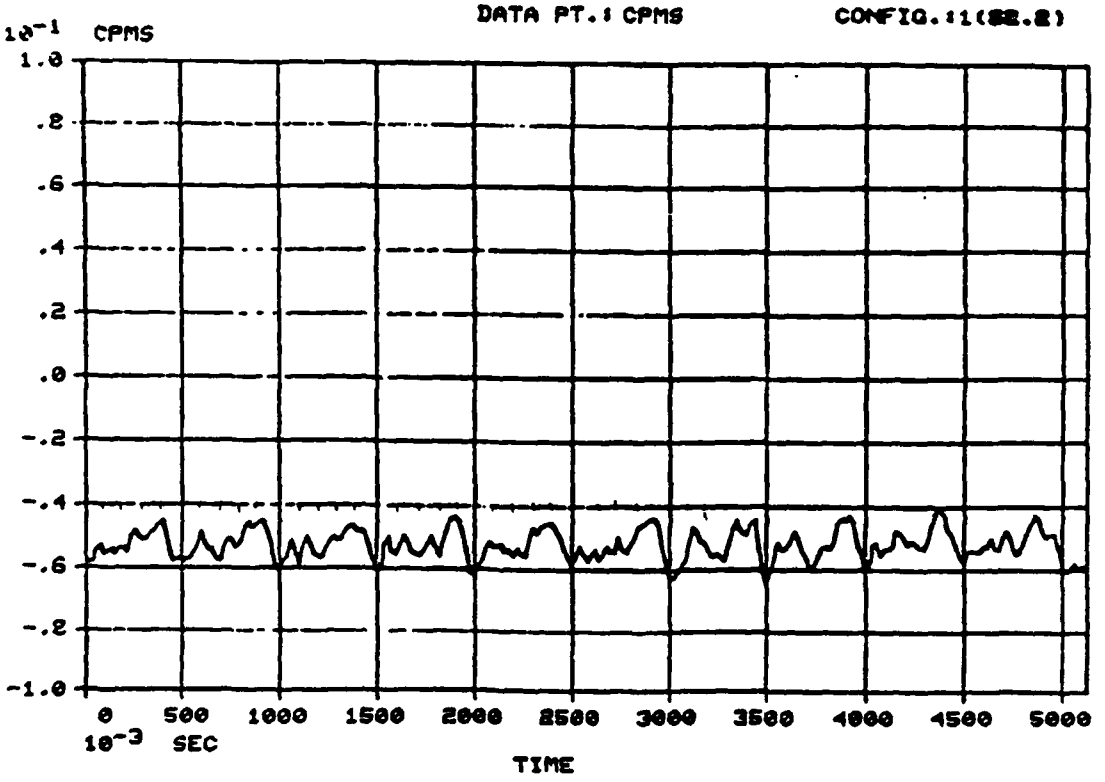

Figure C-2. Subsonic Pitching Motion Data (Run 82.2)

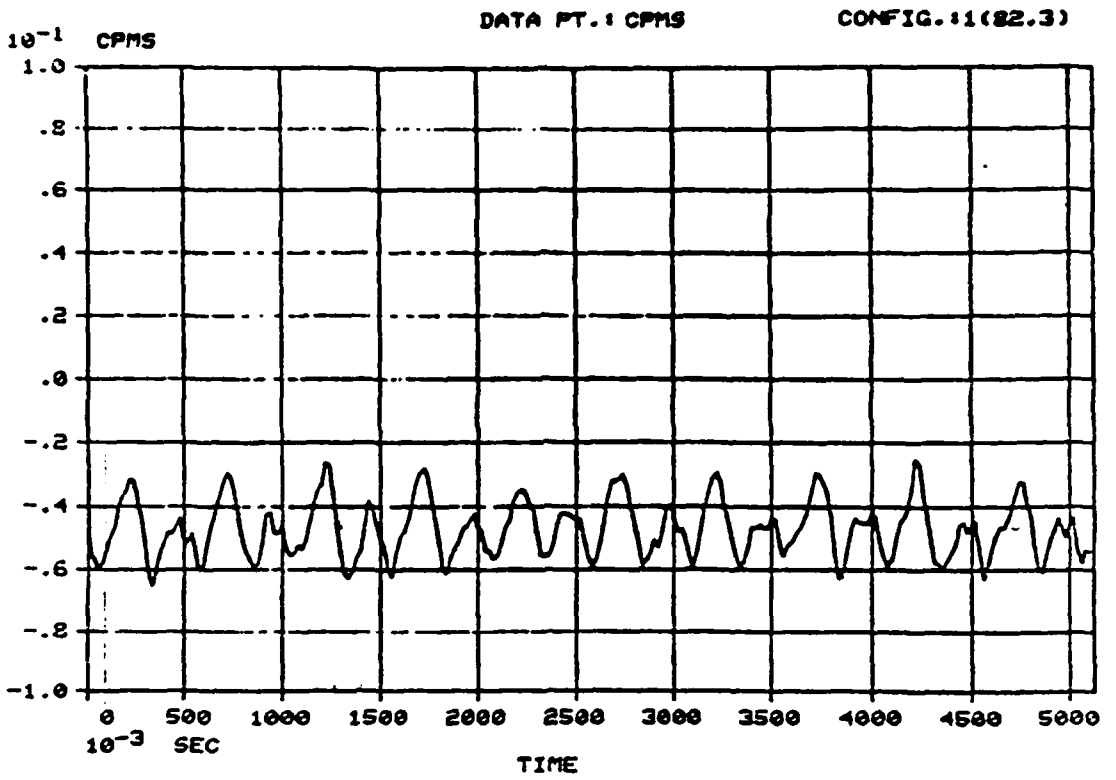

Figure C-3. Subsonic Pitching Motion Data (Run 82.3)

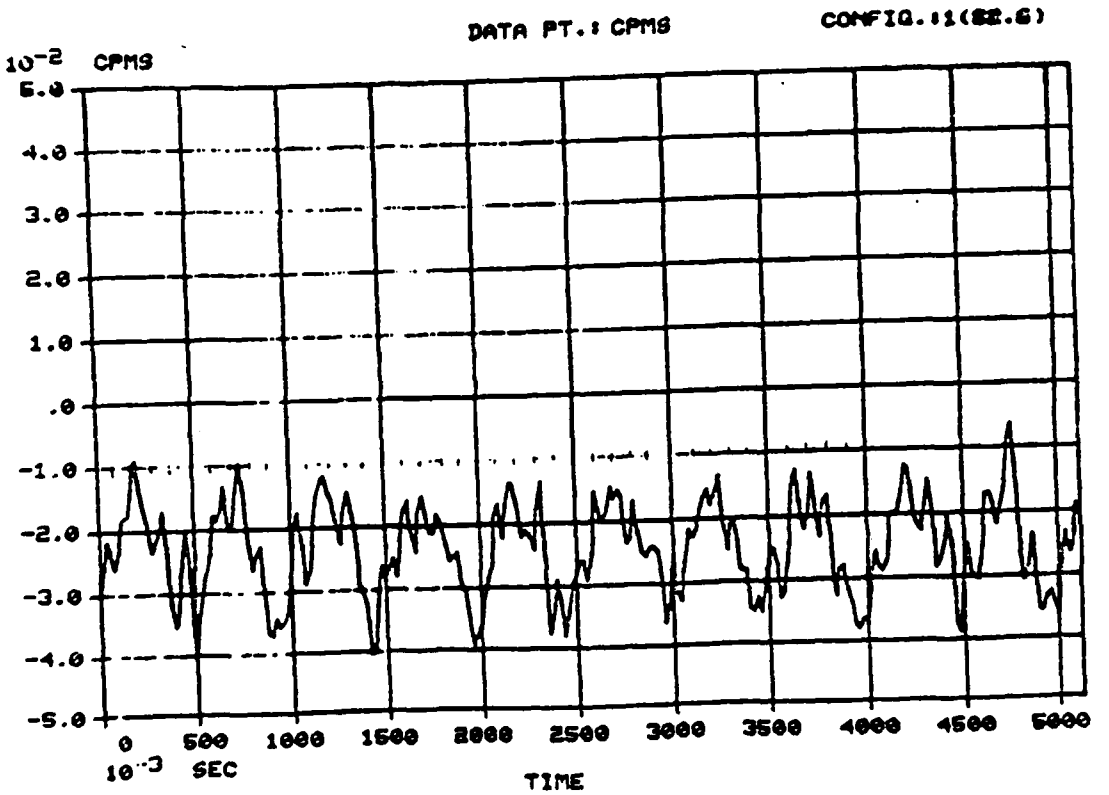

Figure C-4. Subsonic Pitching Motion Data (Run 82.6)

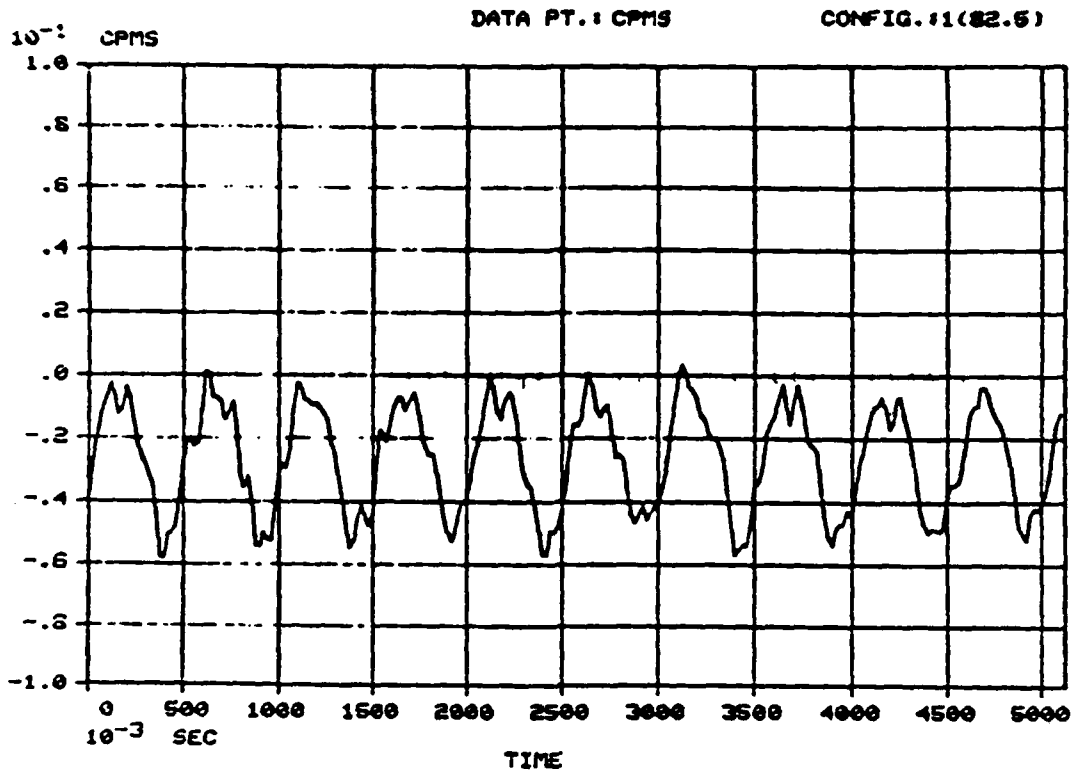

Figure C-5. Subsonic Pitching Motion Data (Run 82.5)

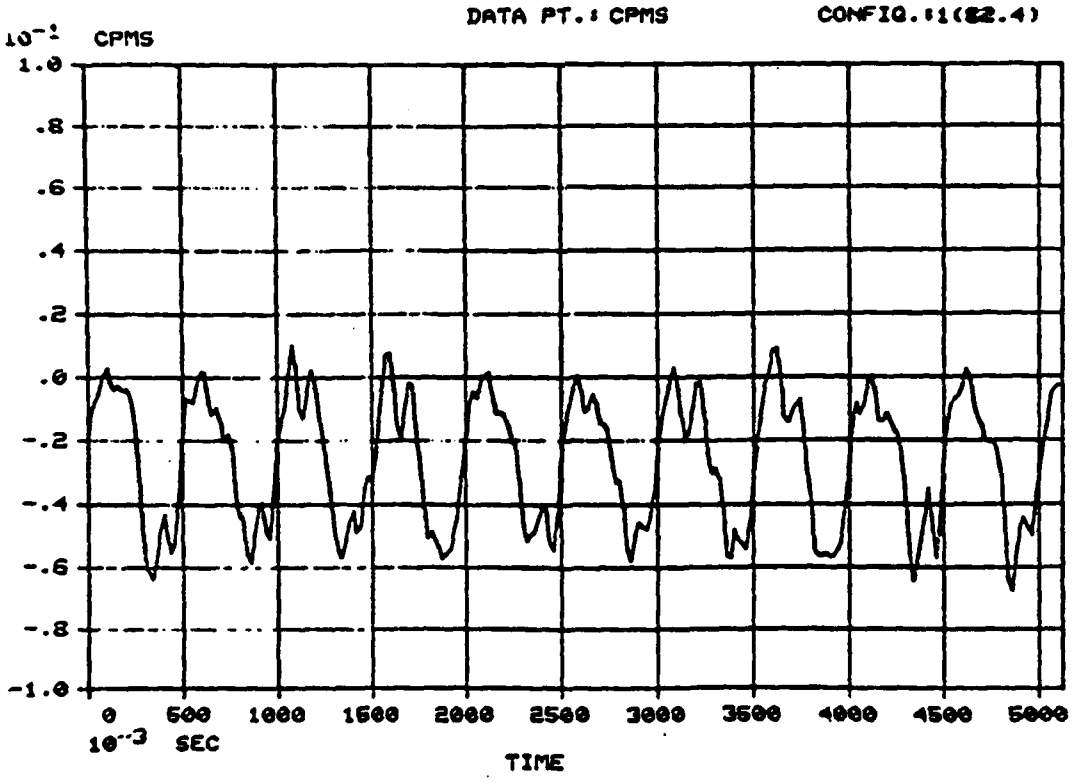

Figure C-6. Subsonic Pitching Motion Data (Run 82.4)

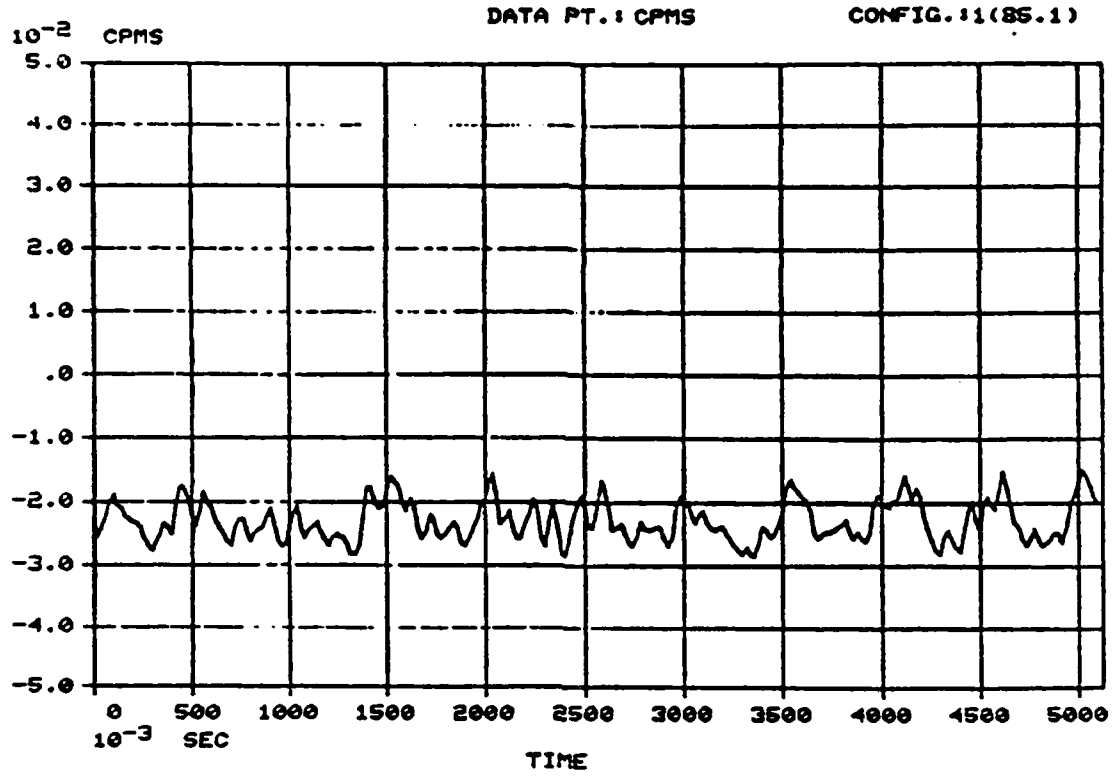

Figure C-7. Subsonic Pitching Motion Data (Run 85.1)

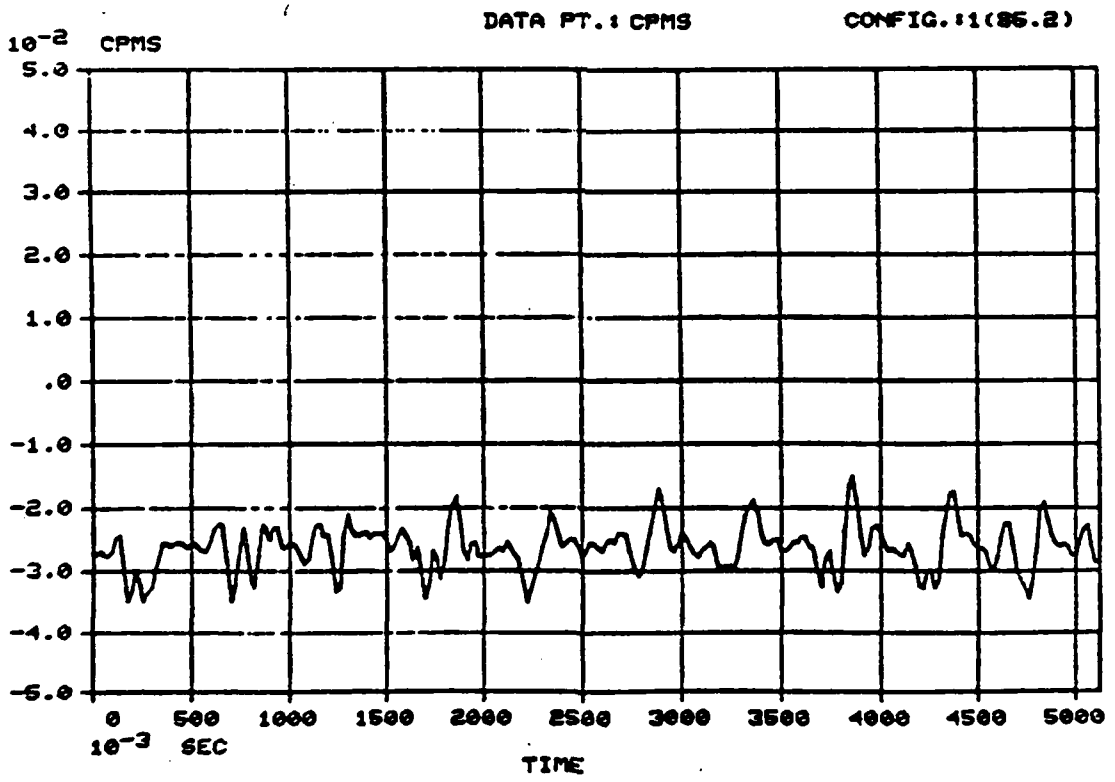

Figure C-8. Subsonic Pitching Motion Data (Run 85.2)

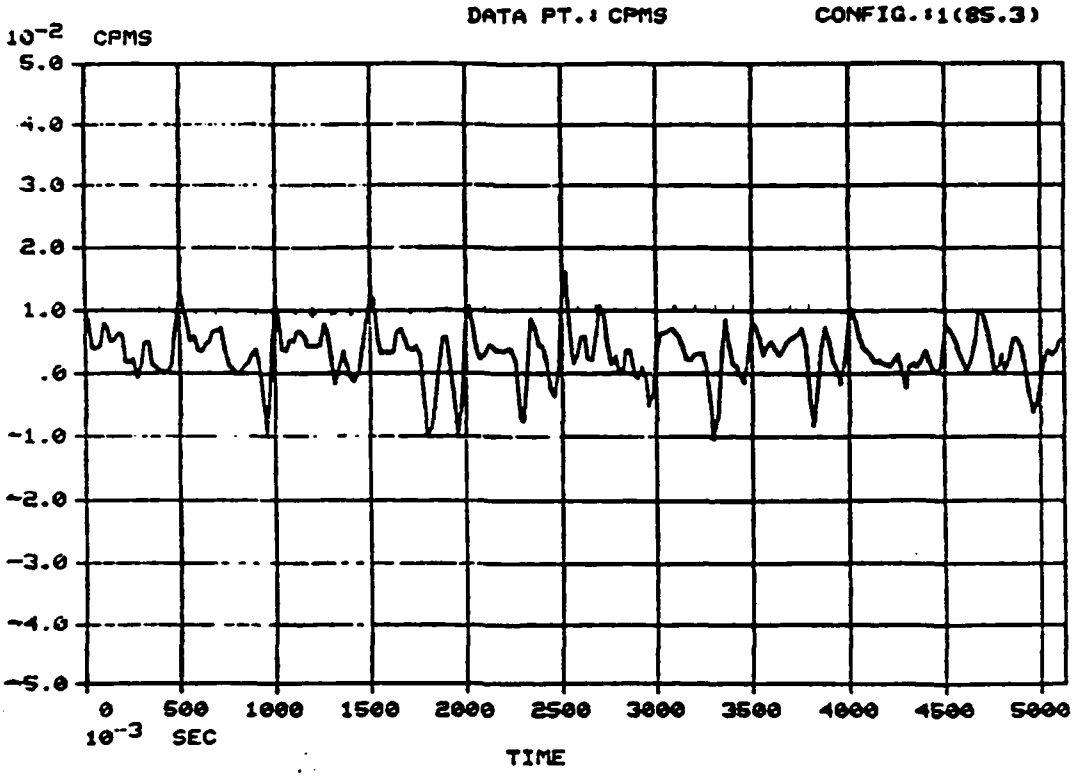

Figure C-9. Subsonic Pitching Motion Data (Run 85.3)

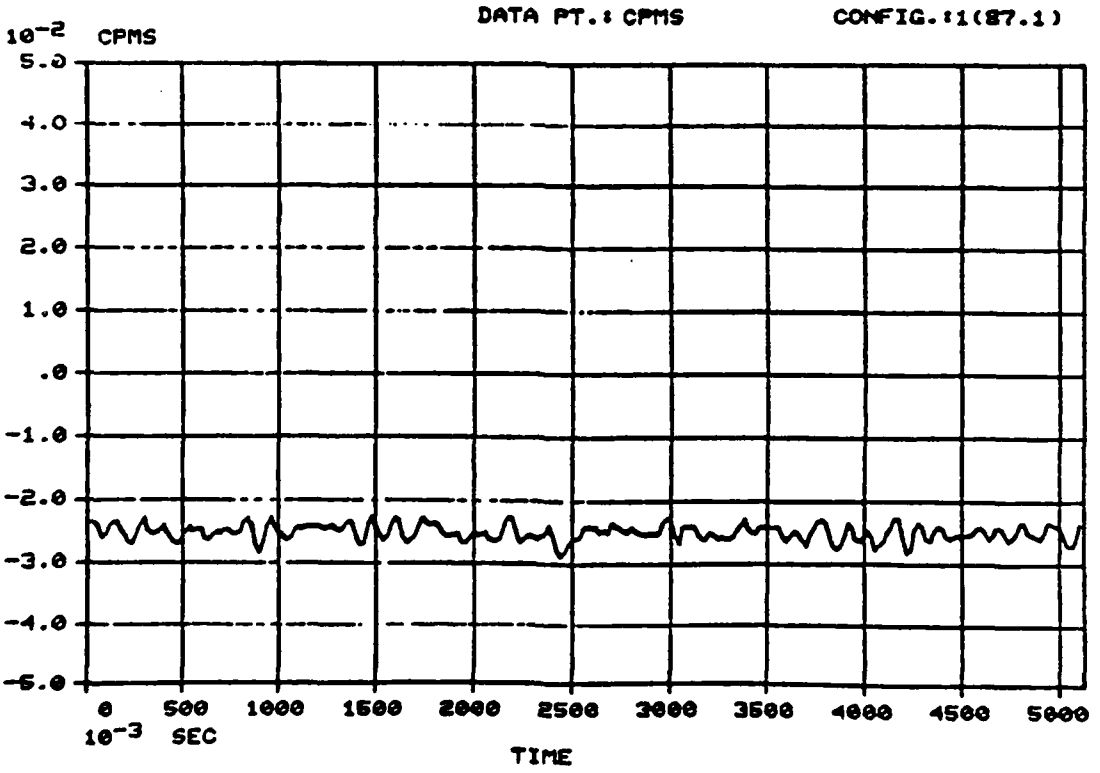

Figure C-10. Subsonic Pitching Motion Data (Run 87.1)

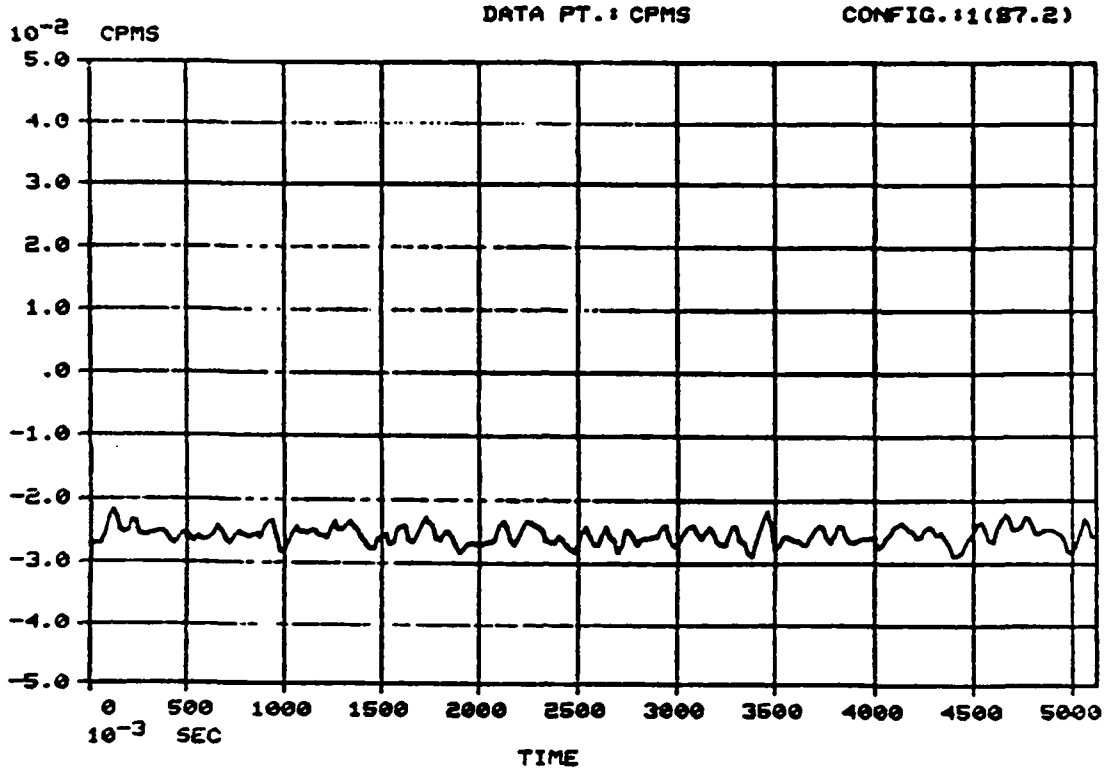

Figure C-11. Subsonic Pitching Motion Data (Run 87.2)

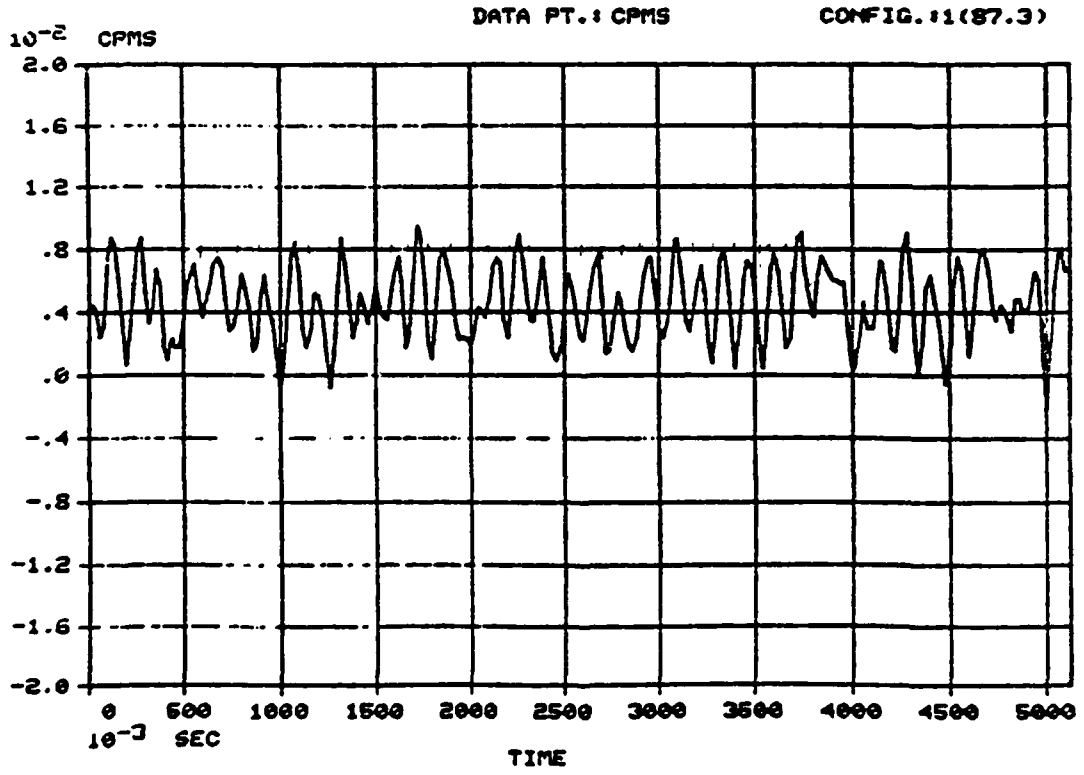

Figure C-12. Subsonic Pitching Motion Data (Run 87.3)

APPENDIX D

SUBSONIC ROLLING MOTION DATA

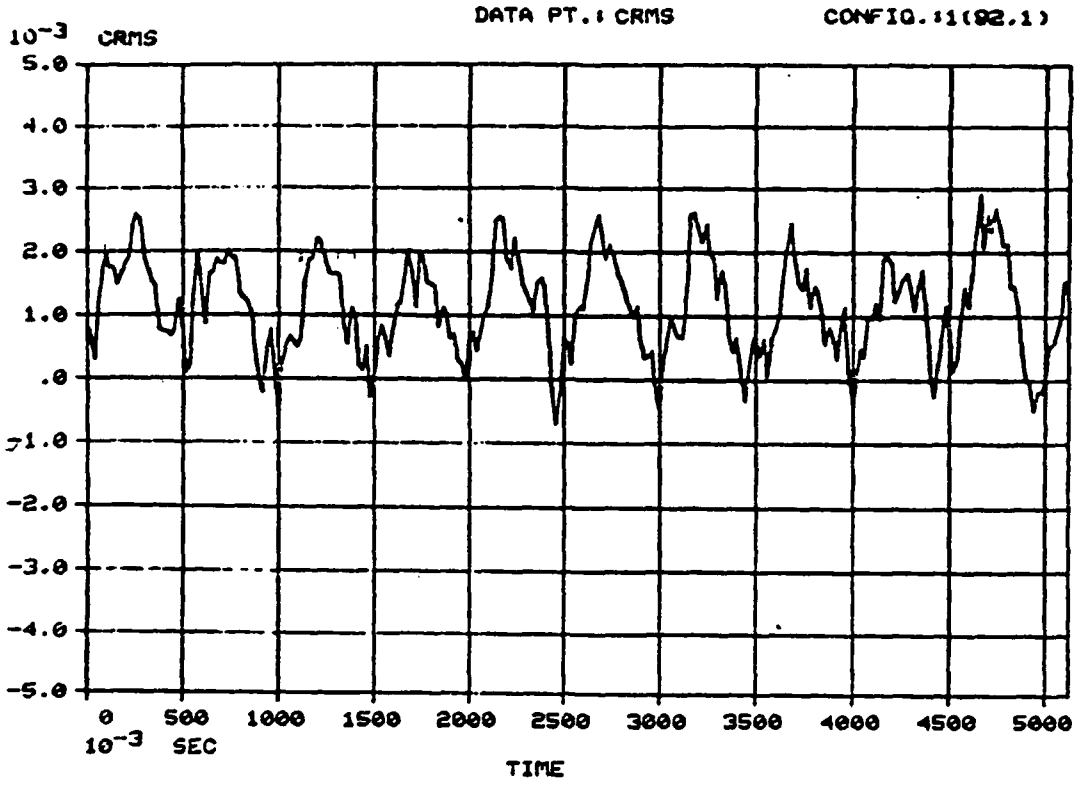

Figure D-1. Subsonic Rolling Motion Data (Run 92.1)

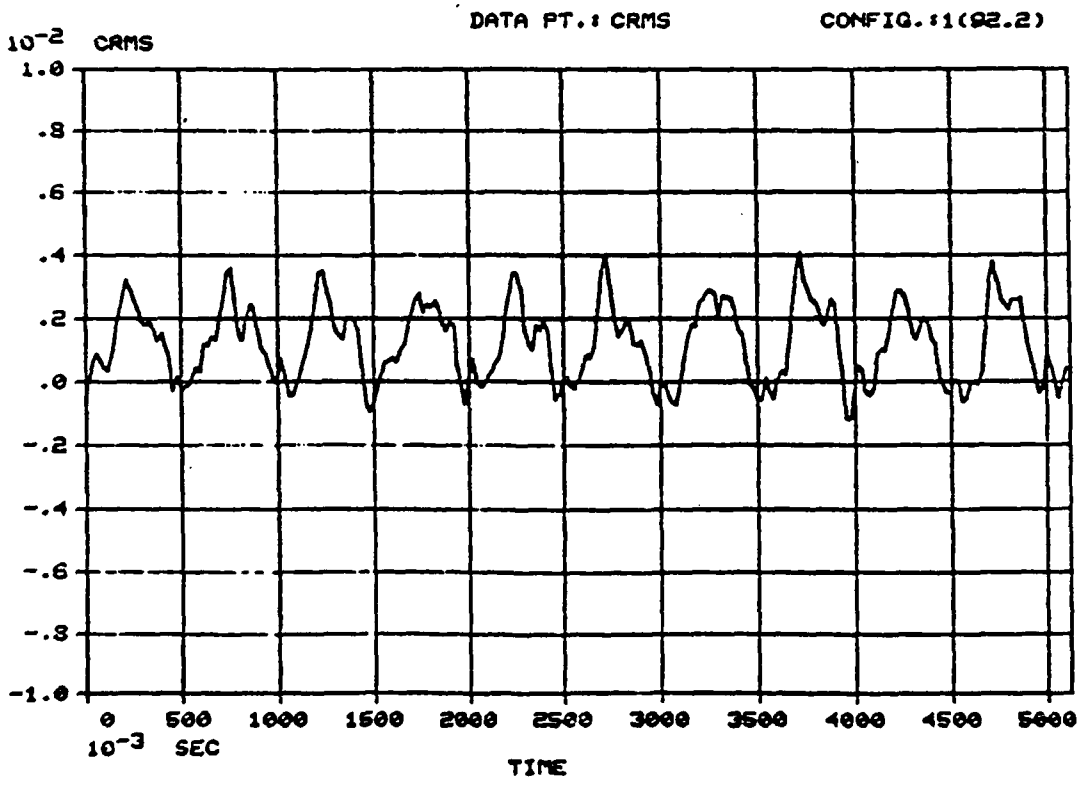

Figure D-2. Subsonic Rolling Motion Data (Run92.2)

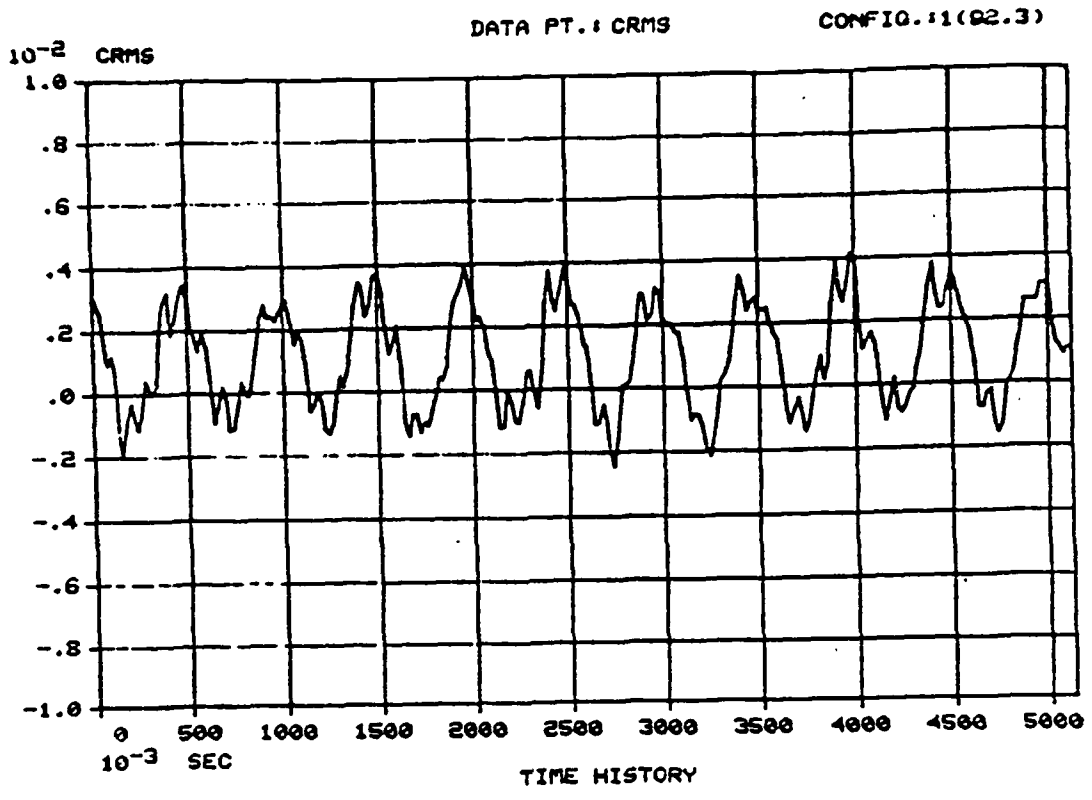

Figure D-3. Subsonic Rolling Motion Data (Run 92.3)

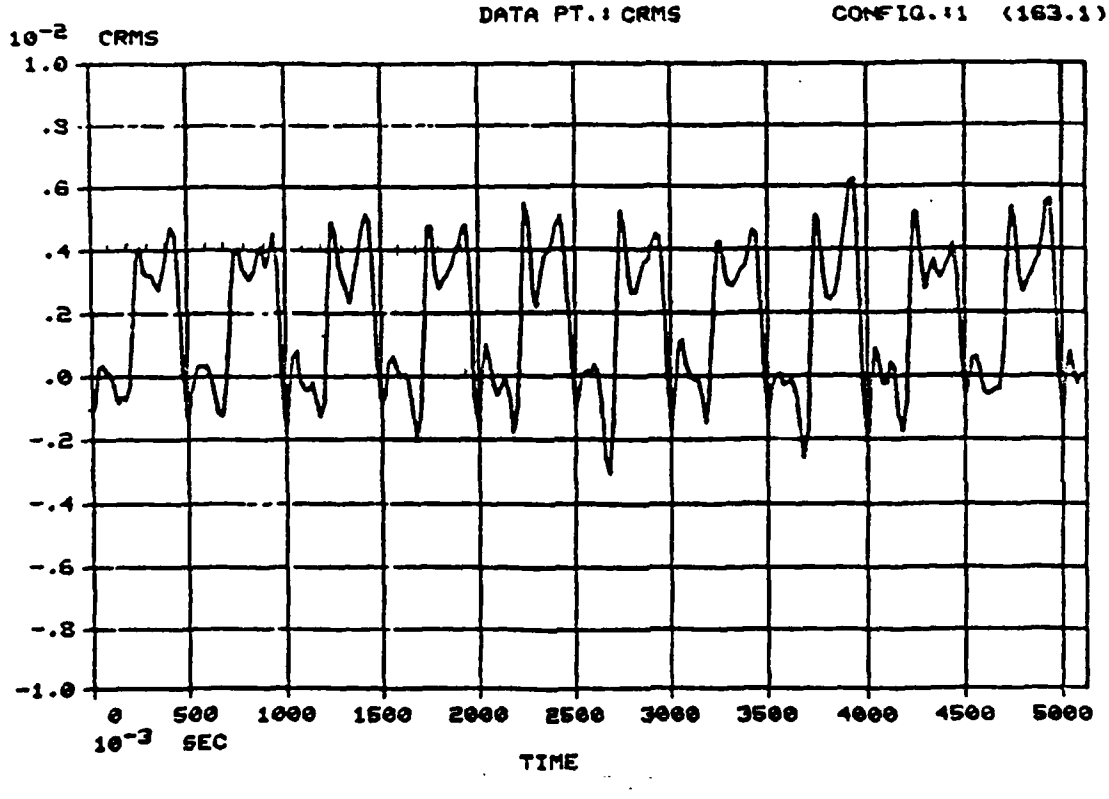

Figure D-4. Subsonic Rolling Motion Data (Run 163.1)

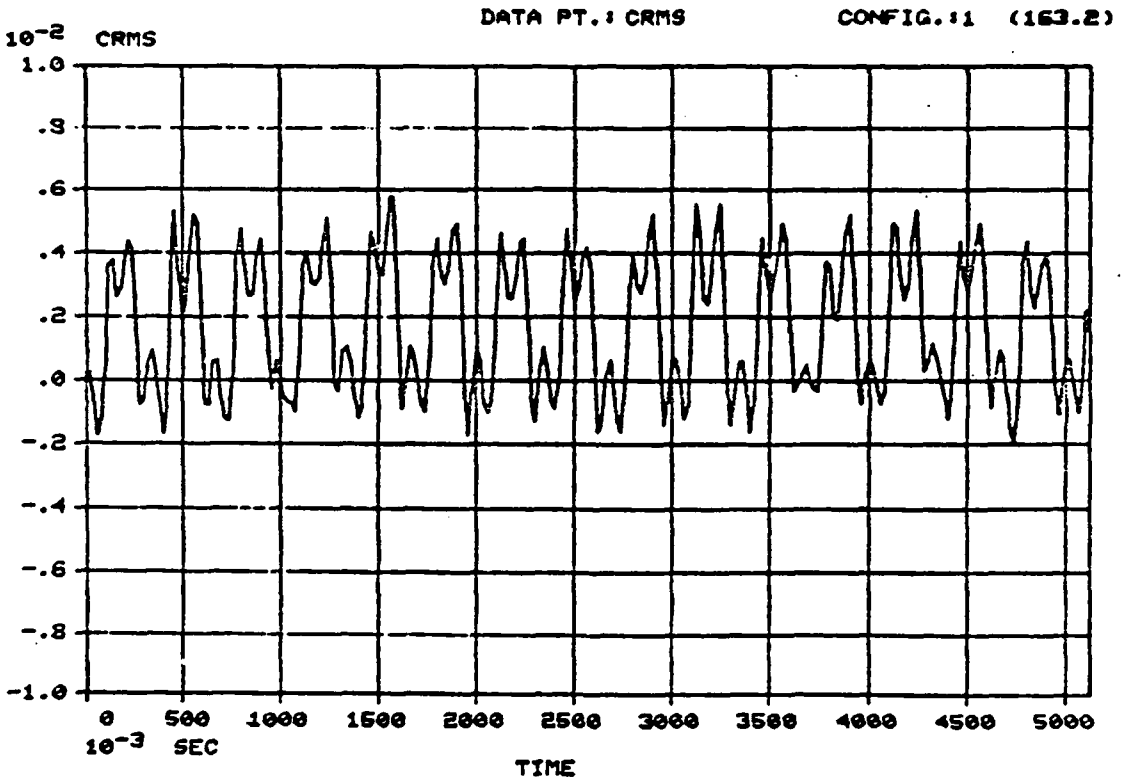

Figure D-5. Subsonic Rolling Motion Data (Run 163.2)

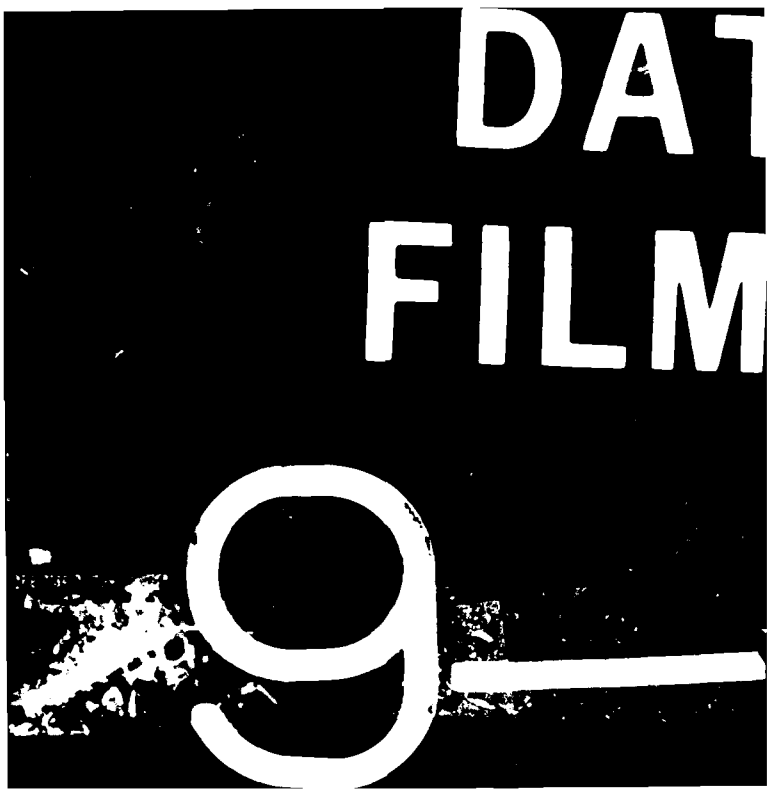
DAT
FILM
9